



cea



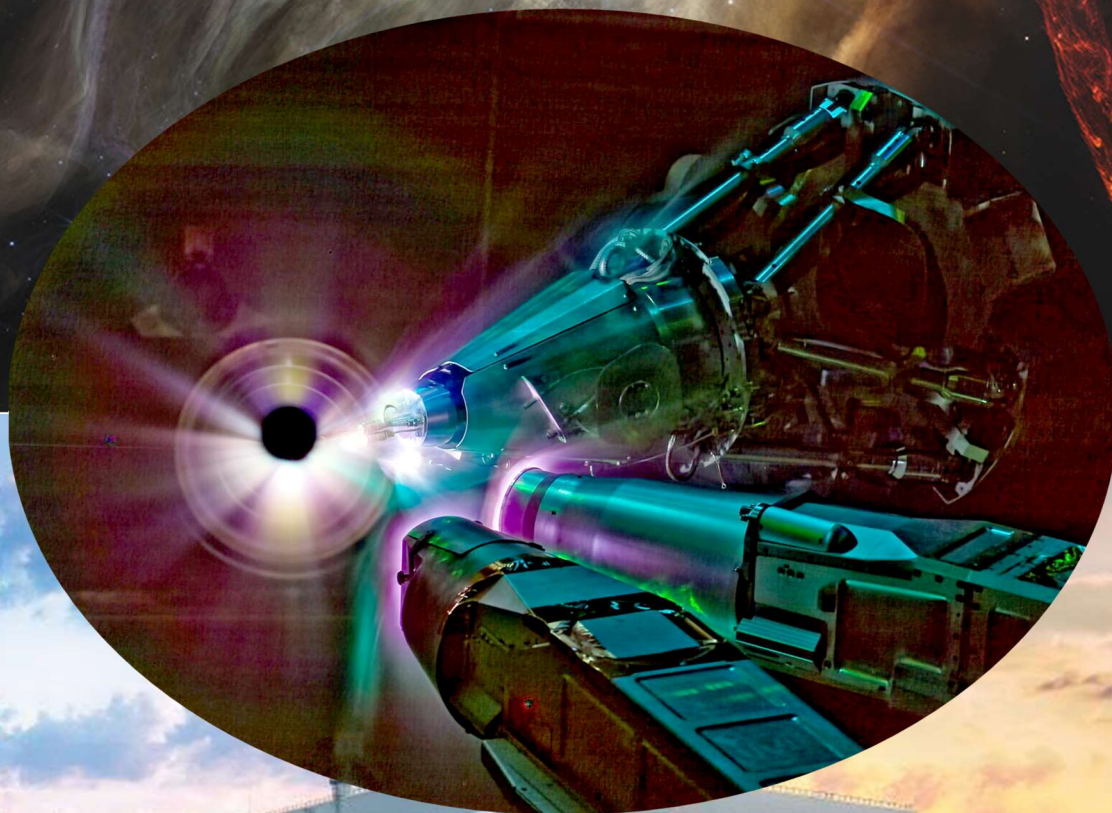
User Guide

LMJ

Laser MegaJoule

PETAL

PETawatt Aquitaine Laser



Version 2.1. Release September 2024

Updated version available at <https://www.asso-ALP.fr> and <http://www-lmj.cea.fr/LMJ-PETAL-User-Group>

CEA-DAM Île-de-France, Bruyères-le-Châtel, F-91297 Arpajon Cedex, France

CEA-CESTA, 15 avenue des Sablières, CS 60001, F-33116 Le Barp Cedex, France

Front page picture: NASA, CEA

Disclaimer

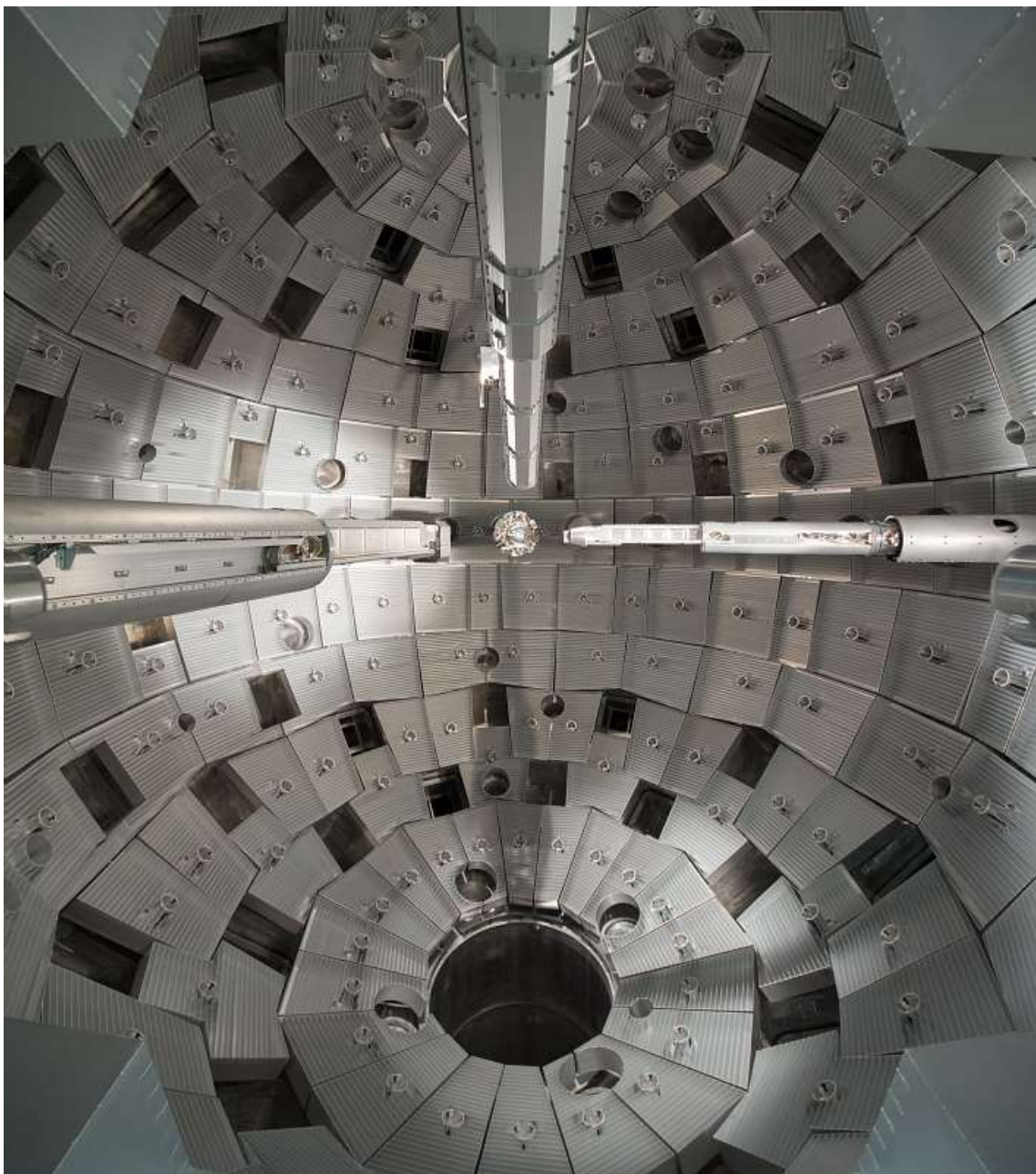
This document describes the status of the LMJ-PETAL facility and provides the necessary technical references to researchers intending to perform experiments on LMJ-PETAL for the 2027-2029 period.

Some devices presented in this document are under development; the data given here, concerning their characteristics, correspond to the specifications. Some small differences could exist between the specification and the realization.

Unless otherwise stated, all the presented devices should be available at the beginning of 2027, but some delays are possible.

Requested experimental configurations may be subject to restrictions in order to ensure compliance to operation procedures and avoid potential damage to facility.

Shot dates will depend on the global planning of the facility operation and constraints induced by the required configuration.



Contents

I- Introduction.....	1
II- LMJ-PETAL Overview.....	2
III- Policies and Access to CEA-CESTA and LMJ facility.....	4
III.1- Driving Directions and Accommodations.....	4
III.2- CEA-CESTA Access and Regulations.....	4
III.3- Confidentiality Rules.....	5
III.4- Selection Process.....	6
III.5- Experimental Process.....	7
III.6- Responsibilities during Shot Cycle.....	7
III.7- Access to LMJ-PETAL during Shots.....	8
III.8- Data Access.....	8
III.9- Publications and Authorship Practices.....	9
III.10- Calls for Proposals History.....	9
IV- LMJ Building Description.....	11
V- LMJ Laser System.....	12
V.1- Laser Architecture.....	12
V.2- LMJ Frequency Conversion and Focusing Scheme.....	15
V.3- Beam Smoothing.....	16
V.4- Spot Sizes.....	16
V.5- Energy and Power.....	17
V.6- Pulse Shaping Capabilities.....	17
V.7- LMJ Performance.....	19
VI- PETAL.....	20
VI.1- Laser System.....	20
VI.2- PETAL Performance.....	22
VII- Target Area and Associated Equipment.....	23
VIII- LMJ Plasma Diagnostics.....	27
VIII.1- X-ray Imagers.....	27
VIII.1.1 - GXI-1, Gated X-ray Imager (high resolution).....	30
VIII.1.2 - GXI-2, Gated X-ray Imager (medium resolution).....	31
VIII.1.3 - SHXI, Streaked Hard X-ray Imager (medium resolution).....	32
VIII.1.4 - UPXI and LPXI, Upper and Lower Polar X-ray imagers.....	32
VIII.1.5 – SXXI, Streaked Soft X-ray Imager (high resolution).....	33
VIII.1.6 – ERHXI, Enhanced Resolution Hard X-ray Imager.....	34
VIII.2- X-ray Spectrometers.....	35
VIII.2.1 – DMX, Broad-band X-ray Spectrometer.....	35
VIII.2.2 - Mini-DMX, Broad-band X-ray Spectrometer.....	37
VIII.2.3 - Mini-DMX-2, Broad-band X-ray Spectrometer.....	37
VIII.2.4 – HRXS, High Resolution X-ray Spectrometer.....	38
VIII.2.5 – SPECTIX, Hard X-ray Spectrometer.....	39
VIII.3- Optical Diagnostics.....	40
VIII.3.1 – EOS Pack.....	41
VIII.3.2 – FABS, Full Aperture Backscatter Stations.....	42
VIII.3.3 – NBI, Near Backscatter Imager.....	43
VIII.4- Particles Diagnostics.....	44
VIII.4.1 – Neutron Pack.....	44
VIII.4.2 – SEPAGE, Electron and Ion Spectrometer.....	45

VIII.4.3 – SESAME, Electron and Proton Spectrometer	46
VIII.5- Other diagnostics.....	47
VIII.5.1 – CRACC and CRACCOPELE, Radiographic Cassette.....	47
VIII.5.2 – DEDIX and DIADEM, Samples Holders.....	48
VIII.6- Diagnostics in Conceptual Design Phase	50
IX- Experimental Configuration for 2027-2029.....	51
IX.1- Laser Beams Characteristics.....	51
IX.2- Target Bay Equipment.....	52
IX.2.1 – SID positions and insertable diagnostics compatibility	52
IX.2.2 – Compatibility with PETAL.....	52
IX.3- Experimental platforms.....	54
X- Targets.....	56
X.1- Assembly and Metrology Process.....	56
X.2- LMJ-PETAL Target Alignment Process.....	57
XI- References.....	58
XII- Acknowledgements	60
XIII- Glossary	61
XIV- Appendix.....	62
XV- Revision Log	63

I- Introduction

The Military Applications Division of the French Alternative Energies and Atomic Energy Commission (CEA-DAM) has promoted for several decades collaboration with national and international scientific communities [1-31]. Regarding laser facilities, according to the decision of the French Ministry of Defense, the CEA-DAM has given access to the scientific communities to the LIL facility, the prototype of Laser Megajoule (LMJ), for a period of 9 years since 2005 until 2014. Ten types of experimental campaigns and a total of one hundred laser shots on targets in collaboration have been performed on the LIL during this period

[32-38]. With the LMJ [39, 40] and PETAL facilities [41], the CEA-DAM is once again in a position to welcome national and international teams, in perfect accordance with its legal obligations to confidentiality.

The Laser Megajoule is part of the French “Simulation Program” developed by the CEA-DAM. The Simulation program aims to improve the theoretical models and data used in various domains of physics, by means of high performance numerical simulations and experimental validations.



Figure I.1: LIL and LMJ aerial view.

LMJ offers unique capabilities for the Simulation Program, providing an extraordinary instrument to study High Energy Density Physics (HEDP) and Basic Science [42, 43]. A large panel of experiments will be done on LMJ to study physical processes at temperatures from 100 eV to 100 keV, and pressures from 1 Mbar to 100 Gbar. Among these experiments, Inertial Confinement Fusion (ICF) is the most exciting challenge, since ICF experiments set the most stringent specifications on LMJ's features [44, 45].

The PETAL project has developed and coupled to LMJ an additional high-energy multi-Petawatt beam. This project has been performed by the CEA under the financial auspices of the Aquitaine Region ("maître d'ouvrage", project owner), of the French Government and of the European Union. PETAL provides a combination of a very high intensity beam, synchronized with the very high energy

beams of LMJ. LMJ-PETAL is an exceptional tool for academic research, offering the opportunity to study matter in extreme conditions.

LMJ-PETAL is open to academic communities, as the previously mentioned LIL. The academic access to LMJ-PETAL and the selection of the proposals for experiments are done by Association Lasers & Plasmas (ALP, Z.A. Laseris – 1 avenue du Médoc – F-33114 Le Barp) through the International Scientific Advisory Committee.

This document provides the necessary technical references to researchers for the writing of experimental proposals to be performed on LMJ-PETAL. A regularly updated version of this LMJ-PETAL User guide is available on the ALP <https://www.asso-ALP.fr> and LMJ <http://www-lmj.cea.fr/LMJ-PETAL-User-Group> websites.

II- LMJ-PETAL Overview

LMJ is a flash-lamp-pumped neodymium-doped glass laser (1.053 μm wavelength) configured in a multi-pass power amplifier system. The 1.053 μm light is frequency converted to the third harmonic (0.351 μm) and focused, by means of gratings, on a target at the center of the target chamber. Once fully commissioned, with 176 beams (44 quads) operational, LMJ will deliver shaped pulses from 0.7 ns to 25 ns with a maximum energy of 1.3 MJ and a maximum power of 400 TW of UV light on the target.

The main building includes four similar laser bays, 128-meter long, situated in pairs on each side of the central target bay of 60-meter diameter and 38-meter height.

The 176 square 37 x 35.6 cm^2 laser beams are grouped into 22 bundles of 8 beams. In the switchyards, each individual bundle is divided into two quads of 4 laser beams, the basic independent unit for experiments, which are directed to the upper and lower hemispheres of the chamber.

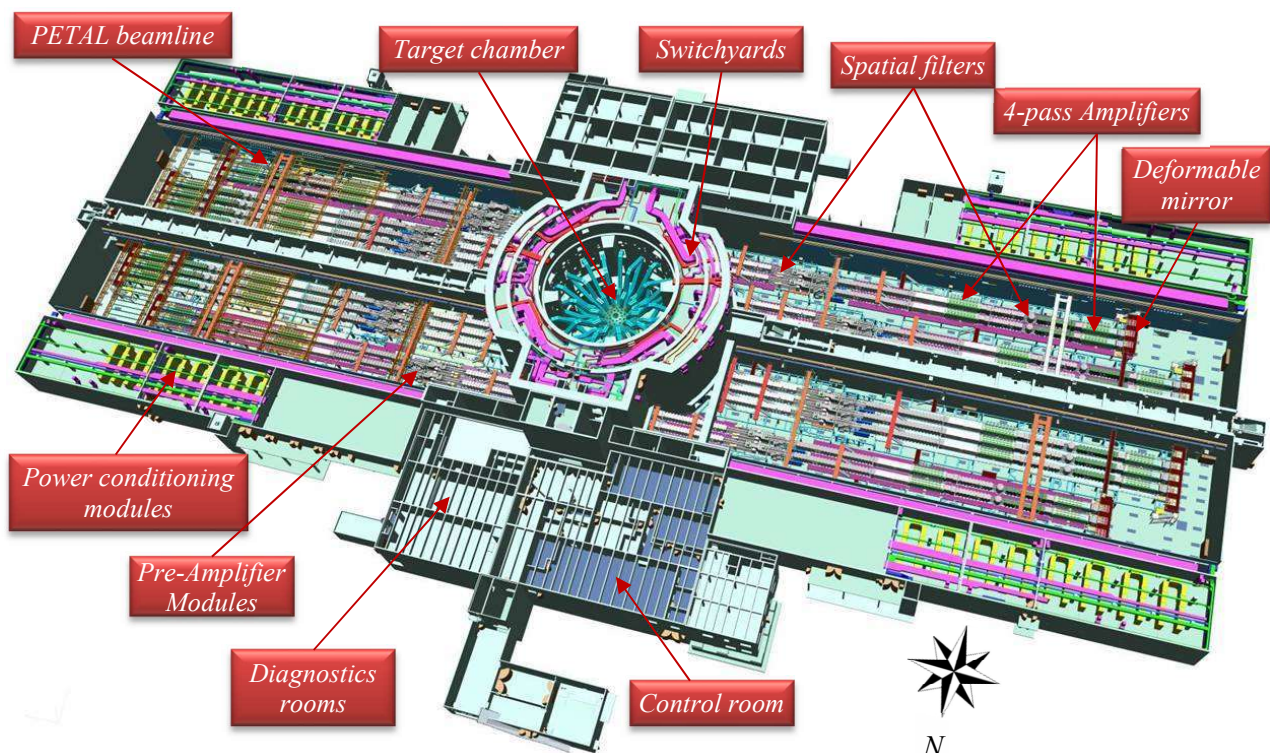


Figure II.1: Schematic view of the Laser Megajoule showing the main elements of the laser system.

At the center of the target bay, the target chamber consists of a 10-meter diameter aluminum sphere, equipped with two hundred ports for the injection of the laser beams, the location of diagnostics and target holders. It is a 10 cm-thick aluminum sphere covered with a neutron shielding made of 40 cm thick borated concrete. The inside is covered by protection panels for X-ray and debris.

LMJ is configured to operate in the “indirect drive” scheme, which drives the laser beams into cones in the upper and lower hemispheres of the target chamber. Forty quads enter the target chamber through ports that are located on two cones at 33.2° and 49° polar angles. Four other quads enter the target chamber at 59.5° polar angle, and are dedicated to radiographic purpose.

The 44 laser beam ports include the final optics assembly: vacuum windows, debris shields and device to check the damages on optics.

Many pieces of equipment are required in the target area:

- a Reference Holder (RH) is used for the alignment of all beams, diagnostics and target,
- a Target Positioning Systems (TPS) for room temperature experiments is operational,
- a cryogenic TPS for ignition target will be installed later,
- a set of visualization stations for target positioning (SOPAC stations, as System for Optical Positioning and Alignment inside Chamber),

- a set of about seven diagnostics manipulators, called Systems for Insertion of Diagnostic (SID), will be installed, they will position 150-kg diagnostic with a 50- μ m precision.

The PETAL laser is a short-pulse (500 fs to 10 ps) ultra-high-power, high-energy beam (ultimately few kJ) which has been coupled to LMJ. The LMJ-PETAL facility, offering the combination of a very high intensity multi-petawatt beam, synchronized with high-energy nanosecond beams, strongly expands the LMJ experimental field on HEDP.

The PETAL design is based on the Chirped Pulse Amplification (CPA) technique combined with Optical Parametric Amplification (OPA). Furthermore, it benefits from the laser developments made for the high-energy LMJ facility allowing it to reach the kilojoule level.

Over 30 photon and particle diagnostics are considered with high spatial, temporal and spectral resolution in the optical, X-ray, and nuclear domains. Beside classical diagnostics, specific diagnostics adapted to PETAL capacities are available

in order to characterize particles and radiation yields that can be created by PETAL [46, 47]. The set of equipment, delivered in 2016 and 2017 has been specified by the academic community in the framework of the PETAL+ project* and has been developed by the CEA. It consists of: one spectrometer for charged particles (SEPAGE), two electron spectrometers (SESAME), one hard X-ray spectrometer (SPECTIX) and radiography cassettes for x-ray or protons (CRACC).

The first CEA-DAM physics experiments on LMJ have been performed in October 2014 with a limited number of beams and diagnostics. The operational capabilities (number of beams and plasma diagnostics) are increasing gradually every year until the completion of the facility. The first academic experiments on LMJ-PETAL have been performed in 2017 with 16 beams (4 quads) and PETAL beam, 3 SID and 12 diagnostics. Other academic experiments have been performed in 2018-2020, 2021-2024, and some other are planned in 2025-2026. The next ones will be performed in 2027-2029 in the final configuration (44 quads) and PETAL beam, 7 SID and more than 20 diagnostics.

<i>History</i>	<i>Date</i>
<i>Beginning of the construction of the LIL facility</i>	<i>1996</i>
<i>First laser shots on LIL</i>	<i>2002</i>
<i>Beginning of the construction of the LMJ facility</i>	<i>2003</i>
<i>First target physics experiments on LIL</i>	<i>2004</i>
<i>Beginning of PETAL on LIL</i>	<i>2005</i>
<i>First academic experiments on LIL</i>	<i>2005</i>
<i>LMJ target chamber installed</i>	<i>2006</i>
<i>LMJ building commissioning</i>	<i>2008</i>
<i>Decision of coupling PETAL with LMJ</i>	<i>2010</i>
<i>Last academic experiments on LIL & closure of LIL</i>	<i>2014</i>
<i>First target physics experiments on LMJ with 2 quads</i>	<i>2014</i>
<i>PETAL most powerful laser beam with 1.2 PW</i>	<i>2015</i>
<i>First associated LMJ and PETAL shot</i>	<i>2015</i>
<i>First PETAL test shots on target</i>	<i>2017</i>
<i>First academic experiments on LMJ with 4 quads and PETAL</i>	<i>2017</i>
<i>First User Meeting</i>	<i>2018</i>
<i>First D₂ fusion experiments on LMJ</i>	<i>2019</i>
<i>First EOS experiments on LMJ</i>	<i>2020</i>
<i>First experiments in LMJ half full configuration (20 quads)</i>	<i>2022</i>
<i>Second User Meeting</i>	<i>2023</i>

Table II.1: Some milestones dates in the history of LIL, LMJ and PETAL facilities.

* The development of PETAL diagnostics took place within the Equipex project PETAL+ led by the University of Bordeaux, funded by the French Research

National Agency (ANR) within the framework of the "Programme d'Investissement d'Avenir" (PIA) of the French Government.

III- Policies and Access to CEA-CESTA and LMJ facility

III.1- Driving Directions and Accommodations

The LMJ-PETAL facility is located at CEA-CESTA, 15 avenue des Sablières, CS 60001, 33116 Le Barp Cedex, France. GPS coordinates are given in the appendix.

In Figure III.1, directions are given for visitors traveling from either the Bordeaux Merignac

Airport, or SNCF Bordeaux railway station. The A63 highway provides direct access to CEA-CESTA. The driving distance from Bordeaux is 35 km, approximately 30 minutes in normal traffic conditions. Note that it is compulsory that all visitors satisfy the badging policy described in Section III.2-.



Figure III.1: Map of Bordeaux South area and transportation routes to CEA-CESTA and LMJ.

There are some hotels close to CEA-CESTA, but numerous hotels can be found in the city of

Bordeaux or in the region of Arcachon (seaside). A list of hotels is given in the appendix.

III.2- CEA-CESTA Access and Regulations

CEA-CESTA is a national security laboratory with regulated access. Visitors must make prior arrangements at least 8 weeks before any visit. The experimental campaigns on LMJ-PETAL will be planned at least 6 months in advance, and the access

to CEA-CESTA could be extended up to a 3 months period. In order to gain admittance, the requested information is the following:

Last name, first name, place of birth, nationality (dual nationality if any), nationality of birth,

passport number and date of validity (CNI number and validity for French citizen), home address, name and address of employer, research institution, funding agency, professional phone number, professional email, contact in case of emergency.

Please notice that access to LMJ-PETAL is of CEA responsibility only. Acceptance of an experimental proposal by ALP doesn't automatically grant access to CEA for all of the collaborators. According to confidentiality rules, no justifications would be given in case of denied access to the facility.

III.3- Confidentiality Rules

CEA-DAM is pleased to promote a wide participation of the academic communities to the scientific and technological researches which will be performed on the LMJ-PETAL facility. However, as an organism which is in charge for the control of scientific disciplines involved in nuclear deterrence, the CEA-DAM has to follow the protection rules regarding French National Defense.

As a consequence, some information and data obtained from laser experiments have to be protected according to the "Guide on the sensitiveness of information in the field of Inertial Confinement Fusion". (General Secretary for Defense and National Security)

This is why some indications are given below to prevent or reduce any risk of proposal rejection due to confidentiality rules infringement.

Most of research themes can be carried out on LMJ-PETAL without any restriction: optics, laser-plasma interaction, plasma physics, particles transport, thermal conduction, mechanics in continuous media, general hydrodynamics, nuclear physics, etc.

Some other research fields can be considered as sensitive: Equation of State (EOS), atomic spectra and opacities, constitutive relations and damage

Professional computers may be authorized on-site provided that the MAC address and physical address of the computer were given with the aforementioned personal information. Internet connectivity will be provided in a dedicated room; however no Wi-Fi capabilities are available inside CEA-CESTA.

All types of cellular telephones are forbidden. This restriction also applies for CEA people inside restricted areas, like the LMJ-PETAL building. The cell phones should be kept secured in a cell phones garage at the badging center entry.

laws of materials, radiative hydrodynamics, turbulent hydrodynamics, X-ray radiation transfer, mixing physics in convergent flows, actinides studies, etc.

For the subjects listed above, sensitivity will depend on materials and parameters quoted in the experimental proposal. EOS and opacities are notably concerned.

Regarding EOS and constitutive relations and damage laws, simple elements or mixture can be studied at any pressure if their atomic number is lower or equal to 71. For atomic number between 72 and 91 (included), the pressure is limited to 1000 GPa. For atomic number greater than 91, the domain is considered as sensitive at any pressure.

Atomic spectra and opacities can be studied for any temperature for element whose atomic number is lower or equal to 36. For other elements, the temperature is limited to 50 eV.

These open domains for experiments are summarized in figure III.3.

In some cases, proposals could be submitted to the General Secretary for Defense and National Security, to verify compliance with security rules.

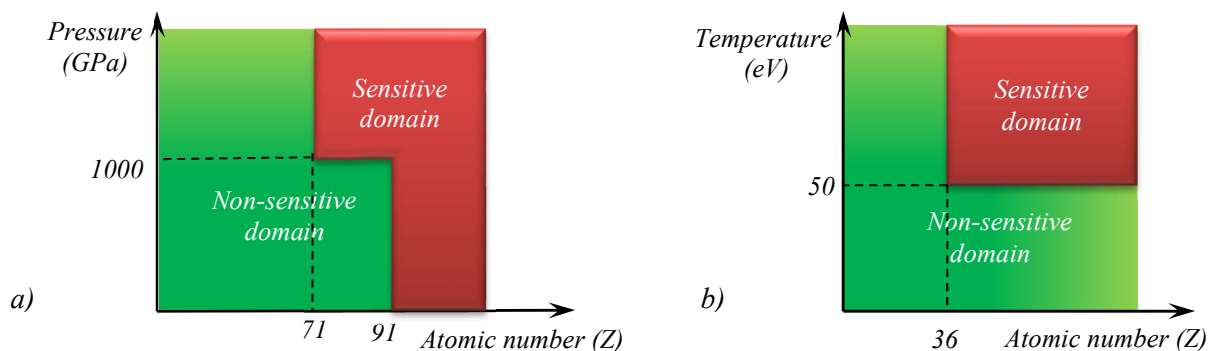


Figure III.3: a) Accessible pressure and atomic number for Equation of State experiments
b) Accessible temperature for Opacities experiments.

III.4- Selection Process

A call for proposals for experiments on the LMJ-PETAL laser facility will be issued regularly roughly every two years by ALP, CEA and Nouvelle Aquitaine Region.

Depending on the experiment complexity, experiments will be approved on a one-year or two-year basis. The more complex selected experiments can be given a few laser shots in the first year, intended to demonstrate the feasibility of the experiment. On the basis of the results of the campaign of the first year, more laser shots can be allocated on the second year.

The selection process for experimental proposals on LMJ-PETAL is the following:

- First a proposal should be addressed by research groups to ALP (contact@asso-ALP.fr) and CEA-DAM (userLMJ@cea.fr). This proposal should describe the scientific motivation and the purpose of the experiment, the research groups involved in the experiment, the laser requirements (energy, power, pulse shape, etc.), the diagnostic requirements, the target requirements, the number of laser shots requested (limited to 6 per campaign). For any question regarding LMJ-PETAL facility and experimental design contact userLMJ@cea.fr. At this stage, the PI may be assisted by a co-PI from CELIA (which can provide modelling and/or numerical simulations for instance).

A pre-selection of the most pertinent experiments is done by the International Scientific Advisory Committee (ISAC), established by ALP. This pre-selection also depends on technical opinion from CEA-DAM concerning the feasibility and impacts on the facility operation of the requested experimental configuration.

- Secondly, the pre-selected groups will be asked to make an oral presentation to the ISAC members, who will assess the quality and originality of the proposals.

In addition to the information already mentioned, the proposal must include:

- 1. Experimental configuration at the target chamber center**, including realistic target dimensions and position of additional targets (backlighter if any).
- 2. Laser configuration**

2.1. For LMJ beams:

- The selected spot sizes (see Table V.2 & Table IX.1) and optical smoothing conditions (2 GHz or 2 + 14 GHz);

- The laser pulse shape per quad (P (TW) as a function of time) and Energy (kJ) per quad (the Energy-Power diagram is presented in Figure V.9);
- The laser aim points per quad.

2.2. For PETAL beam:

- Pulse duration (between 0.5 and 10 ps);
- Energy (the current transport mirrors limits the available energy on target at 600 J for the 2027-2029 timeframe);
- Best focus position.

3. Diagnostics configuration

The primary and secondary diagnostics for the physics goal must be specified.

With regard to diagnostics in SID: 7 SID are available in 2027. Table VII.1 indicates the available locations.

The fixed diagnostics, if needed, are: DMX in MS8 location, SESAME 1 and SESAME 2, UPXI, LPXI, FABS, NBI, Neutron Pack (see VIII- LMJ Diagnostics).

Note that some restrictions apply in the capability to operate insertable diagnostics in the different SIDs (see Table IX.2, and Chapter IX.3 Experimental platforms)

4. Target description

Sketch of the targets, including their dimensions, and the manufacturer of the targets must be provided. Information about materials, approximate thicknesses or dimensions resulting from technological constraints in target manufacturing may help in assessing debris generation risks. A detailed study of target debris generation will be undertaken later during the experimental process.

The CEA/CESTA Target Laboratory is in charge of the alignment of the targets at target center chamber (TCC).

5. Preliminary nuclear safety analysis

In order to later fulfill the CEA LMJ nuclear safety rules, the following information are required:

- A rough estimate of the X-ray and/or neutrons and/or electrons and/or ions emitted spectra, with their angular distribution;
- The list of all the constitutive target materials with estimated mass.

6. Preparation requirements

The list of the experimental capabilities which need to be commissioned prior to the physics experiment is requested: specific ns shaped

pulse, PW laser contrast, characterization of specific hard X-ray or proton backlighting sources, etc.

7. Shots logic and draft failure modes

The order of the shots (6 shots per campaign at maximum) is required, as well as the logic of

the shots and the main possible failure modes (and backup plan).

Final selection of the most pertinent experiments is done by the ISAC in accordance with CEA-DAM.

III.5- Experimental Process

Once the experiments have been selected, the experimental campaigns are included in the schedule of the facility by the CEA-DAM Programming Committee. The selected groups are informed of this planning approximately 2 years in advance of the experimental campaign. At the same time, Experiment Managers from CEA (MOE, see III.7) are appointed in order to prepare the experiment in close collaboration with the selected groups.

The key milestones in the PETAL-LMJ experimental process will include several reviews in order to evaluate the experimental preparations and readiness. During this process the MOE is the point of contact between the research group and the CEA in order to coordinate all activities and optimize experiment preparation within the global planning of all experiments.

- The **Launch Review** is conducted approximately 24 months in advance of the experimental campaign. The selected group, assisted by the MOE, presents the experiment proposal in front of CEA-DAM experts. The primary purpose of this review is to ensure the proposed experiment meets the LMJ-PETAL requirements and to identify additional studies. CEA-DAM will analyze the proposal in terms of confidentiality rules, security rules and feasibility. At this point CEA-DAM could ask the research group to amend their proposal if it does not match the rules or if a feasibility issue is identified.

Following the Launch Review, a detailed report will be provided approximately 18 months in advance of the experimental campaign. This report, written by the MOE and the PI, will complete the proposal with feasibility studies,

simulation results (including X-ray and particles emissions), detailed target description, etc.

- A **Follow-up Review** occurs approximately 6 months later. The selected group exposes the advances of the experimental preparations and results of identified extra studies. This review is based on the abovementioned detailed report. Depending on the progresses made, other Follow-up Reviews may be scheduled.
- The **Design Review** is conducted approximately 12 months in advance of the experimental campaign. In addition to the previous specified data (laser and diagnostic configurations, target description, shots logic ...), this review provides all information required by the facility: consideration of target debris, nuclear safety analysis, diagnostics predictions, etc. This Review also updates the agenda of deliveries (e.g. targets).
- The **Readiness Review** occurs approximately 1 month prior to the date of the experiment. It is the final check to ensure that all preparations for execution of the experiment are complete.
- Approximately 6 months after the end of the campaign when the first scientific outputs are available an **Evaluation Review** is expected either under the form of a formal review or of short report. This review must address briefly the following subjects :
 - Feed back on the execution of the campaign,
 - Assessment of obtained results with respect to goals,
 - Main results obtained,
 - Scientific output : presentations at conferences, papers planed or in progress.

III.6- Responsibilities during Shot Cycle

Several people will be in charge of the management of the experiment, each of them having a specific responsibility.

The Principal Investigator (PI) is in charge of the scientific design of the experiment.

The practical design of the experimental project, taking into account the facility capabilities and the

expected results (laser energy, pulse shape, laser beams, diagnostics, alignment, debris from target, etc.) comes under the responsibility of the CEA Experiment Manager (MOE); he/she will work in close collaboration with the PI.

The execution of the experimental campaign is under the responsibility of the CEA Experiment

Coordinator (RCE); he/she is in charge of the target and laser bay functioning and performance, taking into account all inherent risks for the operation crew and material.

The laser shots during the campaign are under the responsibility of the LMJ Shot Director who is responsible for the LMJ safety.

III.7- Access to LMJ-PETAL during Shots

Access to the LMJ-PETAL facility requires half-day training to LMJ security rules and general information. This course is usually given on Monday.

To ensure personnel and equipment safety, it is mandatory that the LMJ Control Room remains a quiet area during shot operations. Shot preparation is a long process and will take a few hours which include some phases not relevant for physicists. A dedicated meeting room will be available close to

The PI will not be in direct contact with the LMJ Shot Director. Decisions related to the effective performance of the experimental campaign are taken according to the PI's wishes; however communications with the Facility and LMJ Shot Director are the sole responsibility of the MOE and RCE.

the LMJ Control Room for the PI for the final shot phase when his presence is necessary.

To limit administrative duties and escort procedures, the number of external users allowed to follow one shot is limited to 4 people maximum, typically the PI, co-PI (if any), one or two PhD or post-doc student. Those people could rotate during the week or the experimental campaign (providing the access procedures have been followed).



Figure III.4: View of the LMJ Control Room.

III.8- Data Access

The laser pulse shapes and raw laser energy are immediately observable after the shot, like X-ray images acquired on X-ray framing camera or streaked camera when they are directly recorded on electronic devices (CCD). The consolidated laser energy will be communicated at the end of the experimental campaign because it requires evaluation of the vacuum window transmission which could have been modified by laser-induced damages. For data requiring digitizing or scan (like Image Plate) communication will not be possible immediately after the shot, but a few hours later. It is also the case for data depending on material handling inside target bay area, which is regulated by safety procedures for contamination control and radiation monitoring.

Raw experimental data and/or data translated into physics units will be accessible to the PI and the experimental team as soon as possible after the shot. The data release is of CEA responsibility. The release of detailed response functions of some diagnostics, like for example the detailed response functions of DMX-LMJ channels, may be considered as classified information. This is why only consolidated data in physics units will be delivered to the PI in such a case. By any way the CEA Experiment Manager will ensure that all essential physics data are delivered to the PI. He/she is responsible for the quality of the experimental data.

Data support will be either USB key for the data directly available after the shot or CD-ROM for

consolidated and scanned data. The baseline data format of LMJ data is a custom hdf5. CEA will

provide hdf5 structure description and if necessary basic tools to extract the information.

III.9- Publications and Authorship Practices

Results of LMJ-PETAL experiments are expected to be published in major journals and presented in scientific conferences. The PI should inform CEA-DAM of any publication a few weeks before any major conference (APS DPP, IFSA, EPS, ECLIM, ICHED, HEDLA, HTPD, etc.) using the email address userLMJ@cea.fr. It is of PI responsibility to judge who made a significant contribution (or only a minor) to the research study. However CEA Experiment Manager (MOE) and CEA Experiment Coordinator (RCE), as well as CEA Diagnostics leaders, should be co-authors of the first publications of the campaign they have been involved in. The following statement acknowledging the use of LMJ-PETAL should be included in all publications :

“The PETAL laser was designed and constructed by CEA under the financial auspices of the Conseil Regional d’Aquitaine, the French Ministry of Research, and the European Union.

The [CRACC / SESAME / SEPAGE / SPECTIX] diagnostics were designed and commissioned on the LMJ-PETAL facility as a result of the PETAL+ project coordinated by University of Bordeaux and funded by the French Agence Nationale de la Recherche under grant ANR-10-EQPX-42-01.

The LMJ-PETAL experiment presented in this article was supported by Association Lasers et Plasmas and by CEA.”

The sources of financial support for the project (ANR, ALP, ERC, etc.) should also be disclosed.

III.10- Calls for Proposals History

The first call for proposals was launched in September 2014: 16 proposals have been received. In November 2014 the ISAC has preselected 8 proposals, and in May 2015, after the selected groups have provided their full proposals, the ISAC has selected 4 proposals which have been approved by CEA-DAM and included in the schedule of the facility.

The first shots were achieved in December 2017 and the other experiments were performed in 2019-2021

The second call for proposals was launched in April 2016. 9 proposals were received in June 2016. The ISAC pre-selected 6 proposals in September 2016. The full proposals were received on January 2017 and the final selection in March 2017 retained 3 proposals.

Most shots of this second call have been performed in 2022-2023.

The third call for proposals was launched in October 2020. 14 proposals were received in December 2020. The ISAC pre-selected 7 proposals in February 2021. The full proposals were received on July 2021 and the final selection in September 2021 retained 4 proposals

Third call experiments were partly carried out in 2023-2024.

Experiments in the second and third call, relying on x-ray diffractometer, had to be postponed as they revealed to induce risks of damage to the facility, due to potential diffractometer debris.

First call for proposals		
Title of the proposal	Principal Investigators	Home institution
Amplification of magnetic fields in radiative plasmas. [48]	Prof. Gianluca Gregori	Department of Physics, University of Oxford, UK
Study of the interplay between magnetic field and heat transport in ICF conditions, en route to the study of magnetic reconnection.	Dr. Roch Smets	LPP, Ecole Polytechnique, Palaiseau, France
Strong Shock generation by laser plasma interaction in presence or not of laser smoothing (SSD) in the context of shock ignition studies. [49]	Dr. Sophie Baton and Dr. Arnaud Colaitis	LULI, Ecole Polytechnique, Palaiseau, France CELIA, Talence, France
Interacting radiative shock: an opportunity to study astrophysical objects in the laboratory.	Dr. Michel Koenig	LULI, Ecole polytechnique, France

Second call for proposals		
Title of the proposal	Principal Investigators	Home institution
Ramp compression of iron in the TPa regime: a way to investigate super-earths' interiors.	Dr. Erik Brambrink	XFEL, Schenefeld, Germany
Hydrodynamics of laser-produced high-energy-density plasma (HEDP) under kilotesla field to open a new frontier in HEDP physics.	Prof. Shinsuke Fujioka and Dr. Philippe Nicolaï	ILE, Osaka, Japan CELIA, Talence, France
Betatron x-ray radiation in the self-modulated laser wakefield acceleration regime at PETAL.	Dr. Félicie Albert	LLNL, Livermore, USA

Third call for proposals		
Title of the proposal	Principal Investigators	Home institution
FeO at Super-Earth interior conditions for planetary models	Dr. Marion Harmand	IMPMC, Paris, France
Mechanisms and impact of stimulated Raman scattering on hot electron production in ignition-scale plasmas	Dr. Jason Frank Myatt	University of Alberta, Canada
Evaluation and enhancement of proton and neutron sources produced by PETAL	Dr. Julien Fuchs	LULI, Ecole Polytechnique, Palaiseau, France
Driving extreme magnetizations in compressed HED plasmas	Dr. João Jorge Santos	CELIA, Talence, France

Table III.1: List of selected proposals.

The next call is launched in September 2024 for experiments planned in 2027-2029.

IV- LMJ Building Description

The LMJ building covers a total area of 40 000 m² (300 m long x 100 to 150 m wide). It includes four similar laser bays, 128 meters long, situated in pairs on each side of the central target bay. The target bay is a cylinder of 60-meters diameter and 38-meters height, with a 2-meters thick concrete wall for biological protection.

At the center of the target bay, the target chamber consists of a 10-meters diameter aluminum sphere,

fitted with two hundred ports for the injection of the laser beams and the location of diagnostics and target holders. The four lasers bays, completed by the end of 2013, are now equipped with all the infrastructures for optics supports; the final optical components are currently being installed.

The PETAL laser beam takes the place of one classical LMJ bundle inside the South-East laser Bay.

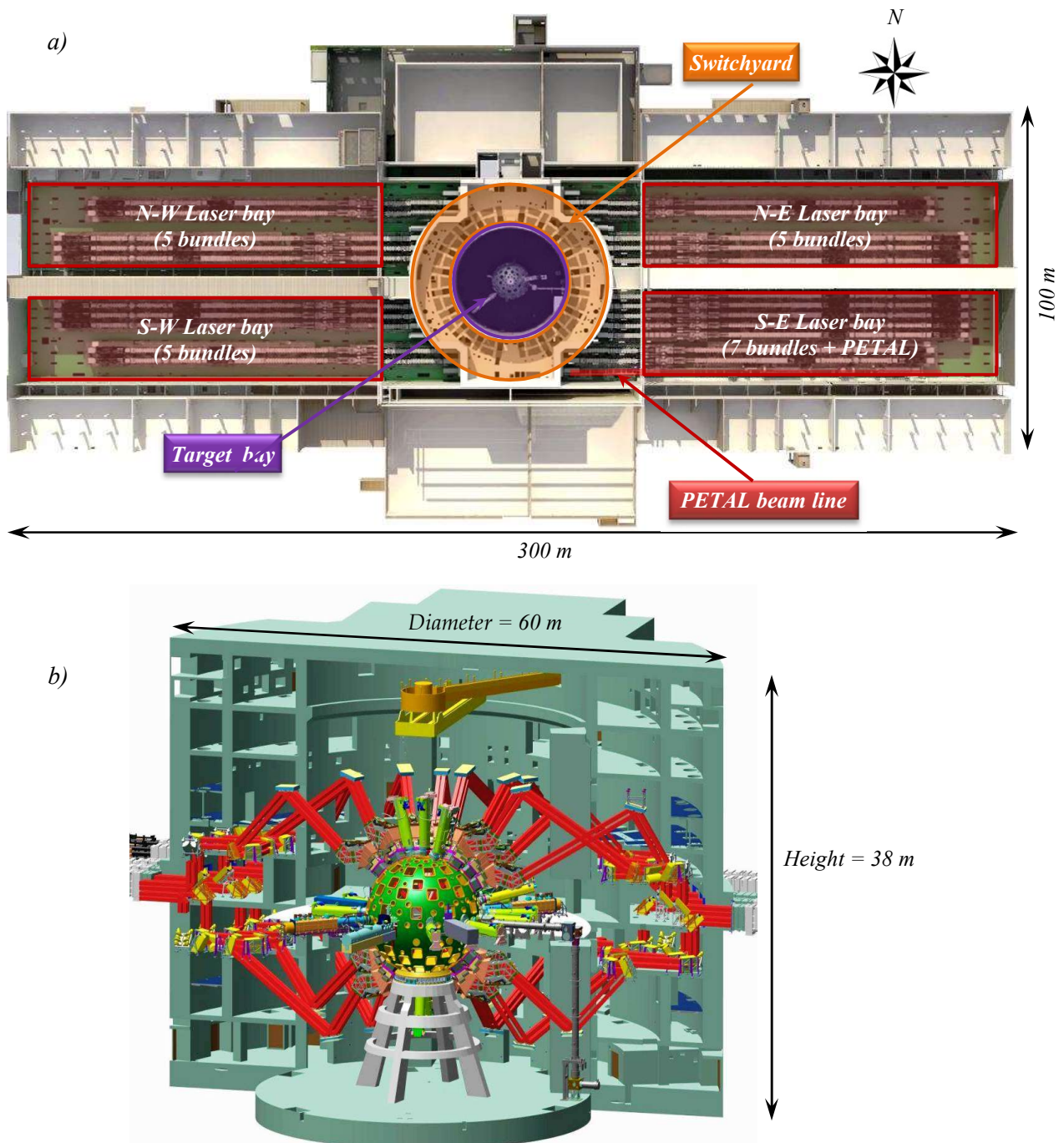


Figure IV.1: a) Drawing of the building with total dimensions b) CAD of the target bay with transport of the beams, the experimental chamber and its equipment: target positioning system, plasma diagnostics.

V- LMJ Laser System

V.1- Laser Architecture

LMJ is a flashlamp-pumped neodymium-doped glass laser (1.053 μm wavelength) configured in a multi-pass power amplifier system. The LMJ's 3100 glass laser slabs will be capable of delivering more than 3 MJ of 1.053 μm light, which is subsequently frequency converted to the third harmonic (0.351 μm) and focused on a target at the center of target chamber. LMJ will deliver shaped pulses from 0.7 to 25 ns with a maximum energy of 1.3 MJ and a maximum power of 400 TW of UV light on target.

The architecture of one beamline is shown in Figure V.1. The front end delivers the initial light pulse and provides its temporal and spatial shape as well as its spectrum and enables synchronization of all the beams. The front end is made of four sources (one per laser hall), which deliver the first photons (about 1 nJ), and 88 Pre-amplifier Modules (PAM, 1 per 2 beams), including a regenerative cavity and an amplifier, which deliver a 500-mJ energy beam to the amplification section.

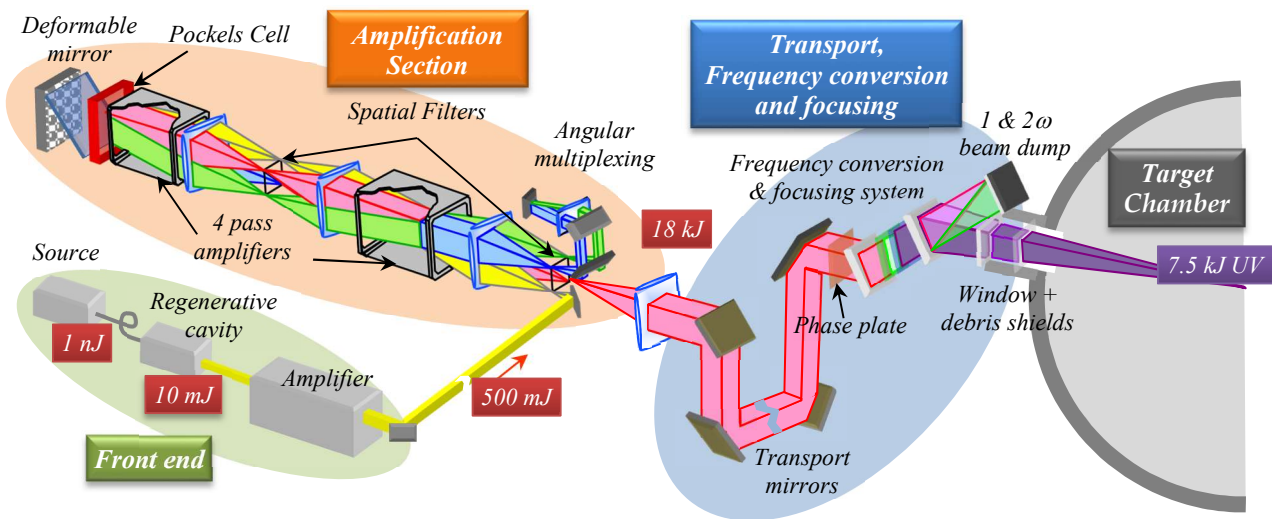


Figure V.1: Architecture of one LMJ beamline.
The basic unit for experiment is a quad made of 4 identical beamlines.

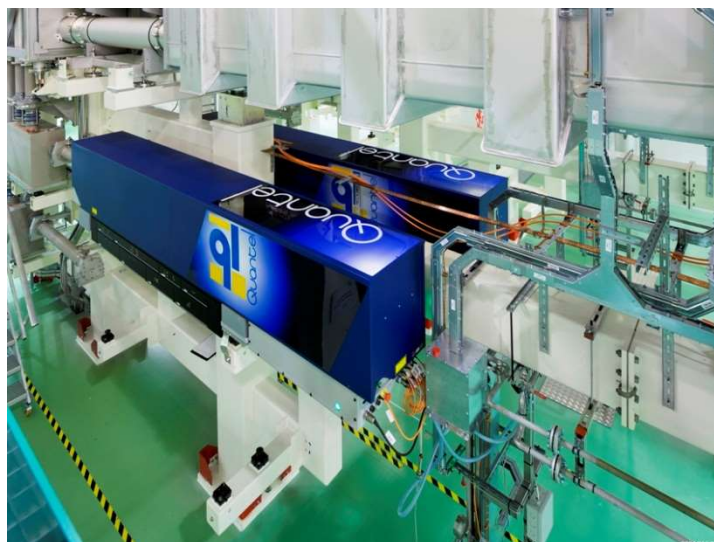


Figure V.2: PreAmplifier Module in the North-East Laser Bay.



Figure V.3: South-West Laser Bay equipped with 5 amplification sections.

In the amplification section, the beams are grouped in bundle of 8 beams and they are amplified 30 000 times to reach energy of 15-18 kJ per beam. The amplification section includes two 4-pass amplifiers, two spatial filters, a plasma electrode

Pockels cell, a polarizer and a deformable mirror for wavefront correction.

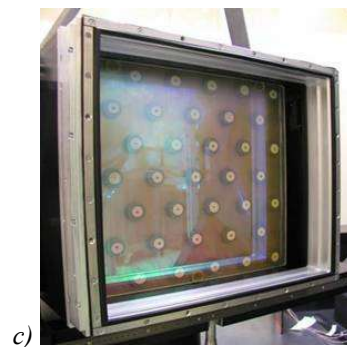


Figure V.4: a) Mounting of 4 laser slabs, b) plasma electrode Pockels cell, and c) deformable mirror.

In the switchyards, each individual bundle is divided into two quads of 4 beams, which are directed to the upper and lower hemispheres of the chamber by the mean of 5, 6 or 7 transport mirrors. The quad is the basic independent unit for experiments.

Both quads of the same bundle cannot deliver very different energies. The ratio of delivered energies cannot be greater than 2.3.

The LMJ target chamber is arranged with a vertical axis. LMJ is configured to operate usually in the “indirect drive” scheme [45], which directs the laser beams into cones in the upper and lower hemispheres of the target chamber. Forty quads

enter the target chamber through ports that are located on two cones at 33.2° and 49° polar angles. There are 10 quads per cone on each hemisphere. Four other quads enter the target chamber at 59.5° polar angle, and will be dedicated to X-ray backlighting purpose (see Figure V.5).

The PETAL beam enters the experimental chamber in the equatorial plane.

A detailed configuration of irradiation geometry is given in Figure V.6 and the spherical coordinates of all beam ports are given in Table V.1.

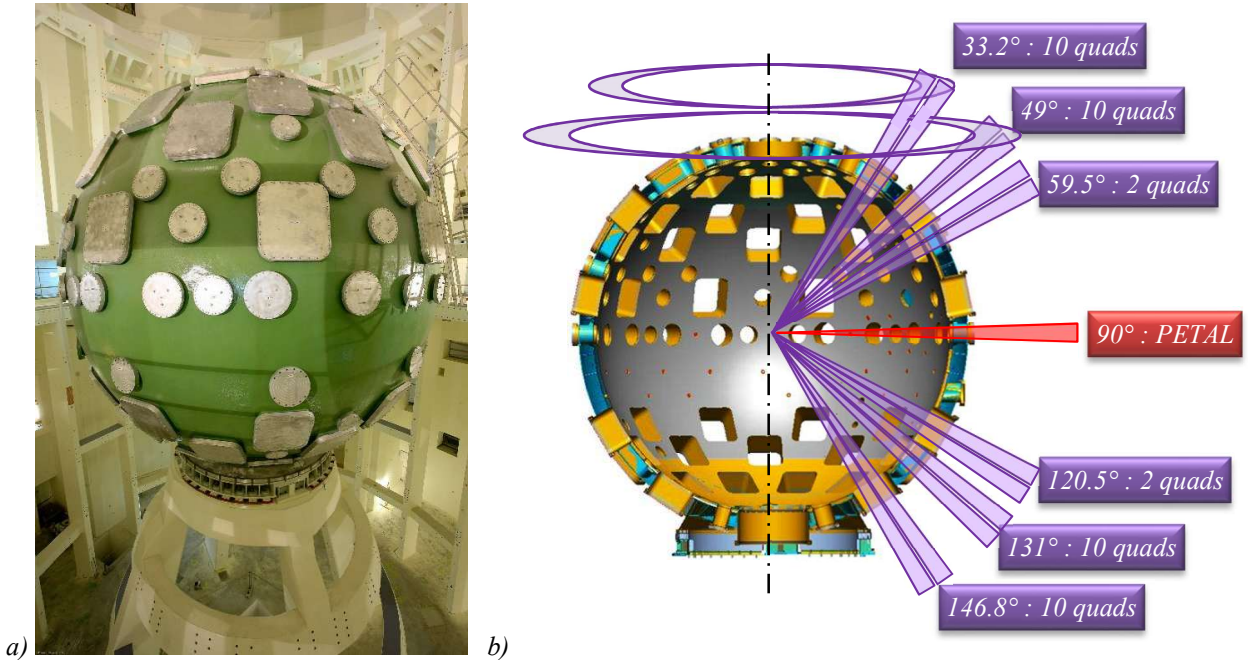


Figure V.5: a) Target chamber and b) geometry of the LMJ irradiation.

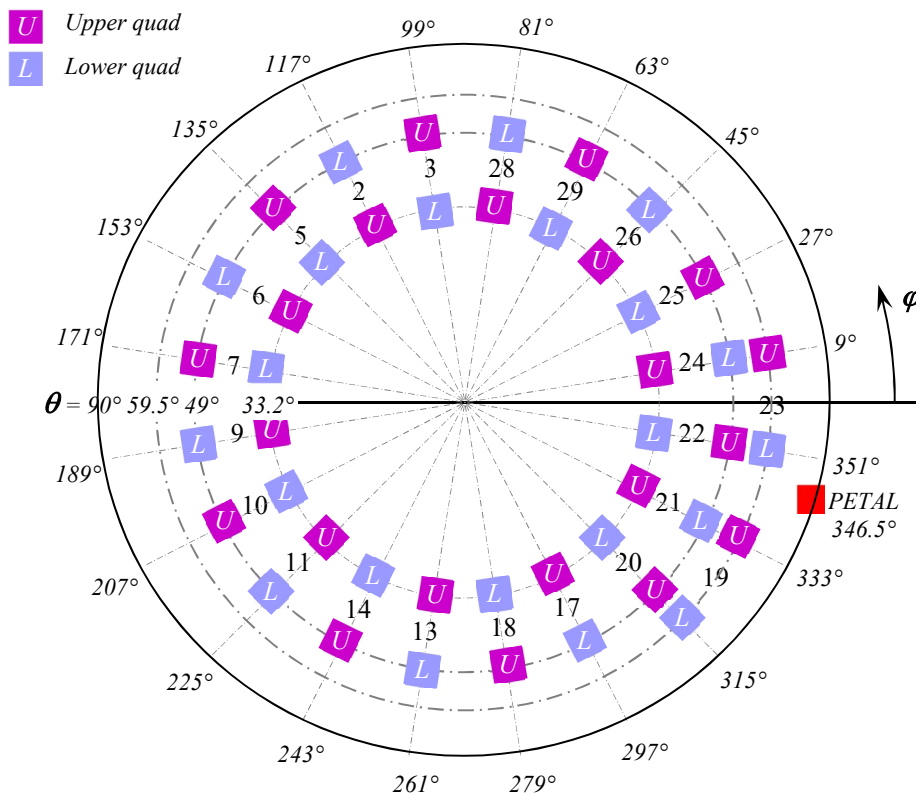


Figure V.6: Irradiation geometry of LMJ quads and PETAL beam.

Beam Port	θ	ϕ	Beam Port	θ	ϕ	Beam Port	θ	ϕ	Beam Port	θ	ϕ
44 Quads operative in 2027 and PETAL											
28U	33.2°	81°	28L	131°	81°	29U	49°	63°	29L	146.8°	63°
17U	33.2°	297°	17L	131°	297°	18U	49°	279°	18L	146.8°	279°
10U	49°	207°	10L	146.8°	207°	11U	33.2°	225°	11L	131°	225°
5U	49°	135°	5L	146.8°	135°	6U	33.2°	153°	6L	131°	153°
22U	49°	351°	22L	146.8°	351°	24U	33.2°	9°	24L	131°	9°
23U	59.5°	9°	23L	120.5°	351°	PETAL	90°	346.5°			
2U	33.2°	117°	2L	131°	117°	13U	33.2°	261°	13L	131°	261°
21U	33.2°	333°	21L	131°	333°	26U	33.2°	45°	26L	131°	45°
9U	33.2°	189°	9L	131°	189°	19U	59.5°	333°	19L	120.5°	315°
7U	49°	171°	7L	146.8°	171°	25U	49°	27°	25L	146.8°	27°
20U	49°	315°	20L	146.8°	315°	14U	49°	243°	14L	146.8°	243°
3U	49°	99°	3L	146.8°	99°						

Table V.1: Spherical coordinates of beam ports.

V.2- LMJ Frequency Conversion and Focusing Scheme

The optics assembly for frequency conversion and focusing is composed of a 1ω grating, two KDP and DKDP crystals for Second and Third Harmonic Generation, and a 3ω focusing grating. The 1ω grating deflects by an angle of 50° the incoming 1ω beam. An angular dispersion of the spectrum is introduced by the grating which allows broadband frequency tripling. The frequency converters use a Type I - Type II third harmonic generation scheme. The 3ω grating deflects back the 3ω beam by an angle of 50° , while the unconverted light is stopped by absorbers. No unconverted light enters the target chamber. As a consequence no volume restrictions and additional shielding around the target for unconverted light issues have to be taken into account in the design of the experiments.

The current available pointing volume is defined by a cubic shape (size 42 mm, see Figure V.8). The quad pointing accuracy in this volume is better than $100 \mu\text{m rms}$ ($75 \mu\text{m}$ in the reduced 30 mm diameter spherical volume). From the operational point of view, the number of different aim points has an impact on the alignment process duration. To reduce this impact, it is recommended to use the micro-offset strategy when some quads aim points are located in a sphere of less than 2 mm diameter. In this case each sphere can be considered as a unique aim point.

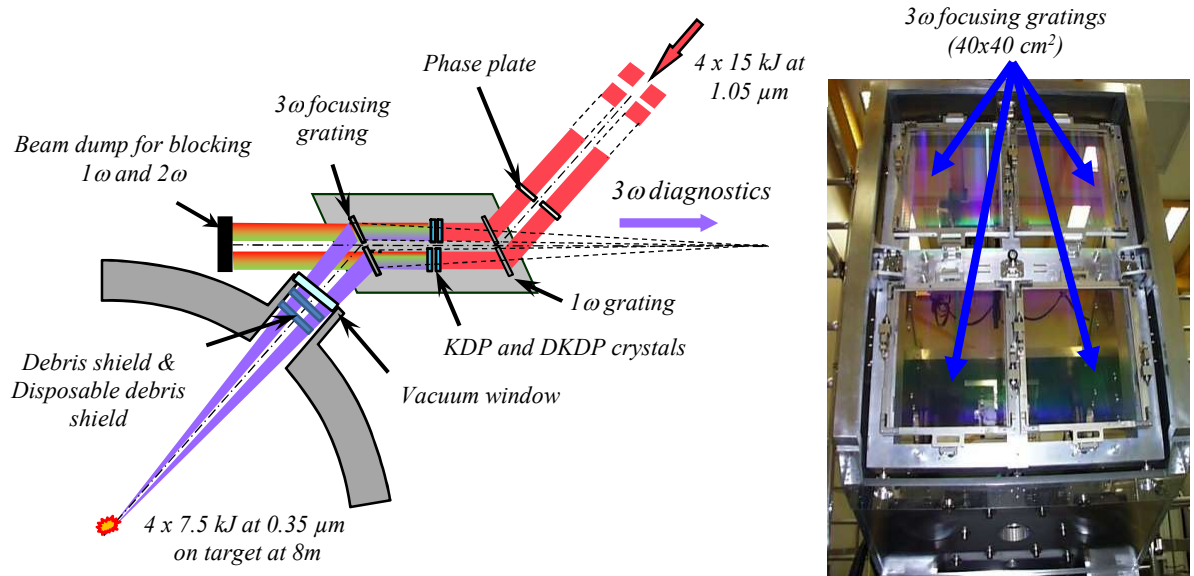


Figure V.7: LMJ frequency conversion and focusing by gratings.

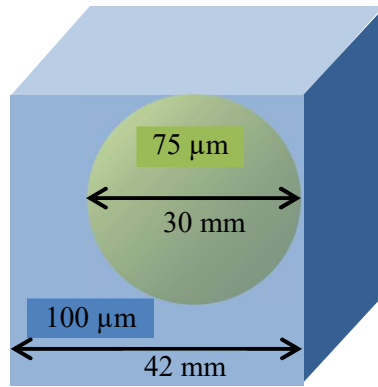


Figure V.8: Current LMJ pointing volume and expected pointing accuracy (rms).

V.3- Beam Smoothing

To reduce the peak intensity of the light on the target, several techniques are available on LMJ: continuous phase plate (see Section V.4) and smoothing by spectral dispersion.

Two phase modulations at 2 GHz and 14 GHz around the central wavelength are realized. The first one (2 GHz) is used to raise the threshold of appearance of the Brillouin effects in optics in the front-end and at the end of the laser chain. The second one (14 GHz) is dedicated to Smoothing by Spectral Dispersion (SSD). The full bandwidth

available with both frequency modulations is 0.5 nm at 1ω in order to reduce the contrast in the speckles of the focal spot on the target down to 20% [50].

Due to the specific LMJ focusing system, the movement of speckles in the focal spot is along the laser axis (longitudinal SSD) instead of being perpendicular to this axis (transverse SSD) as in standard laser facilities. Another smoothing technique, polarization smoothing, will be installed later for ignition experiments.

V.4- Spot Sizes

Various Continuous Phase Plates (CPP) can be considered for the focal spot sizes. Four types have been defined, two for circular focal spots, called CPP Type E, Type F and two for elliptical focal spots called Type A (for external quads) and Type B (for internal quads).

The nominal phase plate are Type A and B, they are used for heating hohlraums which are positioned along the chamber axis. The Type E provides a larger focal spot for uniform irradiation (direct drive

EOS experiments or large backlighter). The Type F provides a smaller focal for radiography purposes.

The available CPP for each quad are indicated in chapter IX.1.

The peak intensity on target for a 5 TW pulse, the diameters of focal spots at $1/e$ and 3 % of the peak intensity and the order of the super-Gaussian describing the intensity profile are given in the Table V.2 below.

CPP	Spot Geometry	Size at $1/e$ (μm)	Size at 3 % (μm)	Intensity (5 TW) (W/cm^2)	Super-Gaussian Order
Type A	Elliptical	Major axis: 870	Major axis: 1430	$1.7 \cdot 10^{15}$	3
		Minor axis: 450	Minor axis: 790		2.4
Type B	Elliptical	Major axis: 1215	Major axis: 1640	$1.1 \cdot 10^{15}$	4
		Minor axis: 775	Minor axis: 1060		2.8
Type E	Circular	Diameter: 980	Diameter: 1460	$7.0 \cdot 10^{14}$	3.7
Type F	Circular	Diameter: 375	Diameter: 680	$4.8 \cdot 10^{15}$	2.1

Table V.2: Characteristics of the Continuous Phase Plates.

V.5- Energy and Power

The available laser energy for user experiments is constrained by optical damages on KDP crystals [51], gratings and vacuum windows, and operating costs. Whereas LMJ nominal laser energy is designed for 30 kJ per quad for ignition experiments, the experiments for the next 5 years will be performed at limited laser energy to reduce the optical damages on final optics, and consequently the maintenance time.

Experimental with a point design up to 15 kJ per quad, for a 3 ns square pulse, are to be considered (the energy on target may be lower according to final optics transmission).

The maximum sustainable laser energy for a given pulse shape will be refined with feedbacks from laser scientists [52, 53] during the preliminary design review of an experiment. Operational limits will also depend on the exact pulse shape and the type of CPP. Figure V.9 gives the available performance as a function of pulse duration for square pulses.

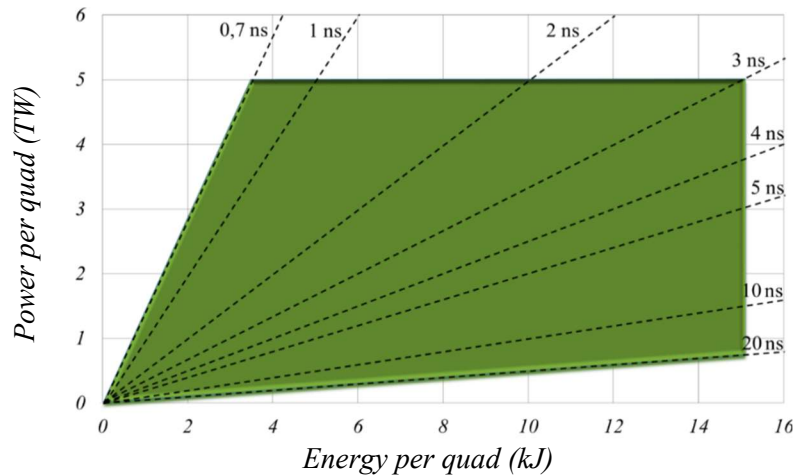


Figure V.9: Current LMJ energy and power available domain.

V.6- Pulse Shaping Capabilities

The LMJ source (master oscillator) is designed to deliver complex ignition pulses. As a consequence, a wide variety of pulse shapes can be produced on LMJ, with a minimum duration of 0.7 ns and a maximum duration up to 25 ns (limited to 20 ns in 2027-29). Complex pulse shapes (rising pulse, decreasing pulse, multiple pulse, with pedestal, etc.) can be tailored, but will require some

test laser shots for fine tuning [53]. Some examples of pulse shapes are given in figure V.10 and V.11.

The LMJ beams have been currently synchronized at the center of the target chamber with a standard deviation of 80 ps, and will be synchronized with a standard deviation of 40 ps later with all the 176 beams.

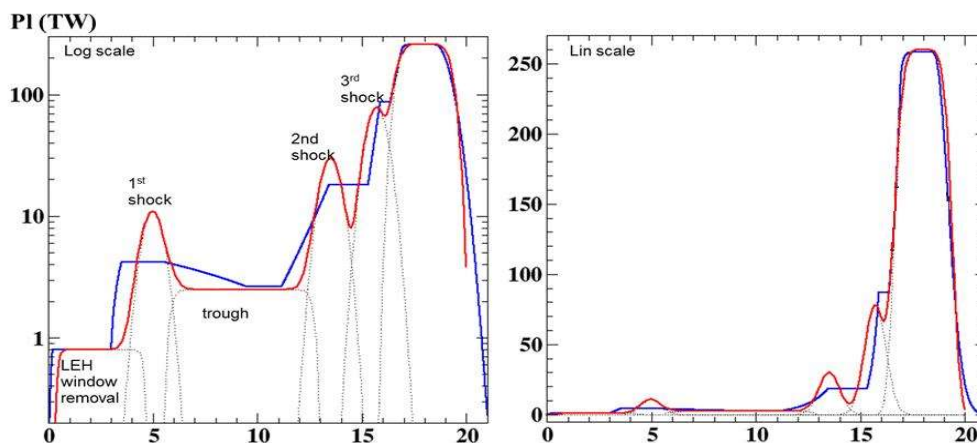


Figure V.10: Different envisioned pulses shapes for ignition target (in red and blue). The dashed black lines are supergaussian used to fit each specific part of the pulse.

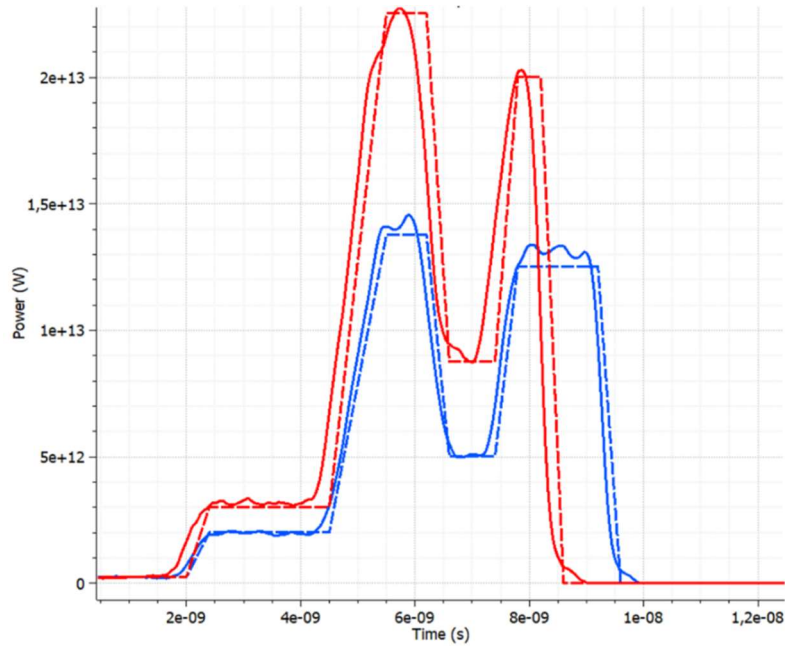


Figure V.11: Typical pulse shape realized on the LMJ facility (request in dashed line).

On LMJ, the Pre-Amplifier Module (PAM) is common to two beams within one quadruplet. However as the two PAMs of a single quadruplet share the same master oscillator (see Figure V.12), only one pulse shape is available per quadruplet. This versatility in pulse shaping will be beneficial

for Polar Direct Drive Shock Ignition [54]. Delays between quadruplets could be defined for example to use one quadruplet as the main driver and one quadruplet to irradiate an X-ray backlighter. The maximum available delays are currently limited to 70 ns.

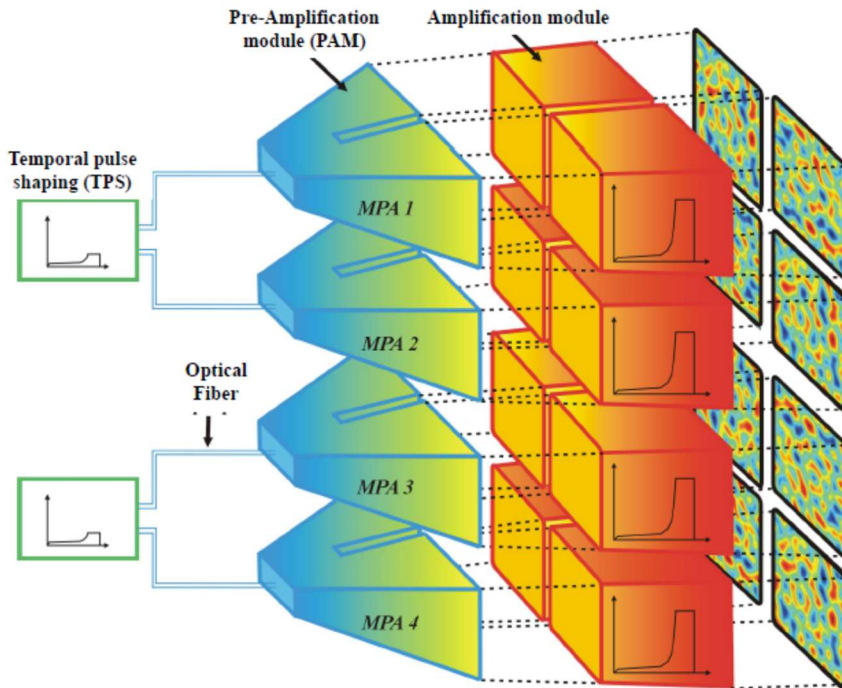


Figure V.12: Schematic of the pulse shaping capability within a LMJ bundle (2 quads, 8 beams)

V.7- LMJ Performance

The first LMJ experiments were carried out in October 2014, with the 8 initial beams (quads 28U and 28L). Until the end of 2023, about 330 laser shots on target have been performed, among them 200 were dedicated to plasma experiments and 65 to plasma diagnostics qualification. All revealed good performance of the whole system.

Figure V.13 shows the history of energy and power delivered per quad on target (from 2nd semester of 2017 to 1st semester of 2024).

In 2024, 100 shots on target have been delivered; the estimated mean pointing accuracy of the quads was better than $75\ \mu\text{m}$, and the quads synchronization was better than $50\ \text{ps}$ for 80 % of the shots. Almost 90 % of the shots delivered the required energy with less than 20 % discrepancy.

For all the experiments, the achieved pulse shapes present a good reproducibility. Figure V.14 shows some examples of pulse shape (radiography and heating pulse).

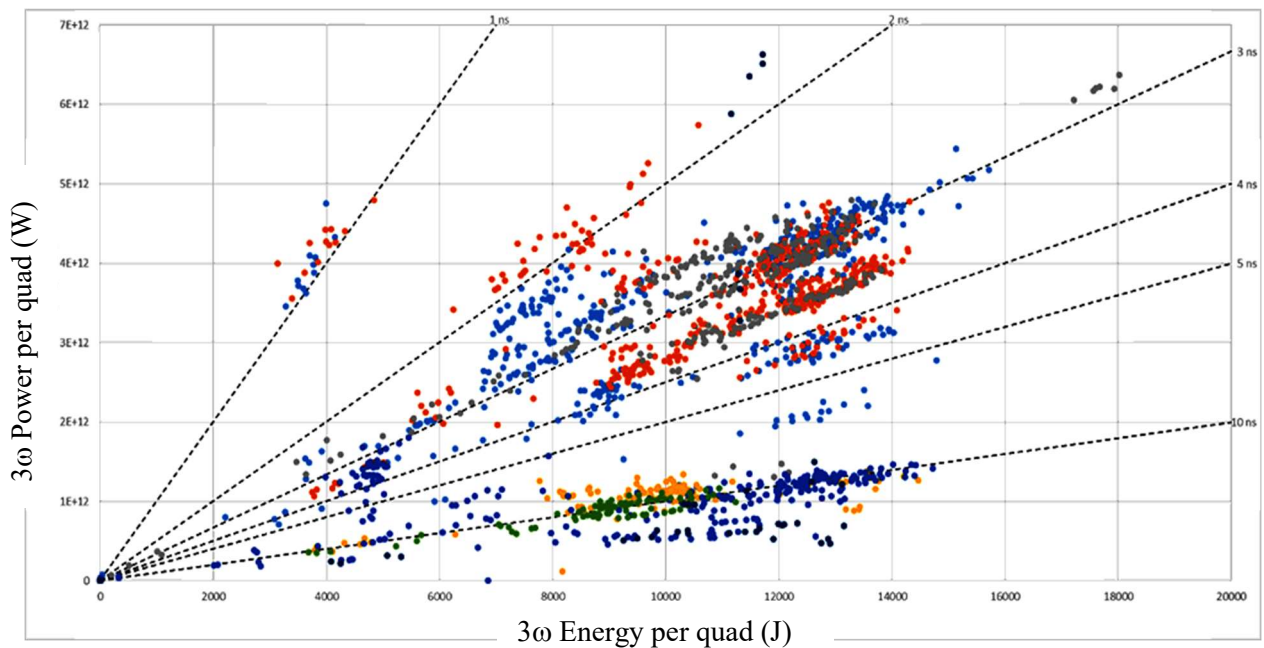


Figure V.13: Delivered pulse energy and power per quad on target (shots above 15 kJ and above 5 TW were used to test damage threshold of final optics, they are not available for experiments).

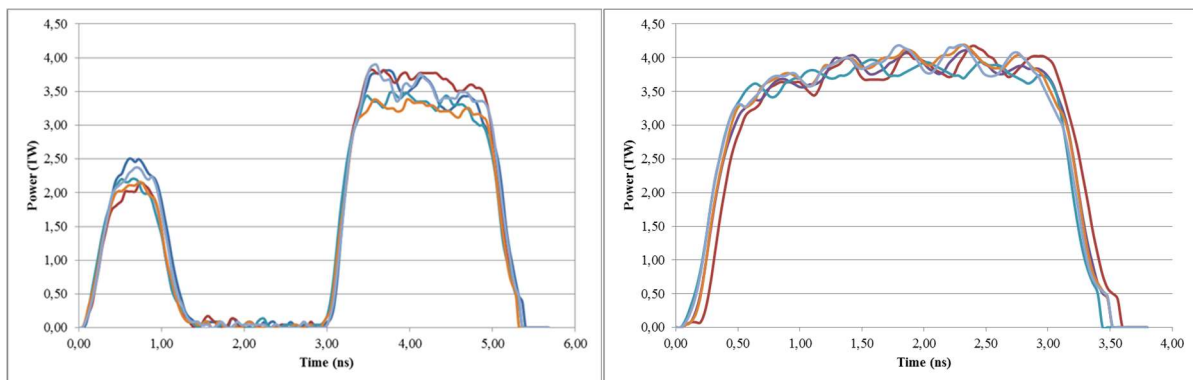


Figure V.14: Pulse shapes of physics campaign on LMJ (Left: radiography pulse, Right: heating pulse)

VI- PETAL

VI.1- Laser System

The PETAL design is based on the Chirped Pulse Amplification (CPA) technique combined with Optical Parametric Amplification (OPA) [55-58]. Moreover, it benefits from the laser developments made for the high-energy LMJ facility, allowing it to reach the kilojoules level.

Figure VI.1 shows the implementation of PETAL in the LMJ facility. The PETAL beamline occupies the place of a LMJ bundle in the South-East laser bay. The compressor stages are situated at the bottom level of the target bay, and after a transport under vacuum, the beam is focused in the equatorial plane of the LMJ chamber via an off-axis parabolic mirror.

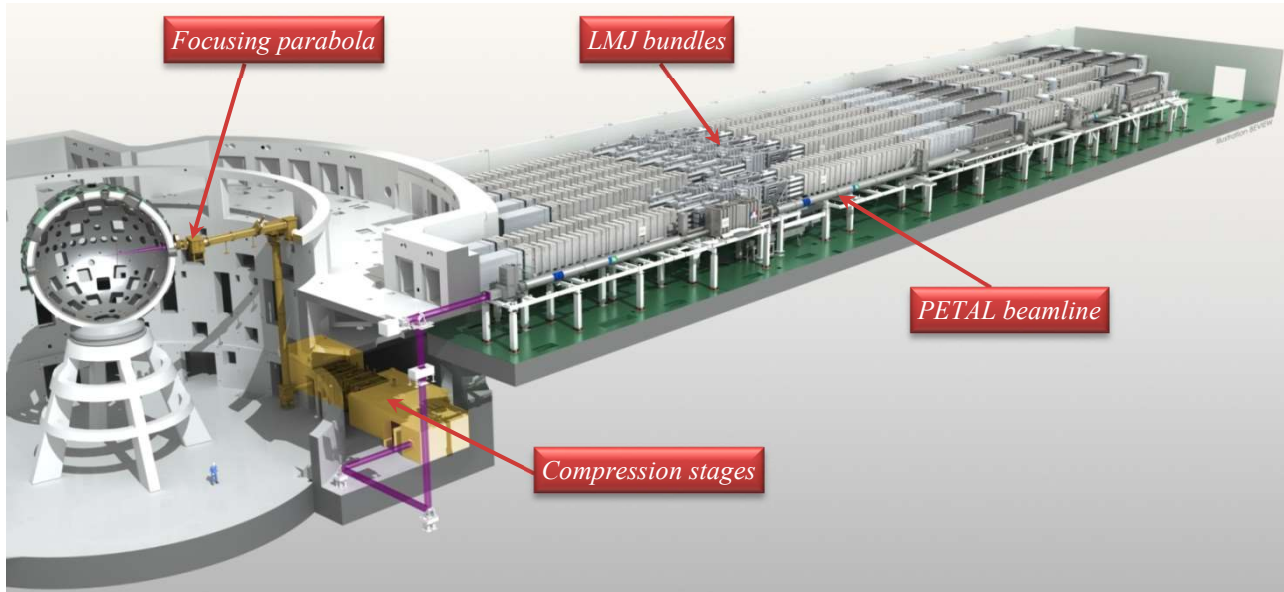


*Fig. VI.1: Implementation of PETAL in the LMJ facility.
The PETAL beam is focused in the equatorial plane of the target chamber*

The front end consists in a standard Ti:sapphire mode locked oscillator delivering 3 nJ /100 fs / 16 nm pulse at 77.76 MHz frequency and 1053 nm wavelength. The pulse is stretched to 9 ns in an Öffner stretcher in eight passes. Then the pulse is sent to the Pre-Amplifier Module (PAM) including OPA stages and pump laser. The OPA scheme consists of two cascaded LBO crystals and a BBO crystal. A 100 mJ amplified signal pulse with a shot-to-shot stability of less than 2 % has been demonstrated on the LIL facility [56, 57].

The PETAL amplifier section has the same architecture as the LIL/LMJ amplifier section using a single 37 × 35.6 cm² beam. It is a four-pass-system with angular multiplexing and a Reverser. It uses 16 amplifier laser slabs arranged in two sets and delivering up to 6 kJ. At this stage, due to gain narrowing, the bandwidth is reduced to 3 nm and duration to 1.7 ns. The main differences with the LIL/LMJ power chain are the wavefront and chromatism corrections [58].

The compression scheme is a two-stage system (see Figure VI.2). The first compressor, in air

atmosphere, reduces the pulse duration from 1.7 ns to 350 ps in an equivalent double pass configuration. The output mirror is segmented in order to divide the initial beam into 4 sub-apertures which are independently compressed and synchronized into the second compressor in a single pass configuration under vacuum [59]. These sub-apertures are coherently added using the segmented mirror with three interferometric displacements for each sub-aperture. The pulse duration is adjustable from 0.5 to 20 ps.

The focusing system consists in an off-axis parabolic mirror with a 90° deviation angle, followed by a pointing mirror (see Figure VI.3). The focal length is 7.8 meters, and the focal spot has a 50 μm diameter, this will result in intensities above 10²⁰ W/cm² on target. The polarization of the PETAL beam on target is linear vertical. Due to the 4 sub-apertures of the beam [60], a multi-beam option could be available: a segmented pointing mirror could redirect the beams towards up to 4 separate focuses. This option will be studied in detail if required.

The depointing is for the moment limited to few hundred of μm (exploration of the actual segmented mirror).

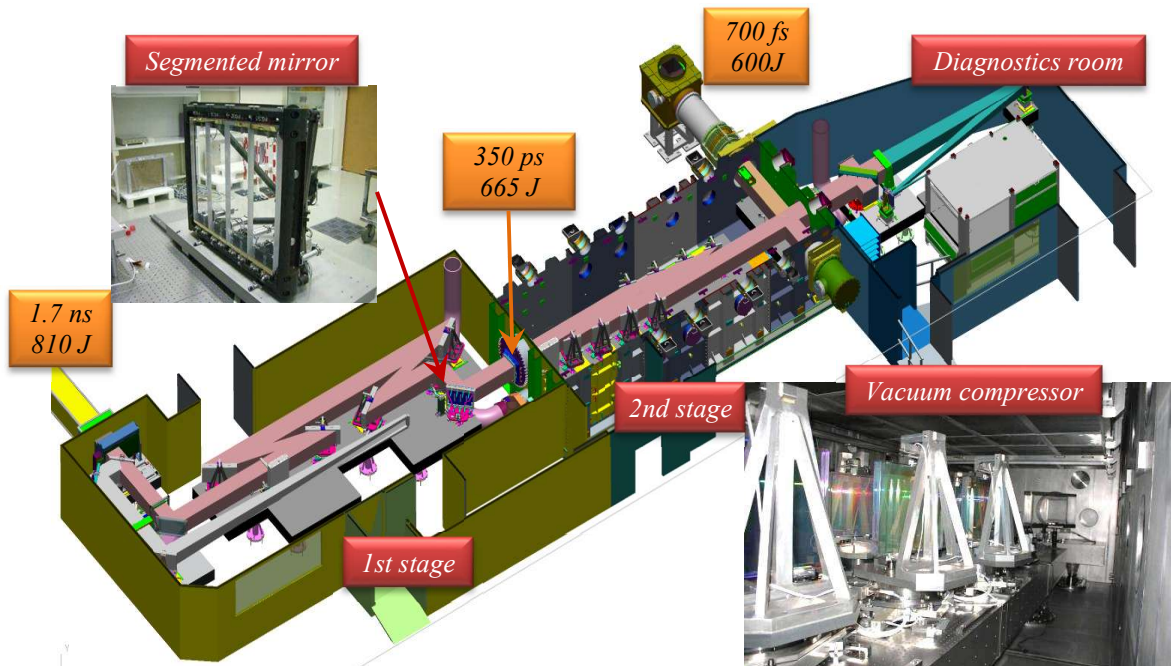


Figure VI.2: Compressor stages with a subaperture compression scheme: first stage in air atmosphere and second stage under vacuum with 4 independent compressors.

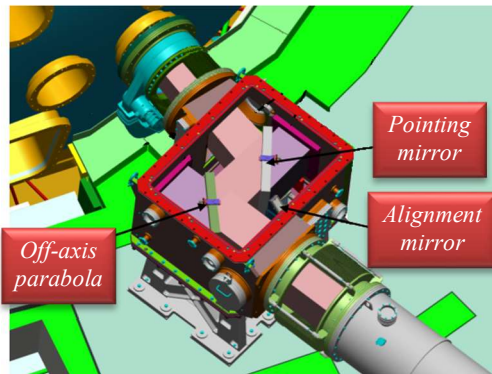


Figure VI.3: PETAL beam and LMJ bundles in the South-East laser bay, and PETAL focusing scheme.

The PETAL performance depends on the damage threshold of optics. Great efforts have been made on gratings in order to improve their strength. The effect of electric field on damages has been demonstrated [61], and the groove profile of PETAL multilayer dielectric gratings has been optimized in order to obtain a damage threshold above 4 J/cm^2 in the ps range. But in fact, the transport mirrors may

not sustain more than 2 J/cm^2 compared to the 4 J/cm^2 specified value required for a 3 kJ output level. **Therefore, the current mirrors will first limit the available energy on target at a $\sim 600 \text{ J}$ level.** New technologies are required to increase this value and the intensity on target. Several ways of improvement are identified and are being explored [62-64].

VI.2- PETAL Performance

The commissioning of PETAL with broadband spectrum pulses began in 2015. The amplification at 1.4 kJ energy of a stretched pulse (2 ns, 3.5 nm) in the amplification section was validated.

The Petawatt capability was demonstrated with several shots in 2015 with the diagnostics located just after the compressor. Several shots at 1.05 kJ energy and 1ps duration were obtained, and on May 29th 2015, PETAL delivered 846 J in 0.7 ps corresponding to a peak power of 1.2 PW [65]. PETAL became the most powerful laser beam in the world, in the high energy lasers category.

Then the PETAL beam was transported and focused into LMJ target chamber. Five PETAL laser shots were carried out in the target chamber on a calorimeter and achieved 635 J at 0.7 ps (0.9 PW) on December 2015. In parallel, the first associated LMJ and PETAL laser shot in the LMJ target chamber was performed.

In 2016, a more comprehensive characterization of the laser performances has been achieved. Thanks to the activation of spectral phase measurements, the pulse duration was improved down to 570 fs (with a 220 J energy shot) which corresponds to a potential

power of 1.8 PW for a full energy shot. The temporal contrast was also characterized ; on a long time scale (10 ns) the energy contrast (ratio between ps-pulse energy and pedestal energy) is 10^{-3} , measured by a silicium integrator, and on a short time scale (250 ps) the power contrast is around 10^{-6} , measured with a single shot 3rd order cross-correlator.

Later, an upgrade of the beam spatial profile was implemented in order to increase the energy on target. Some test shots with longer pulse duration (10 ps) have been successfully performed.

Finally, the focal spot has been characterized (see figure VI-5), leading to a 10^{19} W/cm² intensity.

In 2019 the mean pointing accuracy has been estimated at 42 μ m.

Note that the 4 independent compressors of the last stage can be adjusted to obtain a rectangular focal spot of $\sim 100 \times 25 \mu$ m² with a pulse of 3 ps.

PETAL is currently being upgraded to increase energy on target and temporal contrast, and to add the ability to split the beam into two independently focused beams in space and time.

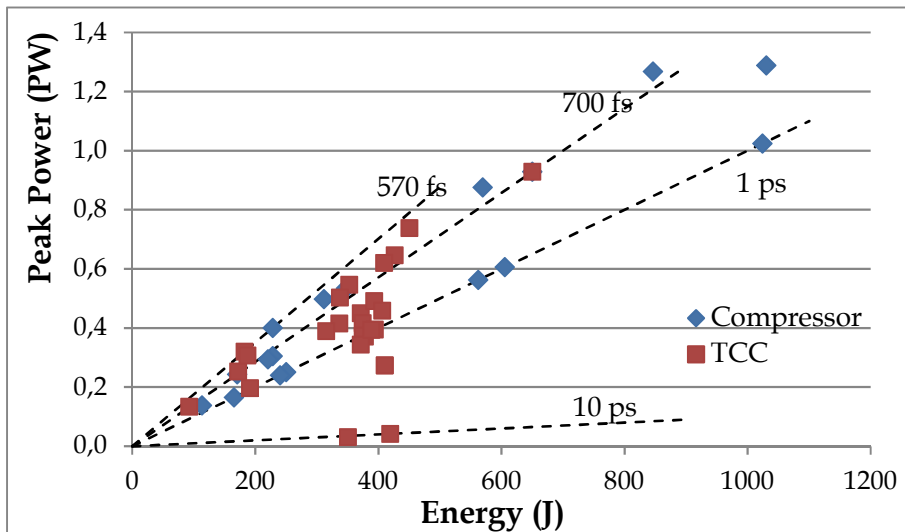


Figure VI-4: Delivered energy and power of PETAL shots, at the compressor end and target chamber center (TCC).

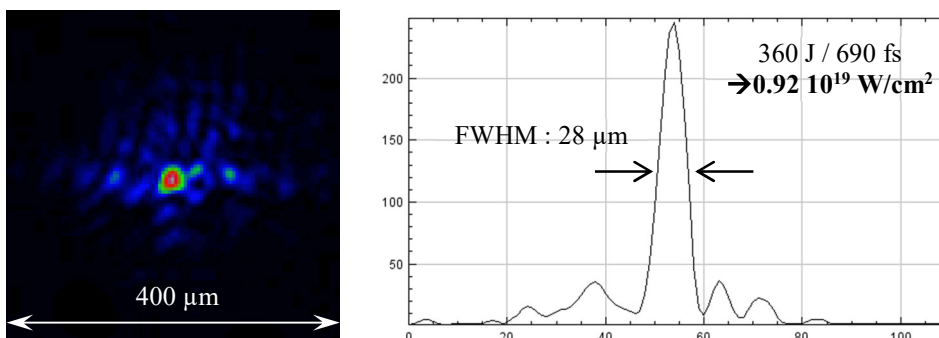


Figure VI-5: Example of delivered PETAL focal spot, and intensity inferred.

VII- Target Area and Associated Equipment

As shown previously in Figure IV.1, the target bay area occupies the central part of the building. There are 8 floors. A detailed CAD of the target chamber with the major target bay equipment is shown in Figure VII.1.

The radius of LMJ target chamber is 5 meters. Beam and diagnostic ports cover the full surface. Most part of the plasma diagnostics are positioned inside the target chamber with the help of a manipulator called SID (System for Insertion of Diagnostics). A SID is a two-stage telescopic system that provides a precise positioning of a diagnostic close to the center of target chamber. It positions 150-kg diagnostic with a 50- μm precision. SIDs are provided on several different port locations. Two kinds of SIDs are available: the polar SIDs can be positioned either on polar axis or in the equatorial plan, and use only electronic detectors; the equatorial SIDs cannot be positioned on polar axis, and can use either passive detectors, due to electromagnetic perturbations induced by PETAL shots, or electronic detectors.

6 SIDs are currently operational, and 1 more is expected by 2025.

Diagnostics are inserted in the SID with the help of a diagnostic transfer box (BTDP, see figure VII.5.b). This box is used to transfer diagnostics from and to the maintenance laboratory. All heavy devices connected to the target chamber (Diagnostics, SID, BTDP, TPS, etc.) are moved with the help of a dedicated means of transportation named intervention vehicle (see figure VII.5b).

The port locations of the target chamber equipment (Reference Holder (RH), Target Positioning System (TPS) and cryogenic TPS, SOPAC viewing stations) as well as the possible port locations for the different SID are listed in Table VII.1. Three Specific Mechanisms ports are also available, 2 of them (MS8 and MS9) being reserved for DMX Broadband time-resolved spectrometer.

The diagnostics manipulators locations are schematically drawn in Figure VII.3. Additional target chamber ports for fixed diagnostics exist and may be considered for future diagnostics developments.

Note that some piece of equipment, like the cryogenic TPS, are not yet available.



Figure VII.1: CAD of the final stage of target area.

Port	θ	ϕ	Remark
Target chamber equipment			
RH	90°	238.5°	Reference holder
TPS	90°	255.5°	Target Positioning System
Cryo TPS	90°	220.5°	Cryogenic TPS, unavailable
SOPAC	16°	9°	Target viewing station
SOPAC	24°	243°	Target viewing and lighting station
SOPAC	90°	13.5°	Target viewing station
SOPAC	90°	103.5°	Target viewing station
SOPAC	90°	193.5°	Target viewing station
SOPAC	90°	283.5°	Target viewing station
SOPAC	164°	9°	Target viewing and lighting station
SOPAC	164°	189°	Target viewing station
Diagnostics manipulators locations			
S1	16°	333°	Close to polar axis, dedicated to UPXI diagnostic
S2	164°	279°	Close to polar axis, dedicated to LPXI diagnostic
S3	16°	153°	Close to polar axis, not equipped
S5	90°	112.5°	
S7	164°	99°	Close to polar axis, laser injection and collection for EOS Pack
S12	90°	148.5°	
S16	90°	58.5°	
S17	0°	0°	Polar axis
S20	90°	292.5°	Optical system of EOS pack
S22	90°	328.5°	Opposite S12.
S26	90°	180°	
Specific mechanisms			
MS 8	24°	99°	DMX position 1 (current position)
MS 18	90°	222°	Reserved for activation diagnostic, unavailable
SESAME 1	90°	166.5°	SESAME diagnostic position 1
SESAME 2	90°	121.5°	SESAME diagnostic position 2

Table VII.1: Spherical coordinate of target chamber equipment and diagnostics manipulators. The unavailable locations for experiments in 2027-29 are indicated.



Figure VII.2 : Reference holder and Target positioning system.

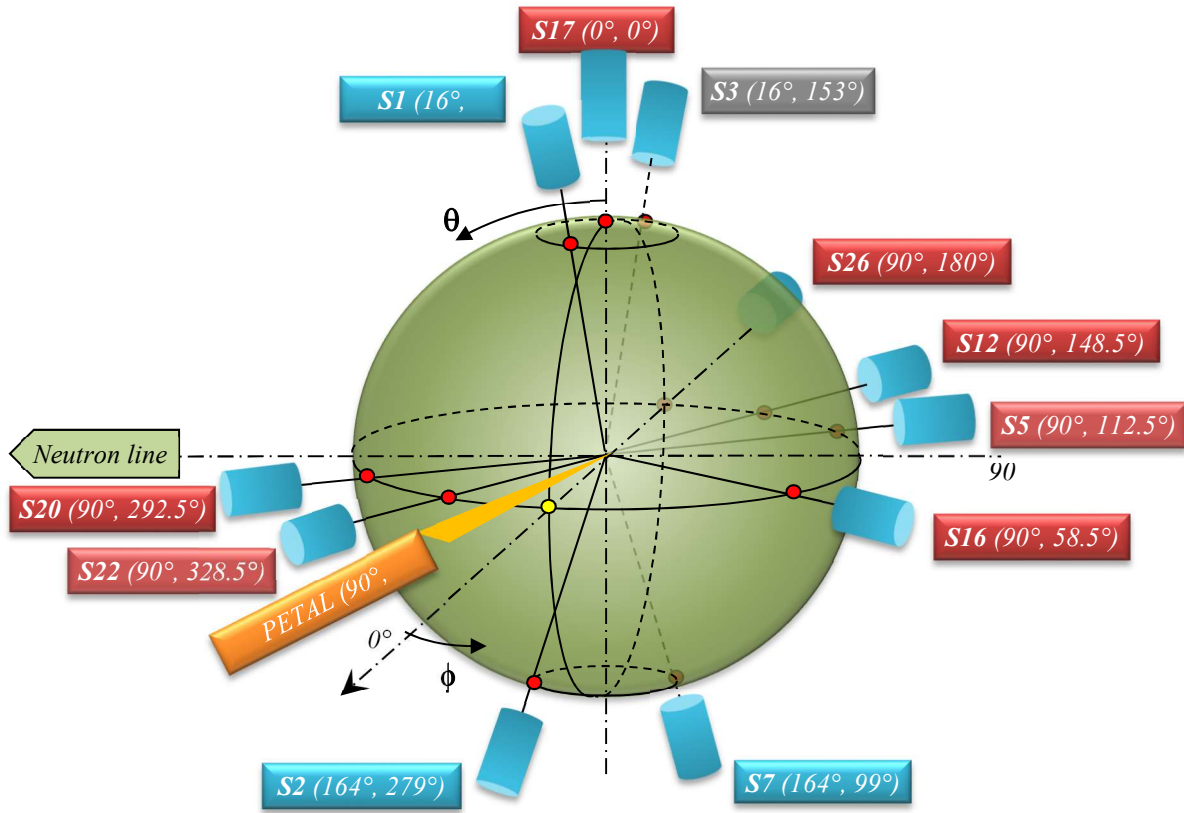


Figure VII.3:3D view of the SIDs location on the target chamber. S3 is unavailable in 2027-29

S1 and S2 are dedicated to Polar X-ray imagers; S7 is dedicated to laser injection and collection for EOS Pack.

All SID locations are not available for any campaign; only the SIDs listed in the available experimental platforms described further can be

used (see Chapter IX.3 Experimental platforms). Moving a SID to another location is not an open option.



Figure VII.4: View of the upper part of the target bay.

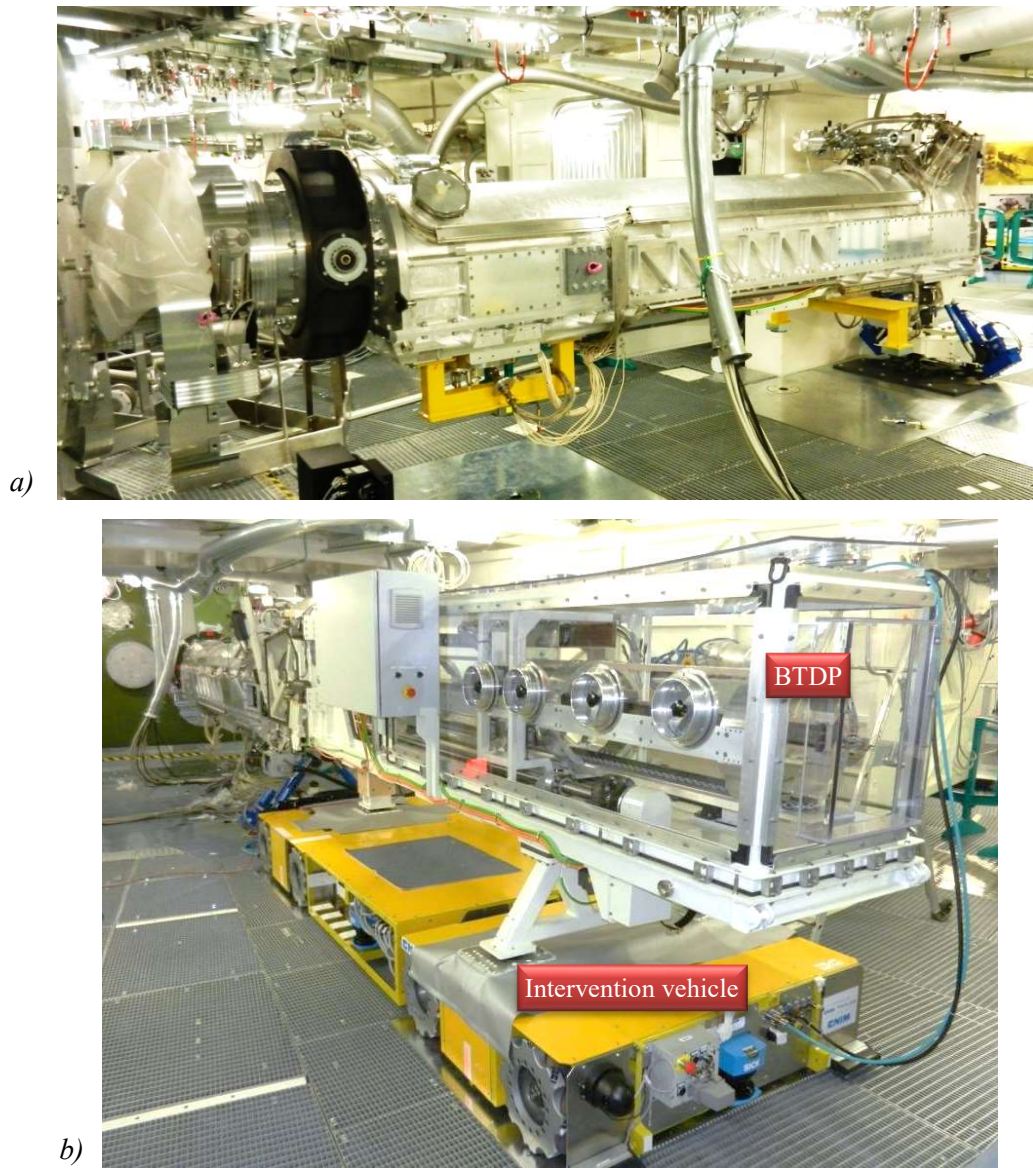


*Figure VII.5: a) Photographs of first LMJ SID
b) Diagnostic transfer box (BTDP) on intervention vehicle connected to the SID.*

VIII- LMJ Plasma Diagnostics

Over 30 diagnostics are considered on LMJ with high spatial, temporal and spectral resolution in the optical, X-ray, and nuclear domains. Development plan for LMJ diagnostics began with the LIL laser facility and relies on decades of expertise in the design, fabrication and commissioning of advanced plasma diagnostics. The OMEGA laser facility (Laboratory for Laser Energetics, University of Rochester, USA) has also been used and will continue to be the test bed for the development of CEA nuclear diagnostics. The early diagnostics, designed using the feedback of LIL's diagnostics, consist of:

- seven hard and soft X-ray imaging systems (30 eV to 15 keV range) with a 15 to 150 μm spatial resolution and a 30 to 120 ps time resolution, providing over 40 imaging channels,
- a diagnostic set for hohlraum temperature measurements including an absolutely calibrated broadband X-ray spectrometer (30 eV - 20 keV), a grating spectrometer, an imaging system of the emitting area,
- two absolutely calibrated SID insertable broadband X-ray spectrometer (30 eV - 7 keV),
- a time resolved high resolution X-ray spectrometer (0.8 - 15 keV) coupled to a framing camera,
- a time integrated hard X-ray spectrometer (7 - 150 keV),

- an optical diagnostic set dedicated to EOS measurements including 2 VISAR (Velocity Interferometer System for Any Reflector), 2 SBO (Shock Break Out), a pyrometer and a reflectivity measurement,

- two Full Aperture Backscatter Systems, and a Near Backscatter Imager to measure the power, spectrum, and angular distribution of backscattered light to determine the laser energy balance,
- two electron spectrometers (5 - 150 MeV),
- a charged particles spectrometer for electrons (0.1 - 150 MeV) and ions (0.1 - 200 MeV) including an imaging module for proton-radiography,
- a neutron pack, to measure neutron yield, ion temperature and neutron bang time along several lines of sight,
- two cassette holders for X-ray or proton radiography (stack of radiochromic films, and/or Image Plates and filters),
- two sample holders dedicated to X-ray induced shock waves or electromagnetic currents.

Companion Table-top laser facilities [66] or X-ray sources [67] are used to perform metrology of the X-ray diagnostics.

Diagnostics development takes into account the harsh environment [28, 68] which will be encountered on LMJ, as well as the electromagnetic perturbations induced by PETAL [69].

VIII.1- X-ray Imagers

The development of grazing-incidence X-ray microscopes is one of the skills of CEA diagnostics development laboratory. On LMJ, debris [70] and X-ray production [28] impose to place any imager as far away from the source as possible, which would degrade the spatial resolution. Grazing incidence X-ray microscopes allow overpassing this limitation. Compared to standard pinhole imagers, they offer also the best solution in terms of resolution versus signal to noise ratio. The design of LMJ X-ray imagers benefits from years of expertise either on OMEGA [71] or LIL X-ray imagers [72, 73].

Four of these imagers, either gated (GXI-1 and GXI-2) or streaked (SHXI and SSXI), share a common mechanical structure (see Figure VIII.1) with the X-ray optical assembly itself, a telescopic extension and the optical analyzer (X-ray framing camera or streak camera) working inside an air box mechanical structure (see Figure VIII.2) [74].

Two others (UPXI and LPXI) are dedicated to the observation of the LEHs from the upper and lower poles of the chamber. A last one (ERHXI) offers an enhanced spatial resolution with the help of channels including two toroidal mirrors.

The main characteristics of the first seven X-ray Imagers are described in Table VIII.1.

<i>X-ray Imagers</i>					
<i>Diagnostics & Setting</i>	<i>Characteristics</i>	<i>Spectral range</i>	<i>Spatial resol. (μm) / Field of view (mm)</i>	<i>Time resol. (ps) / Dynamic (ns)</i>	
GXI-1 <i>Gated X-ray Imager (high resolution)</i>	<i>Magnification = 4.3</i>				
		<i>2x4 time-resolved toroidal mirror channels</i>	<i>0.5 - 10 keV</i>	<i>35 / 3</i>	<i>110 - 130 / 20</i>
	<i>SID</i>	<i>4 pinhole channels</i>	<i>2 - 15 keV</i>	<i>40 / 3</i>	<i>110 - 130 / 20</i>
		<i>1 time-integrated mirror channel</i>	<i>0.5 - 10 keV</i>	<i>50 / 5</i>	<i>N / A</i>
GXI-2 <i>Gated X-ray Imager (larger FOV, medium resolution)</i>	<i>Magnification = 0.9</i>				
		<i>2x4 time-resolved toroidal mirror channels</i>	<i>0.5 - 10 keV</i>	<i>150 / 15</i>	<i>110 - 130 / 20</i>
		<i>4 X-ray refractive lenses channels</i>	<i>6 - 15 keV</i>	<i>150 / 15</i>	<i>110 - 130 / 20</i>
	<i>SID</i>	<i>1 time-integrated mirror channel</i>	<i>0.5 - 10 keV</i>	<i>140 / 20</i>	<i>N / A</i>
SHXI <i>Streaked Hard X-ray Imager (medium resol.)</i>	<i>Magnification = 1 or 3</i>				
		<i>1 time-resolved toroidal mirror channels</i>	<i>0.5 - 10 keV</i>	<i>150 / 15 or 50 / 5</i>	<i>17 / 2 to 120 / 25</i>
<i>SID</i>		<i>1 time-integrated mirror channel</i>	<i>5 - 10 keV</i>	<i>130 / 20 or 50 / 6.5</i>	<i>N / A</i>
SSXI <i>Streaked Soft X-ray Imager (high resolution)</i>	<i>Magnification = 3</i>				
		<i>1 time-resolved bi-toroidal mirror channel</i>	<i>0.1 - 0.8 keV</i>	<i>30 / 5</i>	<i>17 / 2 to 120 / 25</i>
		<i>1 time-integrated bi-toroidal mirror channel</i>	<i>0.05 - 1.5 keV</i>	<i>30 / 5</i>	<i>N / A</i>
	<i>Equatorial SID</i>	<i>Spectral selection by grating</i>			
UPXI <i>Upper Pole X-ray Imager</i>	<i>1 pinhole channel</i>				
	<i>Passive detector</i>	<i>CID detector</i>	<i>> 3 keV</i>	<i>80 / 12 to 65 / 5</i>	<i>N / A</i>
<i>Magnif. = 2 to 5</i>	<i>Image Plate</i>	<i>80 / 50 to 65 / 25</i>			
LPXI <i>Lower Pole X-ray Imager</i>	<i>Optional camera</i>	<i>Streak camera</i>		<i>65 / 2</i>	<i>17/2 to 120 / 25</i>
	<i>Specific mechanics</i>	<i>Magnif. = 6</i>	<i>Framing camera</i>		<i>110 - 130 / 20</i>
ERHXI <i>Enhanced Resolution Hard X-ray Imager</i>	<i>Magnification = 8.2</i>				
	<i>SID</i>	<i>8 time-resolved channels with two toroidal mirrors</i>	<i>0.5 - 12 keV</i>	<i>10 / 0.5</i>	<i>70-80 / 20</i>

Table VIII.1: LMJ X-ray Imagers acronyms and their main characteristics

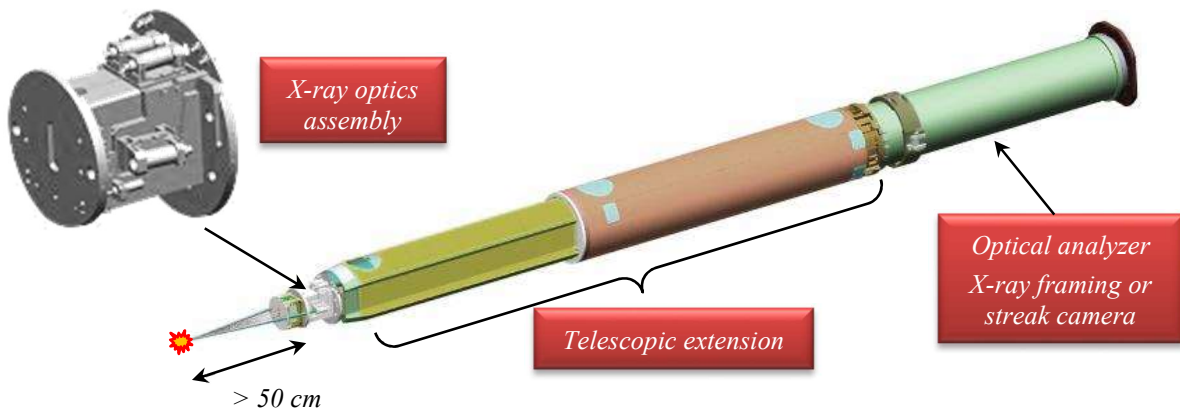


Figure VIII.1: Common mechanical structure of some LMJ X-ray imagers

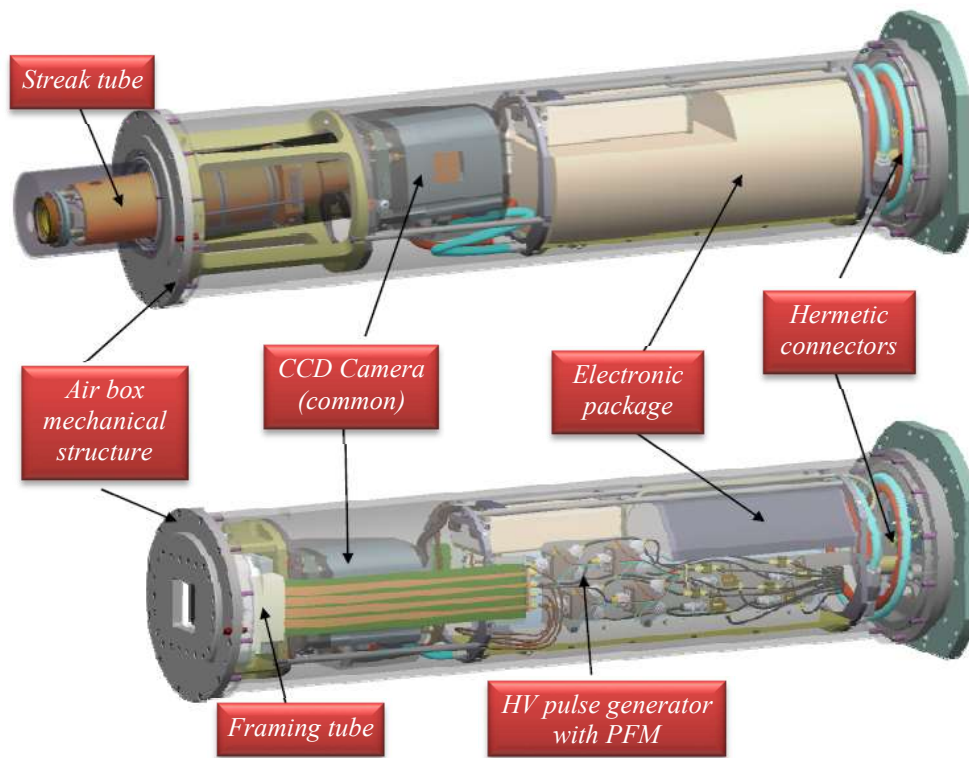


Figure VIII.2: Current design of LMJ optical analyzers [74]

VIII.1.1 - GXI-1, Gated X-ray Imager (high resolution)

The first LMJ X-ray imager GXI-1 records time-resolved 2D images in the hard X-ray spectral region. It is dedicated to X-ray radiography of target motion and to hard X-ray target emission [75].

GXI-1 incorporates a microscope with large source-to-optic distance (61 cm) and a large size gated micro channel plate detector. The microscope includes twelve X-ray channels: eight consisting of grazing angle-of-incidence mirrors [76-79] and a filter, and four straight-through channels consisting of pinholes with a filter. Each image of the twelve X-ray channels is produced along four micro channel striplines (ARGOS detector) [80].

GXI-1 also includes a three-film holder to protect optical components from damages caused by target debris and UV radiation. A filter holder is dedicated to select a broad band energy range on each column of four images on the detector. A CID camera, implemented close to the main detector, monitors X-ray emission with time integration. It allows to control internal alignment of the diagnostic.

GXI-1 is set up in the target chamber by a SID (System for Insertion of Diagnostics, see VII. Target area and associated equipment).

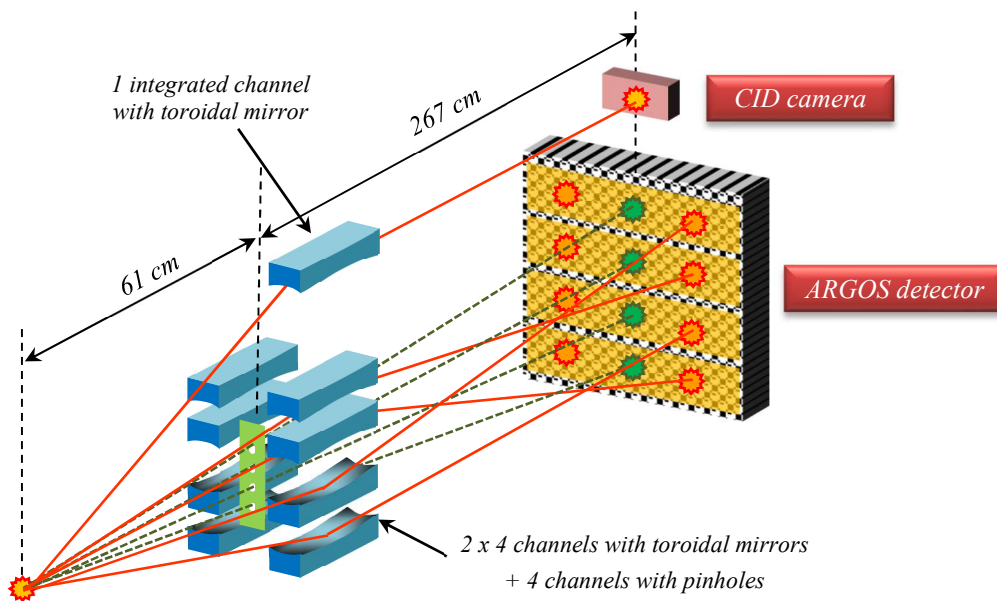


Figure VIII.3: Details of the acquisition channels of GXI-1.

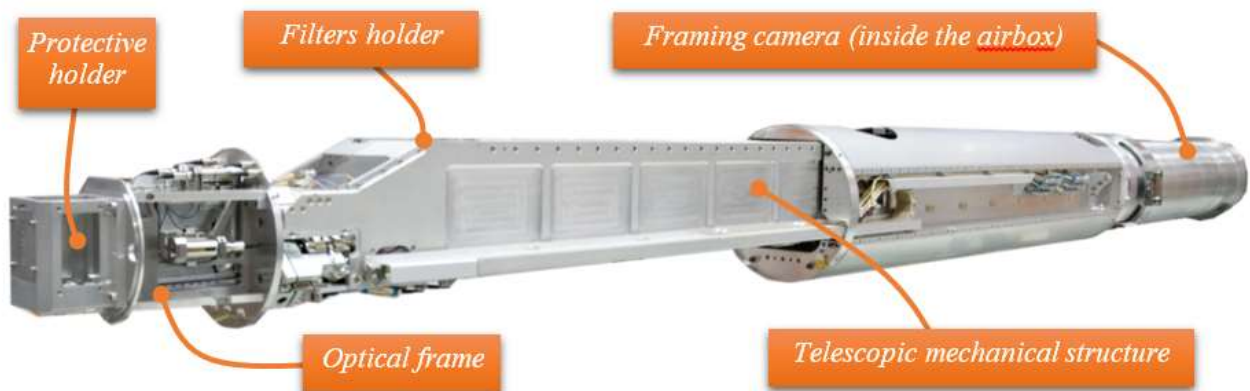


Figure VIII.4: Photograph of GXI-1.

VIII.1.2 - GXI-2, Gated X-ray Imager (medium resolution)

The second X-ray imager, GXI-2, records time-resolved 2D image, in the hard X-ray spectral region, on a large field of view. It is mainly dedicated to the control of laser beams pointing [75].

GXI-2 incorporates a microscope with a very large source-to-optic distance (303 cm) and a large size gated micro channel plate detector. Like GXI-1, the microscope includes twelve X-ray channels: eight consisting of grazing angle-of-incidence mirrors and a filter, and four straight-through channels consisting of refractive lenses with a filter. Each image of the twelve X-ray channels is produced along four micro channel striplines (ARGOS detector) [80].

GXI-2 also includes a three-film holder to protect optical components from damages caused by target debris and UV radiation. A filter holder is dedicated to select a broad band energy range on each column of four images on the detector. A CID camera, implemented close to the main detector, monitors X-ray emission with time integration and also controls internal alignment of the diagnostic. A photoconductive detector with a high bandwidth is mounted close to the framing camera to provide fiducial.

GXI-2 is set up in the target chamber by a SID (see VII. Target area and associated equipment).

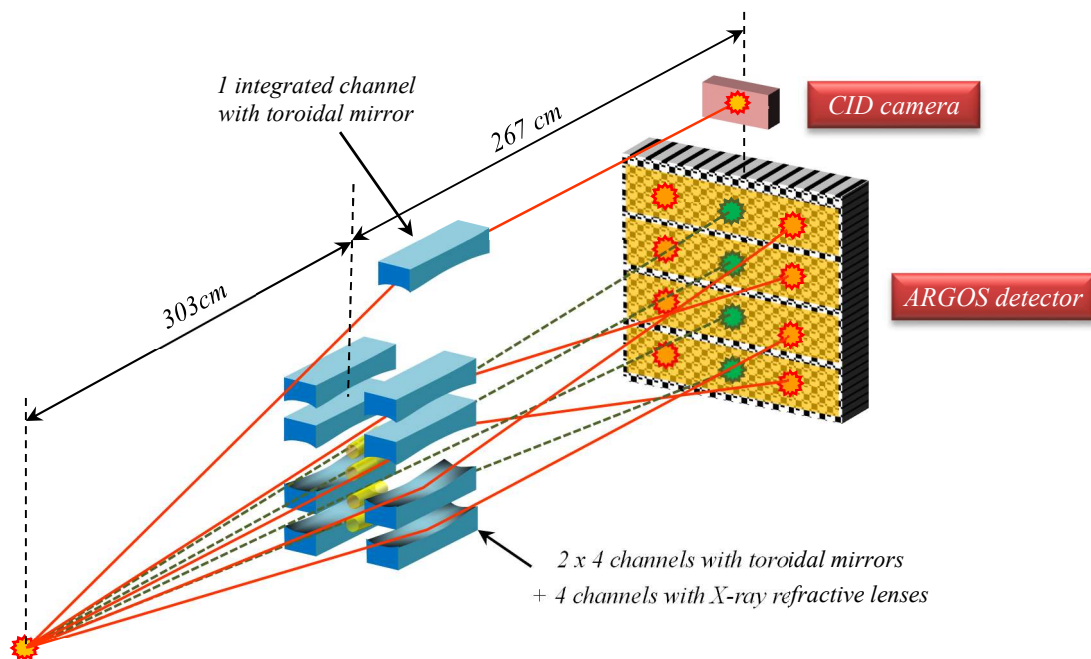


Figure VIII.5: Details of the acquisition channels of GXI-2.



Figure VIII.6: GXI-2 during qualification test.

VIII.1.3 - SHXI, Streaked Hard X-ray Imager (medium resolution)

The streaked X-ray imager, SHXI, records time-resolved 1D images in the hard X-ray spectral region. It is dedicated to X-ray radiography of target motion and to hard X-ray target emission.

The SHXI can be used with two different magnifications, and it has two X-ray channels per magnification, all of them consisting of grazing angle-of-incidence toroidal mirrors and a filter. The image of one of the two X-ray channels is produced

on the streak camera while the image of the other channel is formed on a time integrated detector (CID).

As GXI-1 and GXI-2, a protective holder contains three films to protect optical components from damages caused by target debris and UV radiation.

SHXI is set up in the target chamber by a SID (see VII. Target area and associated equipment).

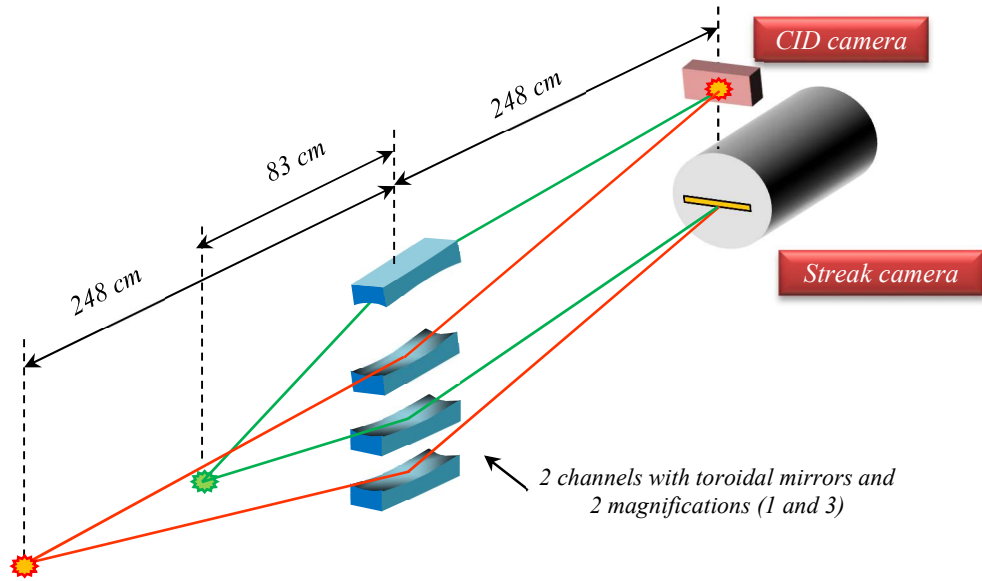


Figure VIII.7: Details of the acquisition channels of SHXI.

VIII.1.4 - UPXI and LPXI, Upper and Lower Polar X-ray imagers

The UPXI and LPXI diagnostics record time-integrated 2D images, or optionally time-resolved 2D or 1D images, in the hard X-ray spectral region. They are dedicated to precision pointing of LMJ laser beams: position and characterization of the laser spots, verification of main-target and backlighter-target positions, and time-resolved size measurement of the Laser Entrance Holes (LEH).

The image is obtained with a single 50 μm diameter pinhole, laser drilled into a tantalum foil. The maximum target to pinhole distance is 250 cm (minimum is 150 cm) for a magnification of 2 (5 or 6).

These diagnostics are available with time-integrated detectors : CID camera or Image Plate (IP) for PETAL experiments.

These diagnostics are set up on the target chamber at fixed place with specific mechanics.

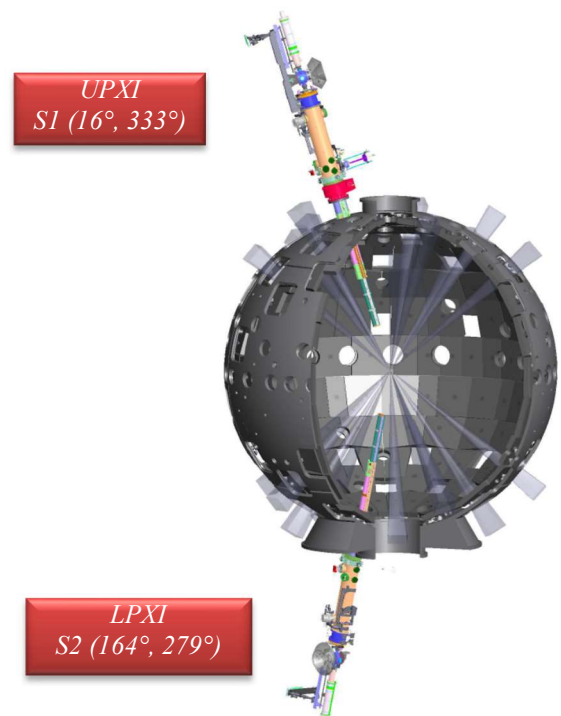


Figure VIII.8: Positions of the UPXI and LPXI diagnostics

VIII.1.5 – SSXI, Streaked Soft X-ray Imager (high resolution)

The streaked soft X-ray imager, SSXI, records time-resolved 1D images or time/space-resolved spectra in the soft X-ray spectral region. It is dedicated to radiative waves analysis (propagation, burn-through, etc.) and soft X-ray target emission.

It consists of the association of an optical assembly and a spectral selection device. As no thick filter can be used due to soft X-ray bandwidth, the optical scheme of the diagnostic is entirely based on grazing incidence optics. The optical assembly is composed of a blast shield consisting of a large flat mirror, with grazing incidence, and an X-ray

microscope with two channels made of two toroidal mirrors to improve spatial resolution.

The spectral selection is provided by two low-pass mirrors combined with a reflective flat field grating.

Currently this diagnostic can be operated in only one equatorial SID due to the availability of specific servicing equipment (see Table IX.2). It is not compatible with polar SID (see VII. Target area and associated equipment). Its use is also restricted to the imaging configuration due to the complexity of reconfiguration from imaging to spectral mode.

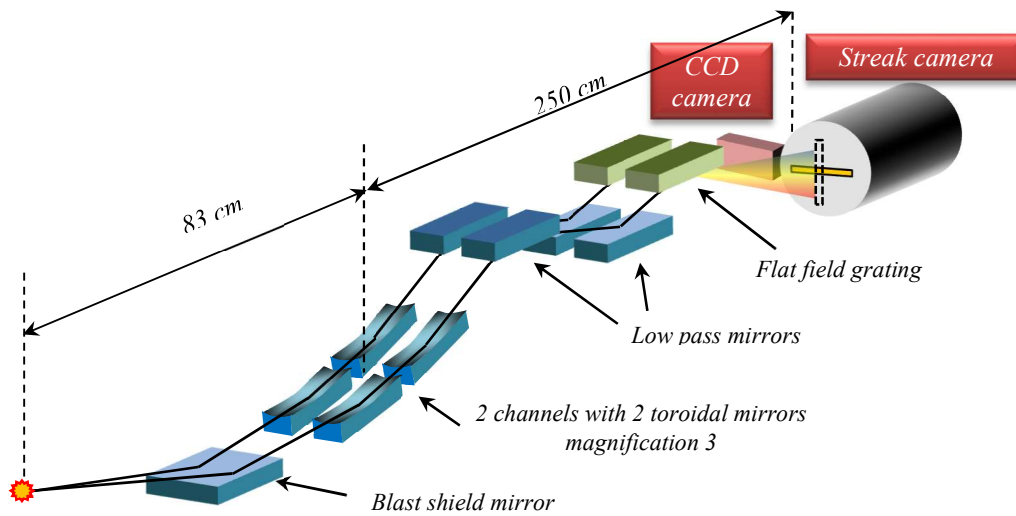


Figure VIII.9: Details of the acquisition channels of SSXI. The streak camera can be rotated in order to commute between a spectrally selected imager and a spatially selected spectrometer.

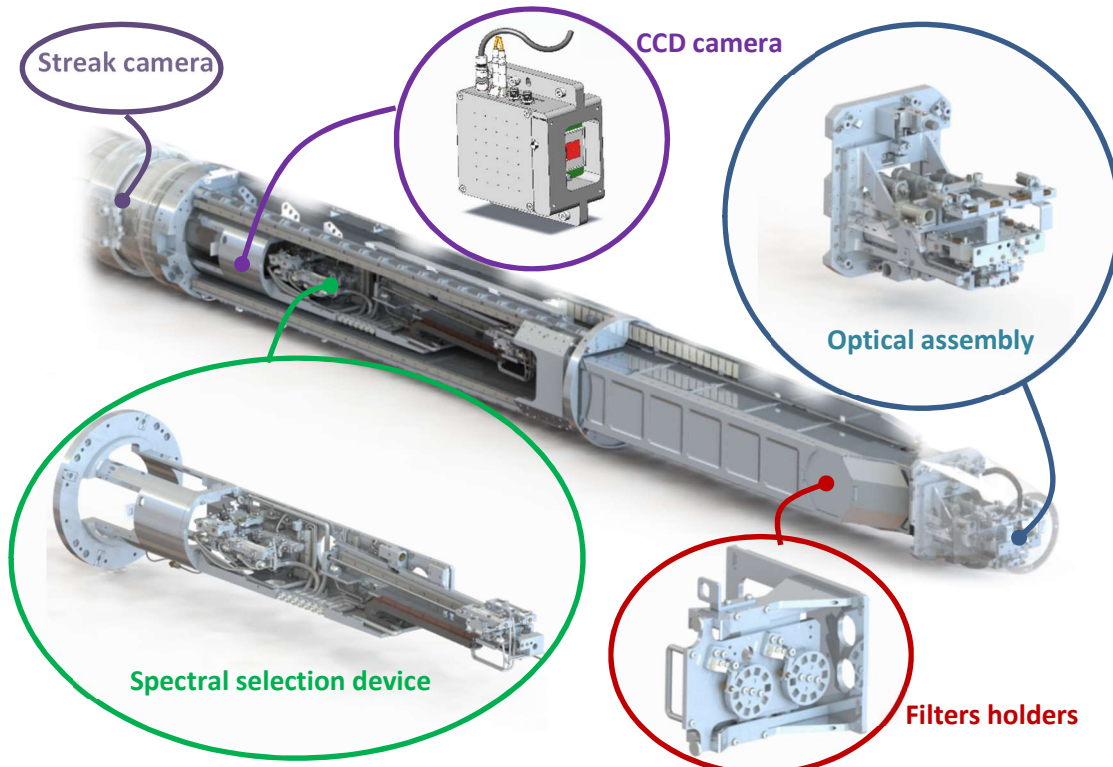


Figure VIII.10: Details of the SSXI diagnostic structure.

VIII.1.6 - ERHXI, Enhanced Resolution Hard X-ray Imager

The enhanced resolution hard X-ray imager, ERHXI, records time-resolved 2D images in the hard X-ray spectral region with high spatial resolution. It is dedicated to X-ray radiography or hard X-ray emission of small size targets (e.g. compressed ICF target).

It incorporates a microscope with large source-to-optic distance and a large size gated micro channel plate detector. The first version (2023) uses the existing ARGOS optical analyzer and a microscope. The second one (in 2025) will bring an improvement of the spatial and temporal performances; it differs by minor modifications of the optical block, and a new analyzer with an advanced tube (ARGOS HD tube type).

The microscope includes eight X-ray channels, each consisting of two toroidal mirrors with a 0.6° grazing angle-of-incidence and a filter. Each image of the eight X-ray channels is produced along four micro channel striplines. The bi-mirrors are mounted in a Wolter-like configuration. They are coated with platinum graded multilayers to have a good reflectivity in the 0.5 to 12 keV range [81, 82].

This imager also includes a film holder to protect optical components from damages induced by target debris and UV radiation.

ERHXI is set up in the target chamber by a SID (see VII. Target area and associated equipment).

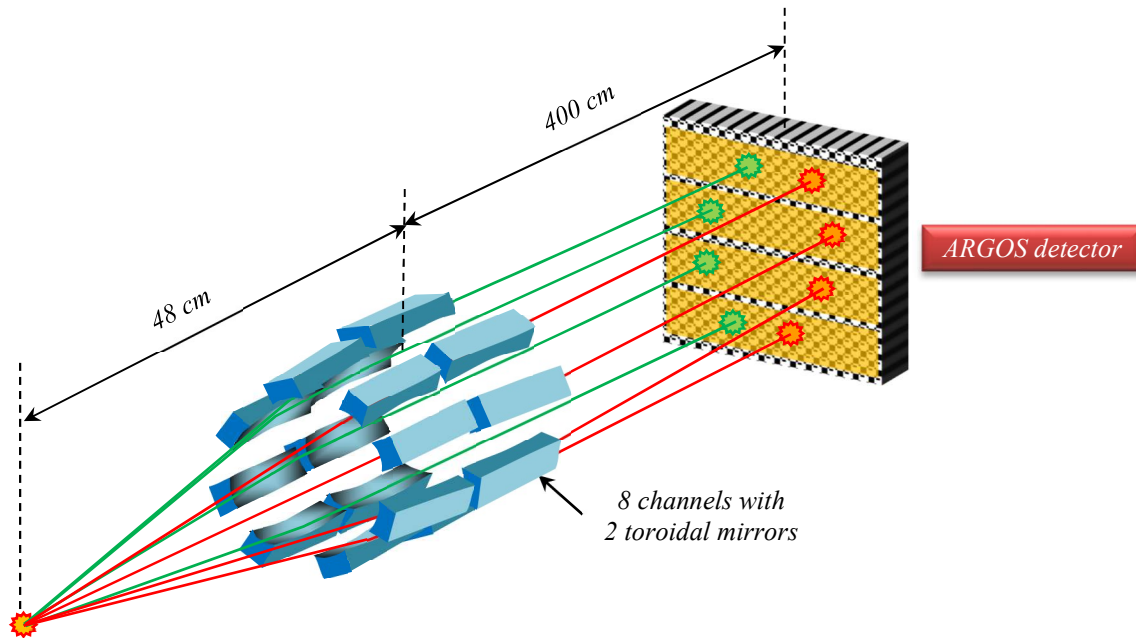


Figure VIII.11: Details of the acquisition channels of ERHXI.

VIII.2- X-ray Spectrometers

Five X-ray spectrometers are available on the LMJ; three of them are made of 16 or 20 broadband channels, and the other ones use crystals for high spectral resolution.

The main characteristics of these spectrometers are described in Table VIII.

<i>X-ray Spectrometers</i>				
<i>Diagnostics & Setting</i>	<i>Characteristics</i>	<i>Spectral range (resol. E/ΔE)</i>	<i>Spatial resol. (μm) / Field of view (mm)</i>	<i>Time resol. (ps) / Dynamic (ns)</i>
DMX <i>Broad-band X-ray spectrometer</i> <i>Specific mechanics</i>	<i>20 time-resolved broad-band channels</i>	<i>0.03 - 20 keV (5)</i>	<i>- / 5</i>	<i>150 / 10⁵</i>
	<i>Grating X-ray spectrometer $\Delta\lambda < 1\text{\AA}$</i>	<i>0.1 - 1.5 keV 1.5 - 4 keV</i>		<i>17 / 2 to 120 / 25</i>
	<i>Laser Entrance Hole Imager 2 frames</i>	<i>0.5 - 2 keV</i>	<i>100 / 5</i>	<i>2ns / frame</i>
	<i>X-ray Power</i>	<i>0.1 - 2 keV 2.0 - 4.0 keV 4.0 - 6.0 keV</i>	<i>- / 5</i>	<i>150 / 10⁵</i>
Mini-DMX <i>Broad-band X-ray spectrometer</i> <i>SID</i>	<i>16 time-resolved broad-band channels</i>	<i>0.03 - 7 keV (5)</i>	<i>- / 5</i>	<i>150 / 10⁵</i>
Mini-DMX-2 <i>Broad-band X-ray spectrometer</i> <i>SID</i>	<i>16 time-resolved broad-band channels</i>	<i>0.03 - 7 keV (5)</i>	<i>- / 5</i>	<i>150 / 10⁵</i>
HRXS <i>High Resolution X-ray Spectrometer</i> <i>SID</i>	<i>4 time-resolved crystal channels Slit magnification = 0.9 or 2.7</i>	<i>0.8 - 25 keV (~500)</i>	<i>70 (1D) / 5</i>	<i>250 - 750</i>
	<i>2x3 time-integrated crystal channels (CID) Slit magnification = 0.65 or 2.2</i>			<i>N / A</i>
SPECTIX <i>Hard X-ray spectrometer</i> <i>SID</i>	<i>1 time-integrated channel Transmission crystals</i>	<i>7 - 150 keV (>100)</i>	<i>N / A</i>	<i>N / A</i>

Table VIII.2: LMJ X-ray Spectrometers and their main characteristics.

VIII.2.1 - DMX, Broad-band X-ray Spectrometer

DMX is a primordial diagnostic for hohlraum energetics measurements [28]. It is composed of a set of four diagnostics:

- a time resolved soft X-ray large band spectrometer made of 20 measurement channels combining mirror, filters and X-ray diodes,
- a time resolved soft X-ray spectrometer with gratings and streak camera,
- a time-resolved soft X-ray laser entrance hole imaging with a hCMOS camera,
- a time resolved X-ray power measurement spectrally integrated.

Beside standard soft X-ray measurements devoted to hohlraum energetics, the filtration of the

channels could be adapted for specific purpose, such as conversion efficiency characterization of backlighters [83-85]. However, as those measurements may require additional filters metrology on synchrotron beam lines (synchrotron SOLEIL at Saint Aubin, France), the request should be done well in advance.

Multilayer mirrors with adjusted spectral response are included for flat-response X-ray channels in the [2-4 keV] and [4-6 keV] domains [86].

DMX is set up on the target chamber at a fixed location, with specific mechanics.



Figure VIII.12: DMX implantation on LMJ

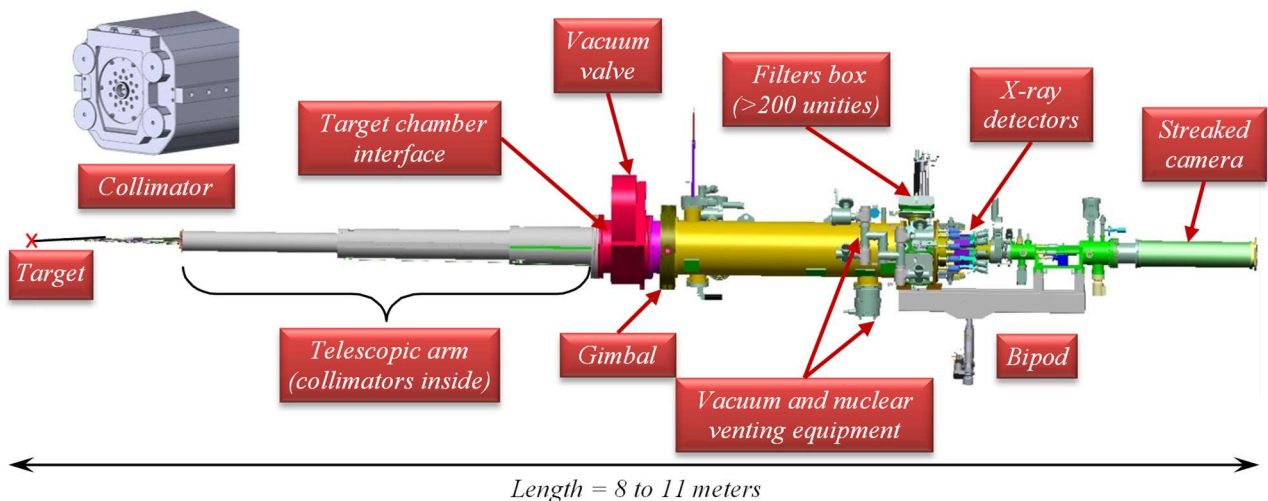


Figure VIII.13: Details of the DMX diagnostic structure.

VIII.2.2 - Mini-DMX, Broad-band X-ray Spectrometer

Mini-DMX is a second hohlraum energetic measurements axis on the LMJ facility.

This diagnostic is composed of 16 broadband channels combining filters, mirrors and coaxial detectors. It can be positioned at two different

working distances (1000 mm or 3500 mm) by a SID (see VII. Target area and associated equipment). This diagnostic, like DMX, is absolutely calibrated.

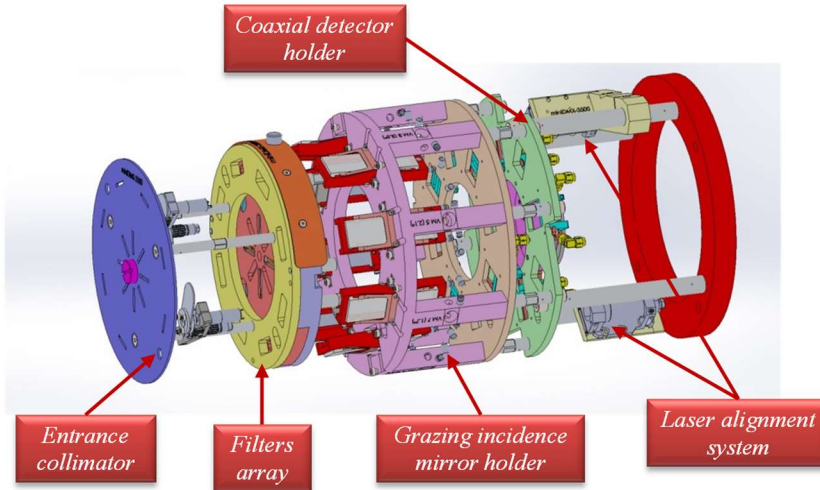


Figure VIII.14: Details of mini-DMX.

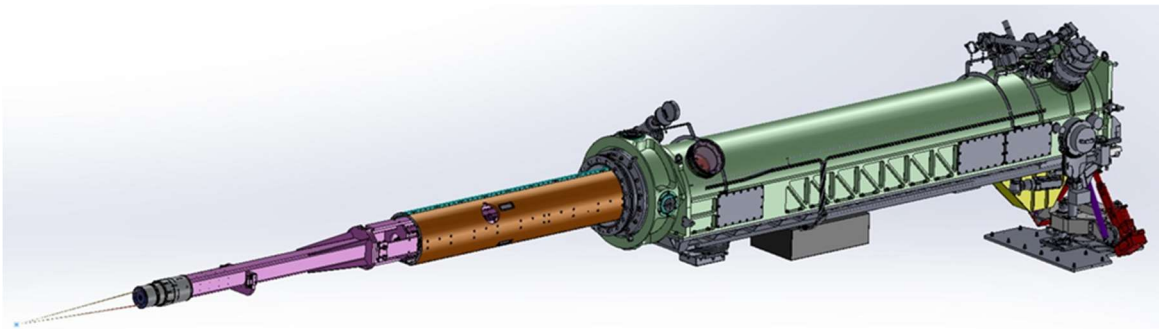


Figure VIII.15: Mini-DMX diagnostic positioned at working distance with SID.

VIII.2.3 - Mini-DMX-2, Broad-band X-ray Spectrometer

MiniDMX-2 is a third hohlraum energetic measurements axis on the LMJ facility.

This diagnostic is composed of 16 broadband channels combining filters, mirrors and coaxial detectors. It can be inserted using a SID. MiniDMX-2 is an evolution of MiniDMX with the ability to position each channel individually at a working

distance of 1 m or 3 m. The working distance can be easily changed before each shot. The dark field has been reduced to 9 mm thus shielding the high radiation from the TEL without the need to add shields on the target. This diagnostic, like DMX, is absolutely calibrated. It is currently under development and is planned to be qualified by 2027.

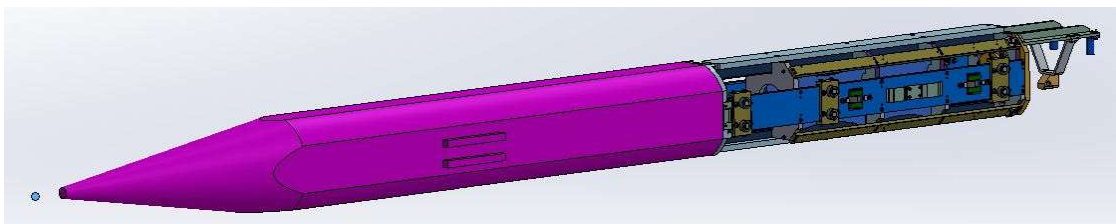


Figure VIII.16: Preliminary design of MiniDMX-2 with its air box hosting the electronics.

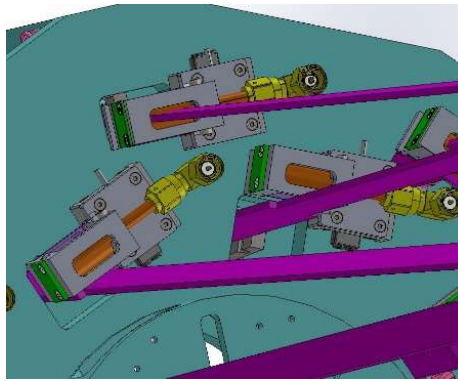


Figure VIII.17: View of the detectors at 1m on their translation plate.

VII.2.4 – HRXS, High Resolution X-ray Spectrometer

HRXS (High Resolution X-ray Spectrometer) is a new plasma diagnostic recently implemented on the LMJ facility. It is dedicated to atomic physics and more specifically to NLTE spectroscopy and opacity measurements.

This diagnostic consists in ten measurement channels implemented in three different boxes. The central box contains four measurement channels associated to a framing camera with CCD detector for time-resolved spectra. Each of the two lateral boxes contains a set of three channels and a CCD camera to record time-integrated spectra.

Each channel is equipped with a cylindrical Bragg crystal in either reflection or transmission geometry, an adjustable shot-to-shot filter (thanks to a four-position filter wheel), and a slit for spatial resolution. The channels are fully customizable,

allowing both spectral range and spectral resolution to be adapted to experimental needs. The slits positions can also be easily changed between experimental campaigns to adjust the magnification and thus the field of view along the spatial dimension.

Opacity measurements can be performed by combining each of the four central channels with a grazing incidence spherical mirror (half-KB). This allows the beam to be angularly split to effectively separate the direct signal from the signal transmitted through the sample on the detector.

HRXS is also equipped with a tungsten alloy collimator at the front end and a debris shield consisting of three successive rolls of aluminized Mylar filters to protect the crystals and detectors.

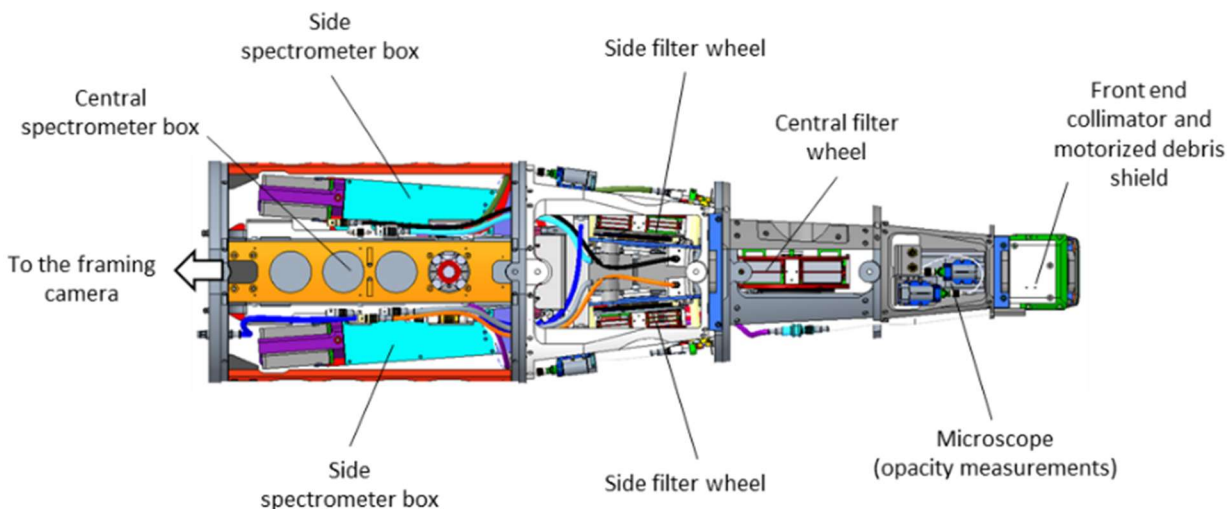


Figure VIII.18: Details of HRXS diagnostic.

VIII.2.5 – SPECTIX, Hard X-ray Spectrometer

SPECTIX is a hard X-ray spectrometer dedicated to K-shell spectroscopy of a large number of materials [87]. This diagnostic has been developed in the framework of the PETAL+ project [46, 47, 88].

The concept is based on diffraction by transmission cylindrical crystals (Cauchy type) associated to a cross-over which absorbs non diffracted x-rays [89, 90]. In this scheme, the diffraction plane is perpendicular to the surface of the crystal and diffracted x-rays are focused at the distance where the cross-over is located. Detection is performed with Image Plates (IP), which are insensitive to electro-magnetic pulses [91, 92].

The wide spectral range 7 – 150 keV is achieved by two different crystals, a quartz crystal (10-10) with a radius of 125 mm for low energies and a LiF crystal (200) with a radius of 250 mm for high energies.

The resolving power of SPECTIX is related to the size of the x-ray source, the distance of the IP to the Rowland circle (distance to crystal = crystal radius) and to the spatial resolution of the IP. The IP can be positioned on the Rowland circle (where spectral resolution is independent on x-ray source size) or farther. A resolving power of ~ 100 can be achieved on all the spectral range.

Identification of contributors to the background noise and shielding optimization were performed with the help of Monte-Carlo simulations [93]. A part of the noise induced by electrons emitted by the target is suppressed by a set of magnets located at the front end of the collimation. The noise created by hard x-ray photons is limited by the use of tungsten alloy in the cross-over and in all parts contributing to the frontal collimation.

SPECTIX is set up in the target chamber by a SID (see VII. Target area and associated equipment).

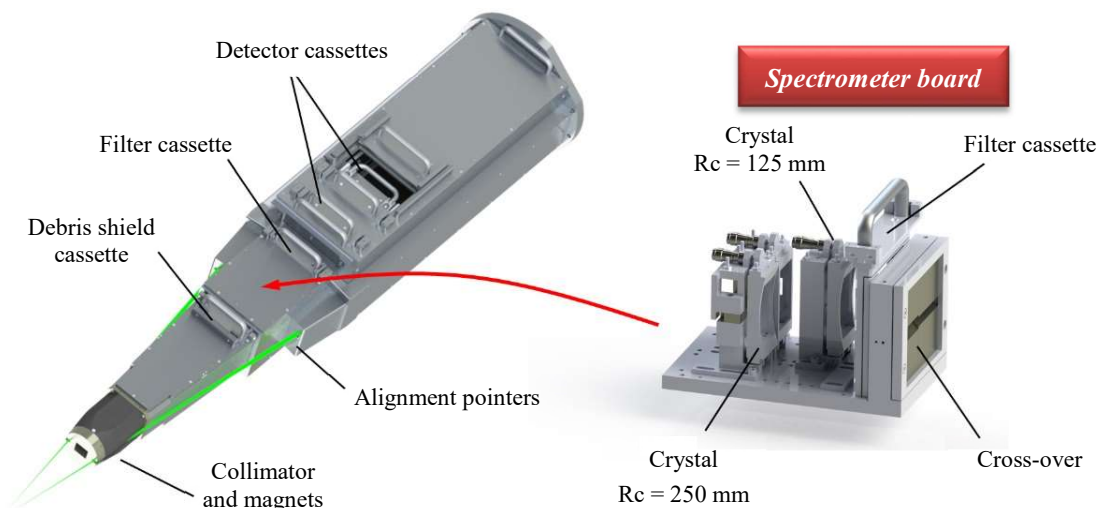


Figure VIII.19: Design of the SPECTIX diagnostic.

VIII.3- Optical Diagnostics

The optical diagnostics of LMJ are composed of a diagnostic set for EOS measurements and two diagnostics for laser energy balance.

The main characteristics of the three optical diagnostics are described in Table VIII.3.

<i>Optical Diagnostics</i>				
<i>Diagnostics & Setting</i>	<i>Characteristics</i>	<i>Measurement or Spectral range (nm)</i>	<i>Spatial resol. (μm) / Field of view (mm)</i>	<i>Time resol. (ps) / Dynamic (ns)</i>
EOS Pack <i>Diagnostics set for EOS experiments</i>	<i>2 VISARs (1064 and 532 nm)</i>	<i>Velocity 0.5 - 200 km/s</i>	<i>30 / 1 to 50 / 5</i>	<i>50 / 5 to 500 / 100</i>
	<i>2 SOPs</i>	<i>490 - 750</i>	<i>30 / 1 to 100 / 10</i>	<i>50 / 5 to 500 / 100</i>
	<i>2 GOIs</i>	<i>490 - 750</i>		<i>75 - 200 / 5 - 20</i>
FABS1&2 <i>Full Aperture Backscattering Station</i> <i>Focusing system quad 28U (available) & 29U (planned)</i>	<i>Brillouin spectrometer Δλ < 0.05 nm</i>	<i>346 - 356</i>	<i>N / A</i>	<i>25 / 5 to 250 / 50</i>
	<i>Raman spectrometer Δλ < 5 nm</i>	<i>375 - 750</i>		
	<i>Time integrated calibration spectrometer</i>	<i>350 - 700 375 - 750</i>		<i>N / A</i>
	<i>3 Brillouin power channels</i>	<i>< 360</i>		<i>150 / 5 to 50</i>
	<i>2 Raman power channels</i>	<i>350 - 750</i>		<i>500 / 25</i>
	<i>1,2,3 ω power channels</i>	<i>1053, 526, 351</i>		
NBI <i>Near Backscatter Imager</i> <i>Chamber wall Around quads 28U & 29U</i>	<i>40 Brillouin/Raman temporal channels</i>	<i>346-356 or 375-750</i>	<i>FOV : 40 mm Without</i>	<i>250 ps (Brillouin) / 1 ns (Raman) / 200 ns Dynamic : 200 ns</i>
	<i>2 Brillouin power channels</i>	<i>346 - 356</i>		
	<i>2 Raman power channels</i>	<i>375 - 750</i>	<i>Angle : 2°/16°</i>	
	<i>Brillouin image</i>	<i>346 - 356</i>	<i>Azimuthal range : 64° Polar range : 46° 150 mm / 4.3 m</i>	<i>N / A</i>

Table VIII.3: LMJ Optical diagnostics and their main characteristics.

VIII.3.1 – EOS Pack

The development of the EOS Pack takes into account the feedback of the same kind of diagnostic that was in operation on the LIL facility [94]. This diagnostic combines two probe lasers with a 10 to 100 ns pulse duration, an optical system, positioned close to the target with the help of a SID, an optical transport system and an analysis table.

The use of the EOS Pack requests the S20 location for the insertion of the optical system inside the chamber and the S7 location for laser injection, as well as collection of laser reflection and self-emission from target.

The diagnostic (laser and optical analyzers) is hardened and protected against EMP inside Faraday cages. The aim is to be fully operational with PETAL so that simultaneous EOS measurements and side-on shock radiography may be possible.

The different acquisition channels are listed in Table VIII.3: two VISAR at 532 nm and 1064 nm, two Streaked Optical Pyrometer (SOP) in the 490-750 nm range combined with 2 two-dimensional Gated Optical Imagers (GOI).

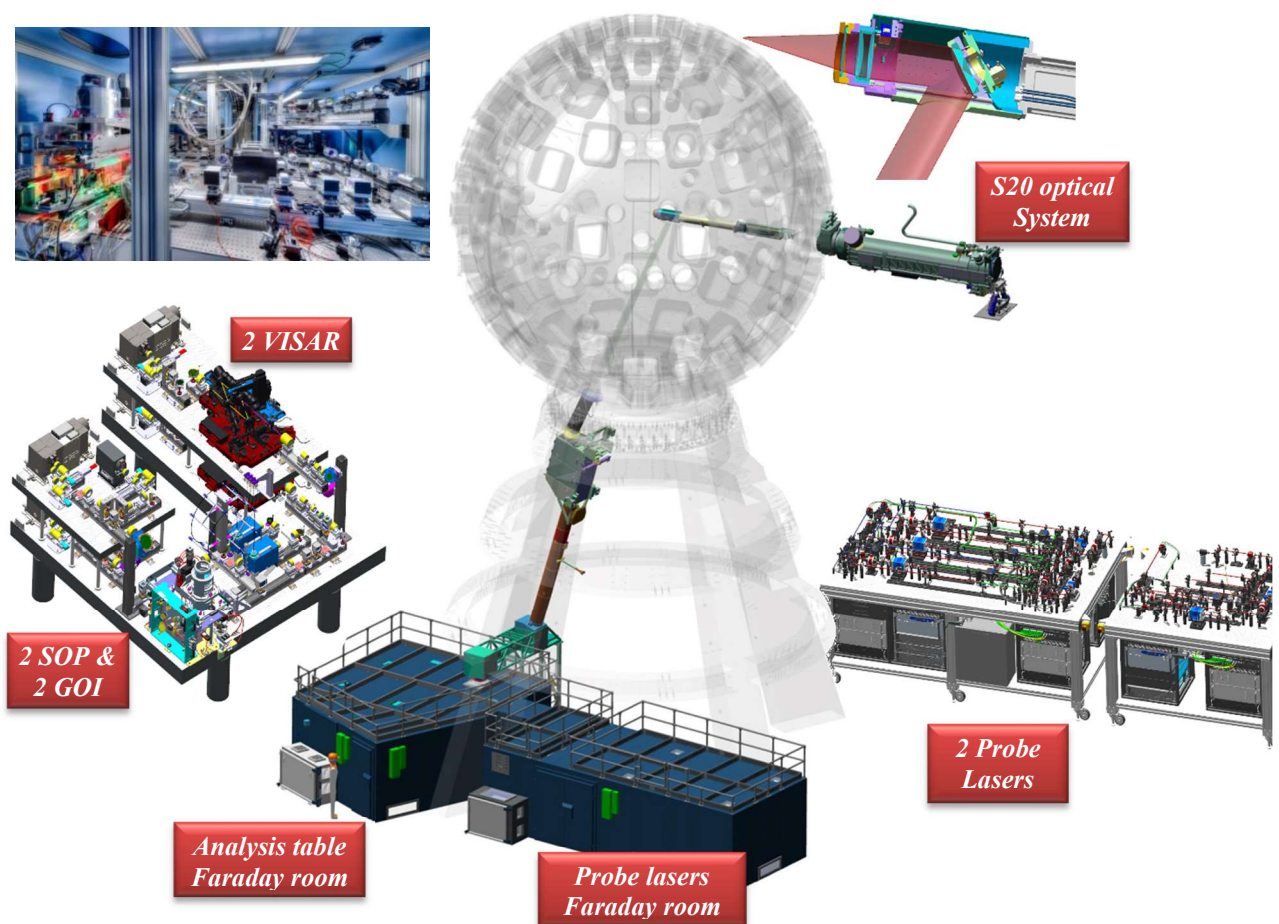


Figure VIII.20: EOS Pack location and closer view on the analysis Table.

VIII.3.2 - FABS, Full Aperture Backscatter Stations

The FABS are dedicated to analysis of backscattered light in the focusing cones of quadruplet 28U (33.2° irradiation cone) and 29U (49° irradiation cone). The backscattered energy is collected with an ellipsoidal Spectralon® scattering panel and sent to the detectors (phototubes and Raman-Brillouin spectrometers).

The ellipsoidal scattering panel is located behind the 3ω gratings that are used on LMJ to deviate, filter, and focus the laser quadruplet on the target. It is positioned so that the first focus of the ellipsoid is the TCC. The detection module is located at the second focus of the ellipsoid. It includes power detection and optical fibers which transport signal to spectrometers.

The Brillouin (346.5 - 355.5 nm) and Raman (375 - 750 nm) backscatter is measured with a 100 ps temporal resolution. *In situ* calibration of the diagnostics is performed using a xenon calibrated lamp located outside the chamber, behind a chamber vacuum window at the opposite of the conversion and focusing mechanical assembly.

The FABS on quadruplet 28U (33.2°) is available since 2019, the FABS on quadruplet 29U (49°) should be available in 2027.

Spectral and temporal characteristics are given in Table VIII.3.

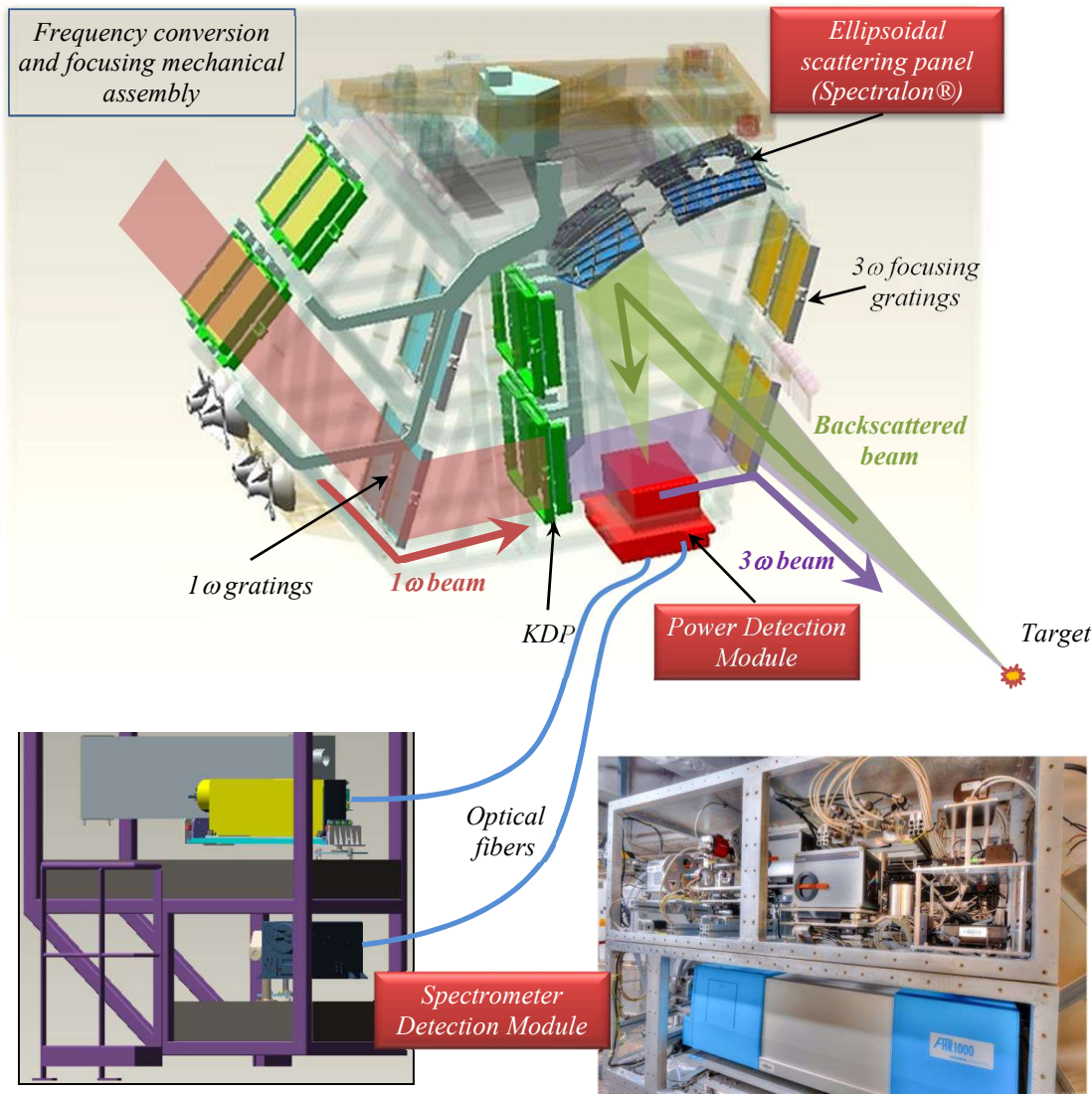


Figure VIII.21: Principle of the FABS.

VIII.3.3 – NBI, Near Backscatter Imager

The Near Backscatter Imager (NBI) [95] is dedicated to analysis of backscattered light outside the focusing cones of quadruplets 28U and 29U. Part of the backscattered energy is collected by an optical system looking at Spectralon® scattering panels inside the chamber, and sent to an optical table where Raman and Brillouin ranges are analyzed.

The NBI is made of:

- 9 flat scattering panels (Spectralon®, 7.1 m²) inside the target chamber, located around the beam ports of quads 28U (33.2° irradiation cone) and 29U (49° irradiation cone);
- an Optical system inserted in a diagnostic port ($\theta = 70^\circ$, $\varphi = 306^\circ$) using 4 lenses to collect

light and send images to the optical analysis table via 4 bundles of 15 m long optical fibers;

- an Optical analysis table surrounded by a Faraday cage, with 4 phototubes (power & energy), 2 iCCD (integrated images), 40 high bandwidth photodiodes and digitizers (time-resolved measurements).

A calibration system is used to control the plates' reflectivity and to determine the diagnostic sensitivity with two modules: a lamp illuminating the surface of the plates and a pulsed laser associated to a mirror steering the laser beam onto numerous positions on the scatter plates with cm-size spots.

This diagnostic is complementing to the FABS measurements.

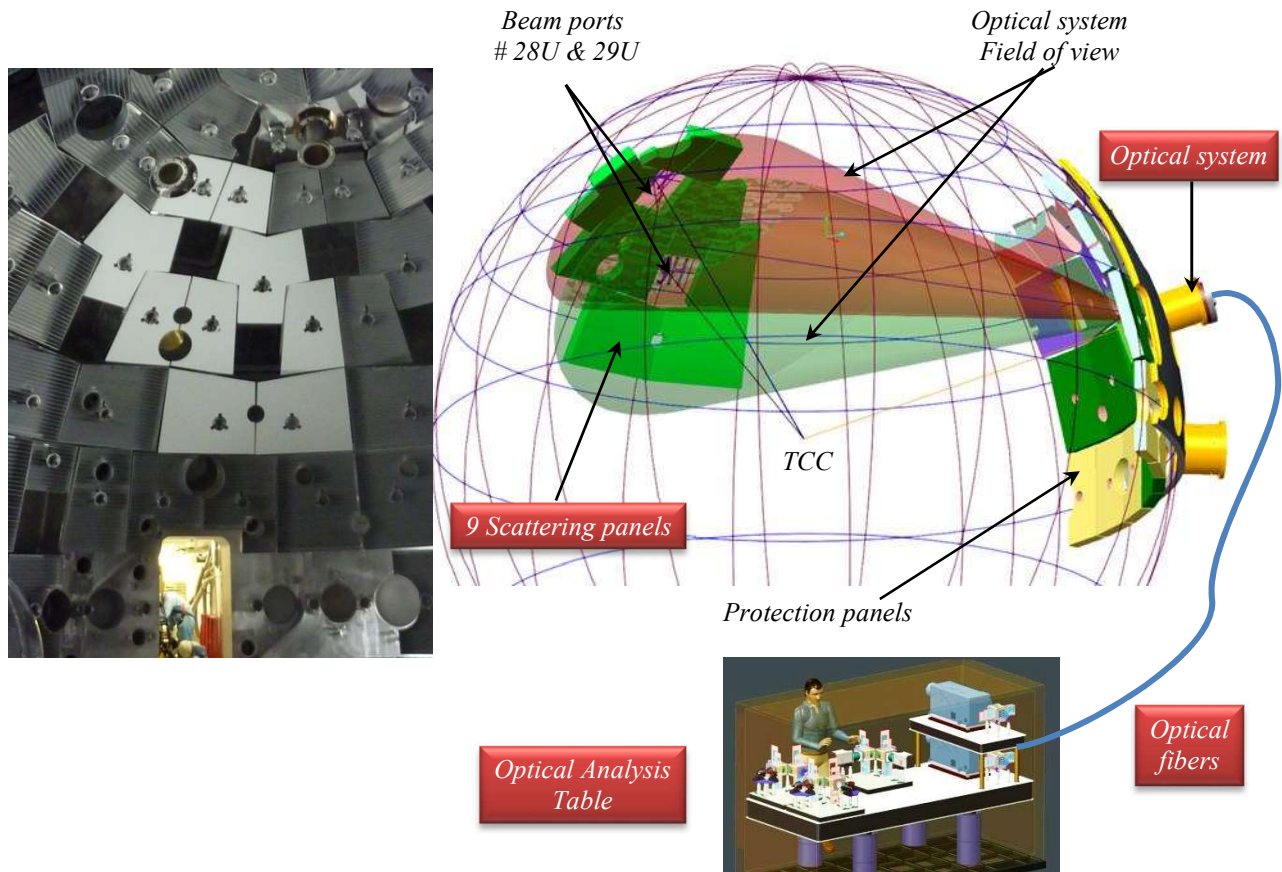


Figure VIII.22: Principle of the LMJ NBI.

VIII.4- Particles Diagnostics

The Particles diagnostics of LMJ include a diagnostic set for neutron emission, and two types of spectrometers for electron and proton/ion emission.

The main characteristics of these Particles diagnostics are described in Table VIII.4.

<i>Particles Diagnostics</i>				
<i>Diagnostic & Setting</i>	<i>Characteristics</i>	<i>Yield / Spectral range</i>	<i>Spatial resol. (μm) / Field of view(mm)</i>	<i>Time resol. (ps)</i>
Neutron Pack <i>Activation and nTOF</i>	<i>Activation</i>	$D_2 : 10^8 \text{ to } 10^{13} \text{ neutrons}$	-	<i>N / A</i>
	<i>Inside and outside the target chamber</i>	<i>GPMT nTOF</i>		$DT : 10^8 \text{ to } 10^{13} \text{ neutrons}$
SEPAGE <i>Electron and proton spectrometer</i>	<i>Low energy Thomson parabola</i> $\Delta E/E < 0.5\% \text{ for } e-, < 6.5\% \text{ for } p$	$e- : 0.1 - 20 \text{ MeV}$ $p : 0.1 - 20 \text{ MeV}$	- / 9	<i>N / A</i>
	<i>High energy Thomson parabola</i> $\Delta E/E < 1\% \text{ for } e-, < 6\% \text{ for } p$	$e- : 8 - 150 \text{ MeV}$ $p : 10 - 200 \text{ MeV}$	- / 2.3	
	<i>SID</i> <i>RCF stack</i>	$3 - 200 \text{ MeV}$	-	
SESAME1 & 2 <i>Electron (& proton) spectrometer</i> <i>Chamber wall</i>	<i>Magnetic spectrometer</i> $\Delta E/E < 5\%$	<i>Electrons : 5 - 150 MeV</i> <i>Protons: 3 - 30 MeV</i>	- / 15	<i>N / A</i>

Table VIII.4: LMJ Particles diagnostics and main characteristics.

VIII.4.1 - Neutron Pack

The Neutron Pack is a set of several diagnostics to measure neutron yield, ion temperature, neutron bang time and the ratio of secondary to primary neutron reactions during D₂ and DT implosions [96] (note that the use of tritium in target is not yet permitted).

This set of diagnostics consists of several neutron Time of Flight detectors (nTOF: Gated PhotoMultiplier Tubes (GPMT) and scintillators, photodiodes) and activation (indium, copper, zirconium, etc.). At this time, these diagnostics include:

- a set of 4 GPMT nTOF detectors placed at 3.8 meters from TCC to describe two perpendicular equator axis.
 - a set of 2 GPMT nTOF detectors placed at 16° from the polar axis.
 - 1 GPMT nTOF detector placed on the south equator line of sight 18 meters away from TCC.
 - a set of 6 Indium disk located outside the target chamber close to nTOF detectors locations.
- Other GPMT nTOF detectors will be placed on long LMJ equator lines of sight (East and West);

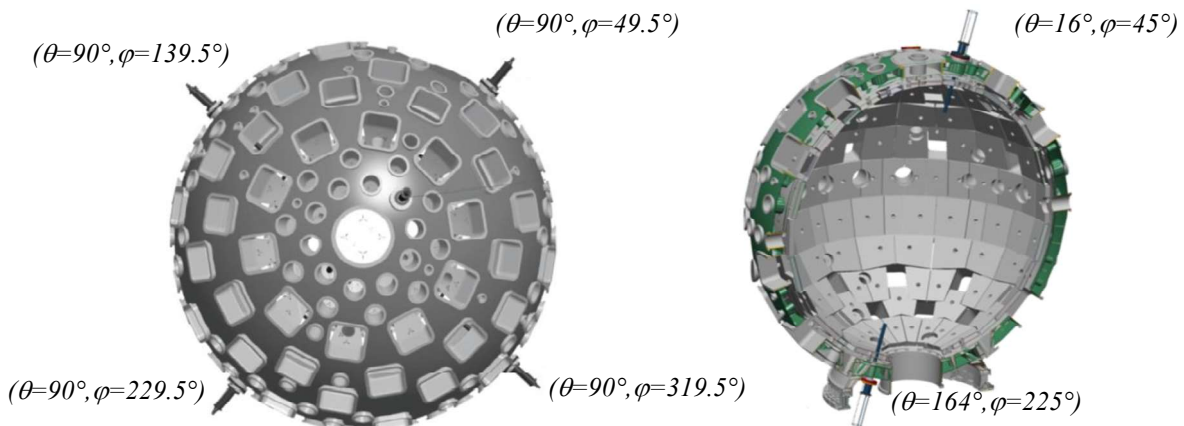


Figure VIII.23: Equator (left) and near polar (right) locations of GPMT nTOF detectors and



Figure VIII.24: Indium disk positions (in red) vs nTOF detector locations around the LMJ target chamber

VIII.4.2 – SEPAGE, Electron and Ion Spectrometer

The SEPAGE diagnostic [97] is dedicated to spectral measurements of high energy particle beams generated by PETAL. SEPAGE was jointly developed by CEA/DRF/IRFU and CEA/DAM/DCRE in the framework of the PETAL+ project [46, 47, 88].

It is composed of three parts:

- A Low Energy Thomson Parabola (TP) measuring the low energy part of the spectrum (100 keV – 20 MeV for protons and electrons)
- A High Energy TP collecting the high energy part of the spectrum from 7 to 200 MeV for protons and from 10 to 150 MeV for electrons.

For both TP, electrons are collected on Image

Plates (IP) located on the sides of the diagnostic whereas protons and ions are collected on the frontal IP.

- A detector cassette located at the front of SEPAGE that can be either used as a radiography module or as a discrete 2D proton spectrometer in addition to the two TP. It is composed of a stack of radiochromic films (RCF) and filters (see also CRACC §VIII.5-.1) and can be positioned at 100 mm to the TCC.

A CAD drawing of the diagnostic as well as examples of experimental results are shown in Figure VIII.22. The SEPAGE working position is in SID S26, facing the PETAL beam with an angle of 13.5

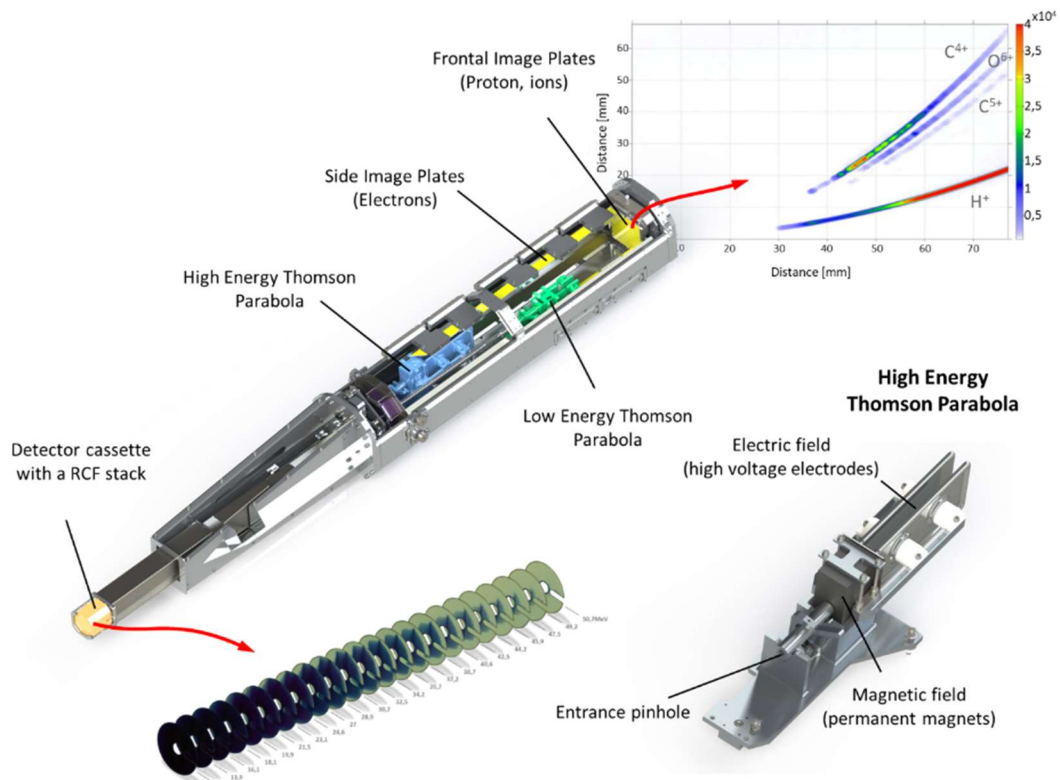


Figure VIII.25 : Design of SEPAGE diagnostic and examples of results obtained during qualification.

VIII.4.3 – SESAME, Electron and Proton Spectrometer

In addition to the SEPAGE spectrometer, two electron / proton spectrometers are set up at fixed positions on the target chamber (see Table VII.1) along the PETAL axis (SESAME 1) and at 45° (SESAME 2).

Each of these two spectrometers is composed of a tungsten collimator, an entrance slit and permanent magnets that deflect charged particles toward Imaging Plates (IP) detectors located around. Since the magnetic field deflects particles according to their charge, electrons and proton (and ions) are collected on two different IP positioned on both sides of the magnet. Unlike SEPAGE, the absence of electric field prevents any differentiation between

proton and other positively-charged particles. Non-deviated neutral particles are collected on the frontal IP (see Figure VIII.23). A recent improvement of the diagnostic allows for high energy X-ray spectrometry by replacing the frontal IP by a stack of IP and filters (bremsstrahlung cannon).

The measurement range for electrons is 5-150 MeV while for protons the range is limited to 1–15 MeV. The bremsstrahlung cannon is designed for X-rays in the 1–200 keV temperature range.

These two spectrometers were developed in the framework of the PETAL+ project [46, 47, 88].

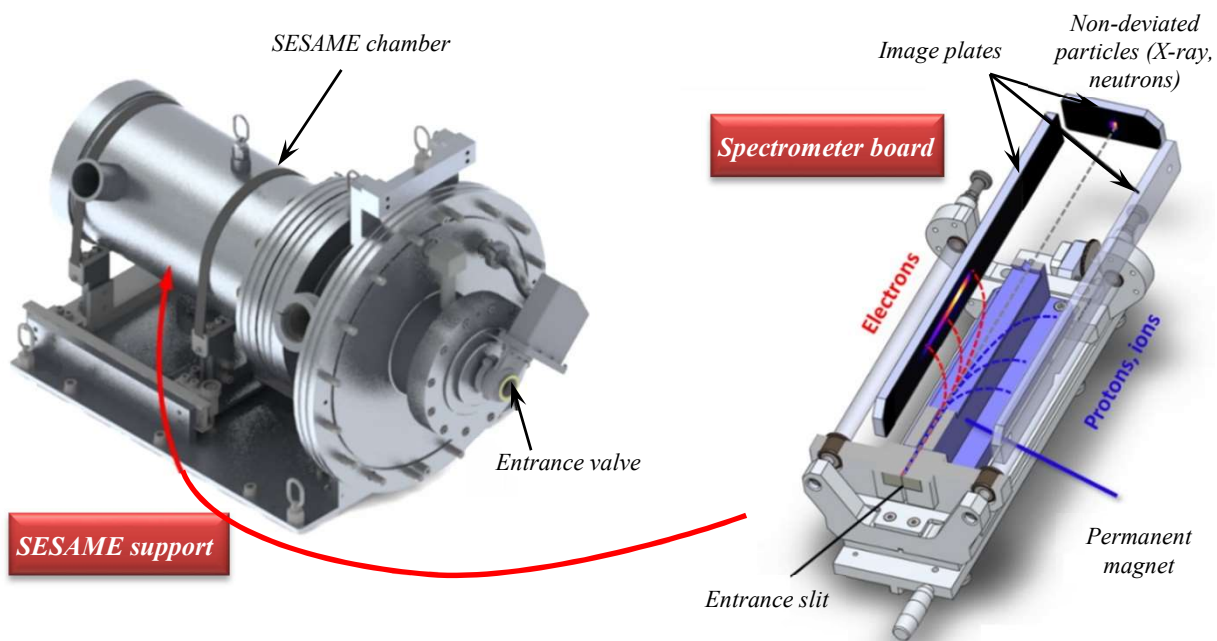


Figure VIII.26: Principle and current design of the SESAME diagnostic.

VIII.5- Other diagnostics

VIII.5.1 - CRACC and CRACCOPELE, Radiographic Cassette

CRACC complements the PETAL diagnostics developed in the framework of the PETAL+ project. It is dedicated to proton or X-ray radiographies but can also be used as a discrete proton or X-ray spectrometer (Bremsstrahlung cannon), or for activation measurements. Unlike the imaging module of SEPAGE, CRACC can be positioned in any equatorial SID.

CRACC is made of an aluminum holder which integrates a translation module carrying the detector cassette close to the TCC (100 mm from the target at the closest, distance is adjustable from 100 mm to 700 mm).

Four different types of cassettes are currently available:

- **CRACC-RCF** is a cassette dedicated to proton radiography or spectrometry in the 3 – 200 MeV energy range. It is composed of a stack of 94 mm diameter radiochromic films (RCF) and filters. A standard configuration with a ~ 1 MeV

- resolution (energy range 3-60 MeV) is available. A user-defined stack can be studied upon request.
- **CRACC-RX** is a X-ray radiography cassette composed of one or more Image Plates (IP). The IP have a diameter of 94 mm.
- **CRACC-X** is a Bremsstrahlung cannon composed of a stack of 20 mm diameter IP and filters allowing for high energy X-ray spectrometry in the 1 – 200 keV temperature range. The stack is inserted in a lead and plastic housing improving signal to noise ratio.
- **CRACC-ACT** is a cassette that can contain both radiographic films and activation samples.

A picture of the diagnostic is shown in Figure VIII.24.

Note that the SESAME diagnostic can also include a Bremsstrahlung cannon module.

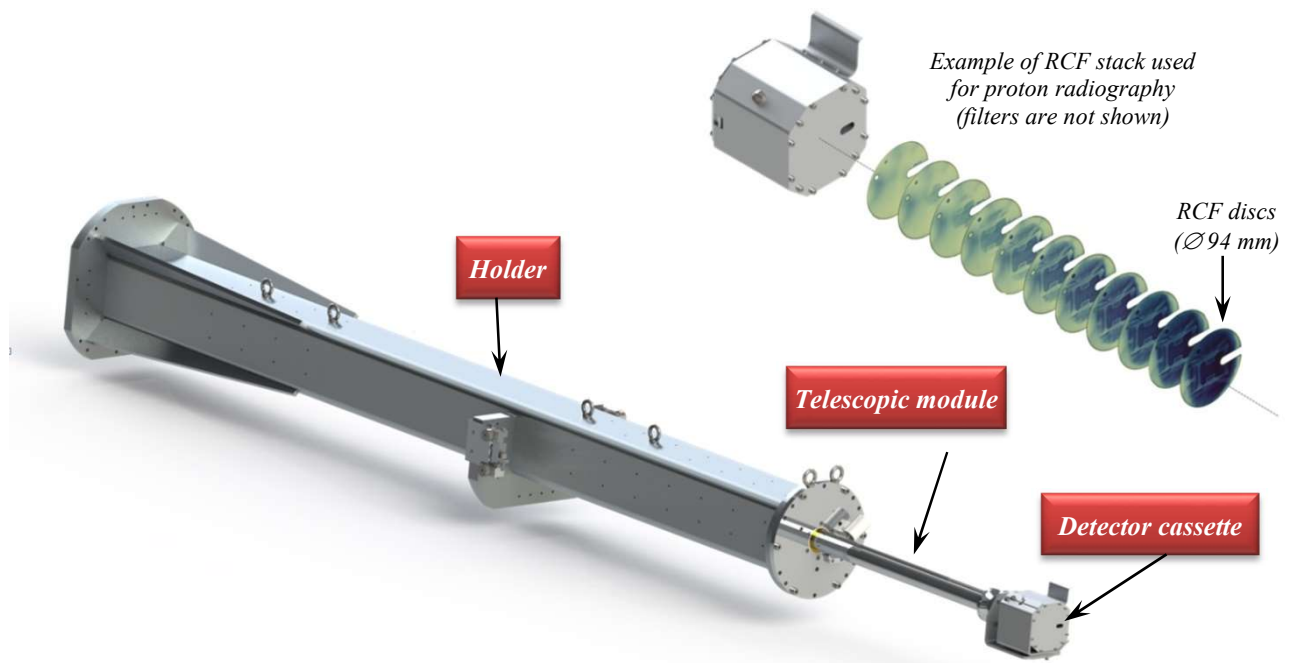


Figure VIII.27: Design of the CRACC diagnostic.

CRACCOPELE is a clone of the CRACC diagnostic that can be positioned either in an equatorial SID or in the vertical position in the polar SID (S17). It is composed of the same elements as CRACC and can hold the same types of cassettes. As CRACCOPELE has a shorter length, the

minimum distance to TCC is limited to 300 mm (100 mm for CRACC).

For a detailed information about available capacities, see the CRACC description.

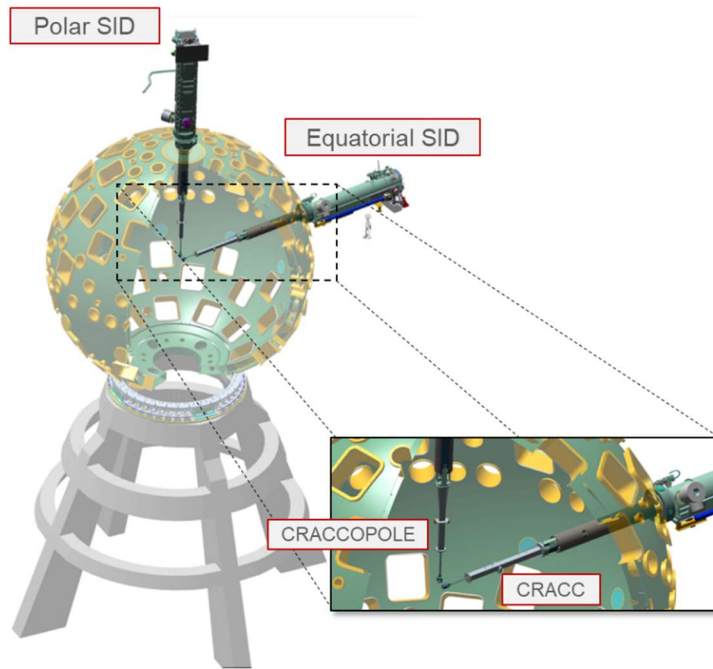


Figure VIII.28 : CRACC and CRACCOPOLE in the LMJ environment.

VIII.5.2 – DEDIX and DIADEM, Samples Holders

The DEDIX diagnostic is mainly dedicated to the study of materials thermomechanical properties under X-ray irradiation, typically Equation-of-States (EoS) or Structural Response (SR). This device holds four samples (30 mm diameter at maximum) at a minimum distance of 70 mm from the TCC, in order to maximize the collection of

radiant energy, e.g. [98]. All-fibered coupled PDV and triature VISAR channels are connected to each sample, enabling shock wave and/or impulse response measurements [99]. In addition, a spectrometer module, made of 4 X-ray diodes with different filters, is used to characterize the X-ray flux, which irradiates the samples.

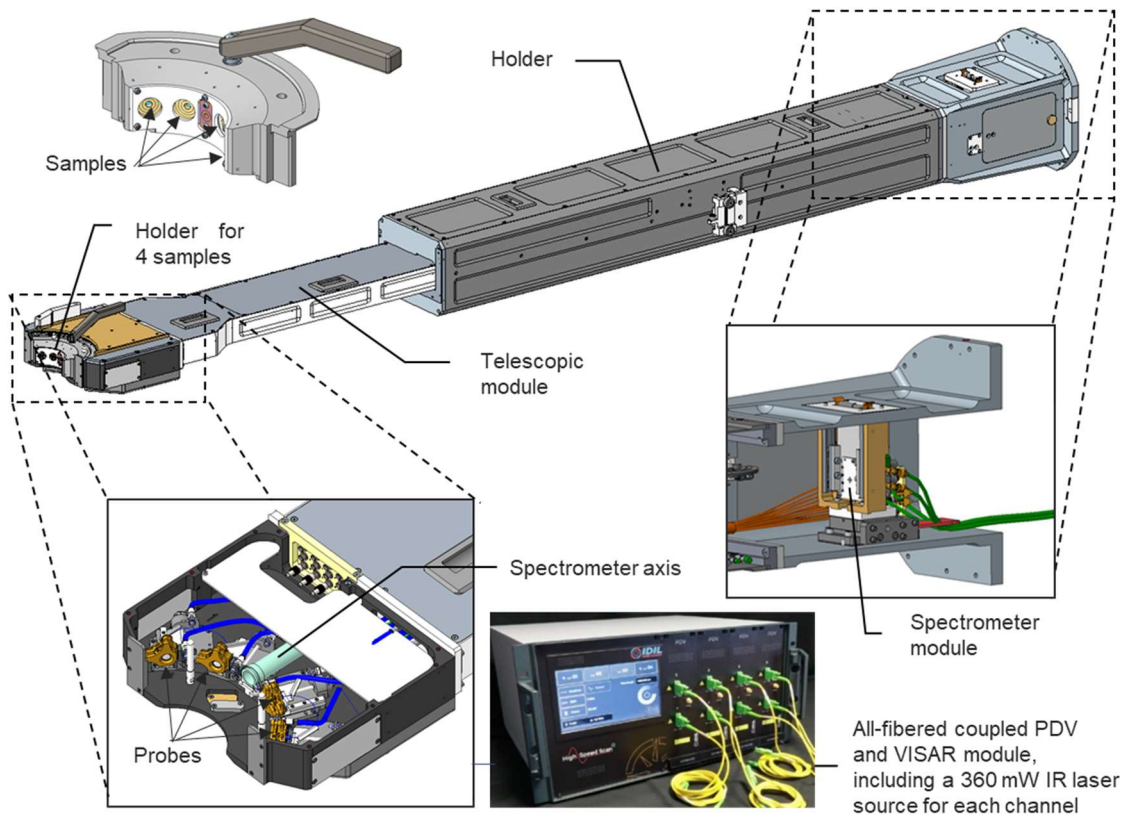


Figure VIII.29: CAD drawing of DEDIX diagnostic. DEDIX diagnostic.

DEDIX				
<i>Diagnostic & Setting</i>	<i>Characteristics</i>	<i>Speed / Spectral range</i>	<i>Field of view</i>	<i>Time resol. / Speed accuracy</i>
DEDIX PDV/VISAR SID	<i>1 all-fibered coupled PDV/triature VISAR interferometer per sample</i> <i>Probe laser: 1550 nm, up to 360 mW for each channel</i> <i>Adjustable frequency shift for PDV: [-3 GHz; +15 GHz]</i>	<i>Fast dynamics mode (EoS): [5; 700] m/s over 1 ms</i> <i>Low dynamics mode (SR): [0.1; 10] m/s over 1s</i>	<i>≈ 200 μm FWHM probe laser (focused on the center of rear side of the sample)</i>	<i>3 ns / 3 m/s</i> <i>1 μs / 0.01 m/s</i>
DEDIX X-ray spectrometer SID	<i>4 time-resolved broad-band channels</i>	<i>[2 - 7 keV]</i>	<i>5 mm</i>	<i>150 ps / 1 μs</i>

The DIADEM diagnostic shares the same architecture (same samples holder, telescopic and spectrometer modules) but it is dedicated to the study of electromagnetic response of materials under X-ray irradiation, such as ElectroMagnetic Pulse (EMP) response, transient radiation effects in electronics (TREE) and System-Generated

ElectroMagnetic Pulse (SGEMP). The samples (30 mm diameter at maximum) must be equipped with 50 ohms coaxial connectors at the rear side. The acquisition system is equipped with tunable high-power attenuation (from -20 dB to -80 dB) and 4 GHz-bandwidth oscilloscopes.

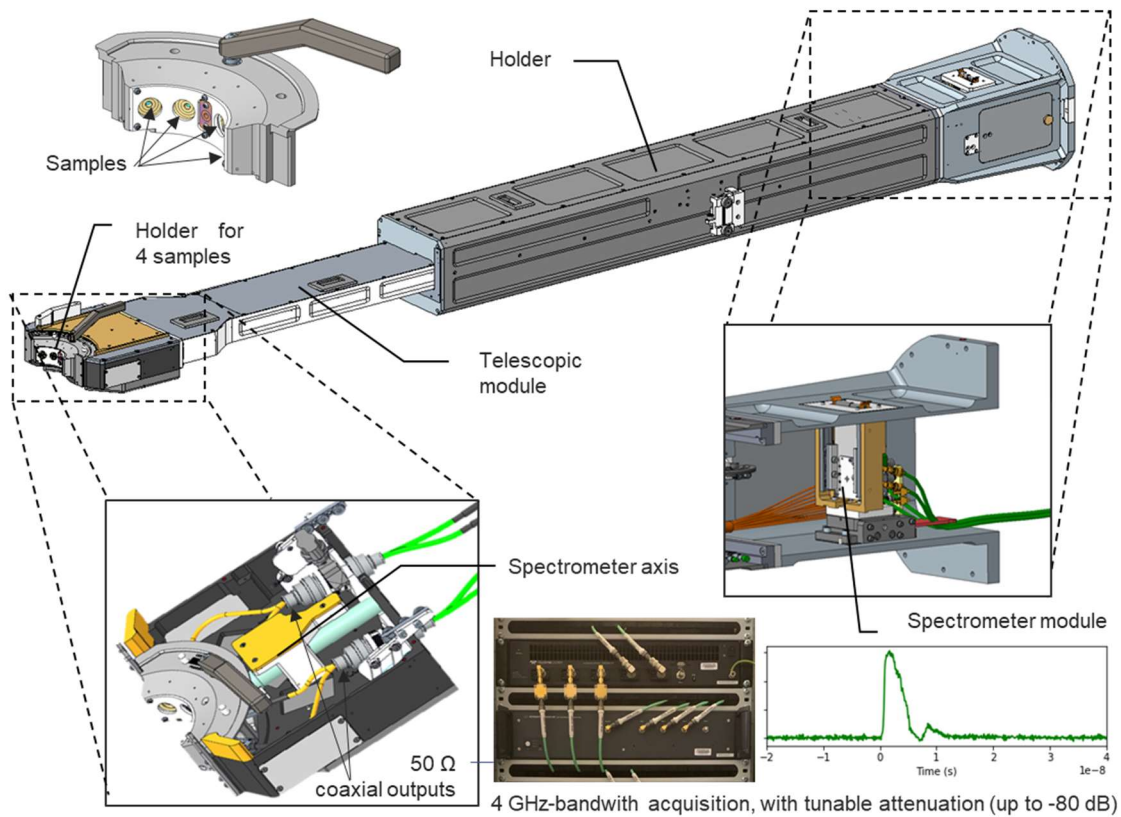


Figure VIII.30: CAD drawing of DIADEM diagnostic.

<i>DIADEM</i>				
<i>Diagnostic & Setting</i>	<i>Characteristics</i>	<i>Voltage / Spectral range</i>	<i>Spatial resol.(μm) / Field of view(mm)</i>	<i>Time resol. (ps)</i>
<i>EM Pulse measurements</i>	<i>4 time-resolved channels (50 ohms impedance)</i>	<i>Detection threshold: 2000 V (50 A) over 10 ns</i>	-	<i>150 ps over 1 μs</i>
<i>X-ray spectrometer</i>	<i>4 time-resolved broad-band channels</i>	<i>[2 - 7 keV]</i>	<i>5 mm</i>	<i>150 ps over 1 μs</i>

It must be noted that due to their large dimensions and short standoff distance to target, these diagnostics blocks the line of sight of some SID ports and precludes their simultaneous use.

VIII.6- Diagnostics in Conceptual Design Phase

Beside the twenty one diagnostics described in the previous sections, other diagnostics have been identified for the next years and are under design.

The future LMJ diagnostics in conceptual design phase include:

- a gated soft X-ray imager;
- high resolution hard X-ray imagers;
- Neutron imaging;
- Thomson scattering diagnostic [100] (not expected before 2030) ;
- ...

IX- Experimental Configuration for 2027-2029

IX.1- Laser Beams Characteristics

In 2027, the experimental configuration of the LMJ facility will include:

- 20 bundles (40 quads) for a 10-order symmetric irradiation;
- at least one other bundle (2 quads) for radiography or other irradiation;
- the PETAL beam.

The spherical coordinates of these beams and the angles between the quads and PETAL are given in Table IX.1, together with the CPP available for each quad.

Regarding Smoothing by Spectral Dispersion, the 2 GHz modulation will be activated for all shots, and the 14 GHz modulation will be activated if required.

Symmetric irradiation									
Beam Port	θ	φ	Angle vs. PETAL	Available CPP	Beam Port	θ	φ	Angle vs. PETAL	Available CPP
2U	33.2°	117°	110.8°	B	24U	33.2°	9°	59.6°	B
2L	131°	117°	119.4°	A	24L	131°	9°	45.8°	A
3U	49°	99°	106.8°	A	25U	49°	27°	55.0°	A
3L	146.8°	99°	102.1°	B	25L	146.8°	27°	65.4°	B
5U	49°	135°	130.1°	A	26U	33.2°	45°	73.4°	B
5L	146.8°	135°	117.8°	B	26L	131°	45°	66.8°	A
6U	33.2°	153°	122.2°	B	28U	33.2°	81°	92.5°	B
6L	131°	153°	137.2°	A	28L	131°	81°	93.4°	A
7U	49°	171°	138.8°	A	29U	49°	63°	79.9°	A
7L	146.8°	171°	123.1°	B	29L	146.8°	63°	82.7°	B
9U	33.2°	189°	120.4°	B	17U	33.2°	297°	69.2°	B
9L	131°	189°	134.2°	A	17L	131°	297°	60.6°	A
10U	49°	207°	125.0°	A	18U	49°	279°	73.2°	A
10L	146.8°	207°	114.6°	B	18L	146.8°	279°	77.9°	B
11U	33.2°	225°	106.6°	B	20U	49°	315°	49.9°	A
11L	131°	225°	113.2°	A	20L	146.8°	315°	62.2°	B
13U	33.2°	261°	87.5°	B	21U	33.2°	333°	57.8°	B
13L	131°	261°	86.6°	A	21L	131°	333°	42.8°	A
14U	49°	243°	100.1°	A	22U	49°	351°	41.2°	A
14L	146.8°	243°	97.3°	B	22L	146.8°	351°	56.9°	B
Radiography or other irradiation									
Beam Port	θ	φ	Angle vs. PETAL	Available CPP					
23U	59.5°	9°	37.2°	E,F					
23L	120.5°	351°	30.8°	E,F					
19U*	59.5°	333°	59,5°	E,F					
19L*	120.5°	315°	120,5°	E,F					
PETAL	90°	346.5°	0°	-					

Table IX.1: Angle of the LMJ quads and PETAL beam in 2027. CPP available for each quad. (*19U and 19L will only be operational in 2028)

IX.2- Target Bay Equipment

At the beginning of 2027, 7 SIDs will be available: 1 polar SID and 6 equatorial SIDs.

The cryogenic TPS is not available and the LMJ facility is not yet configured to handle tritium in target.

For the sake of minimizing the number of facility reconfiguration, the operational positions available in the 2027-2029 timeframe will be:

- S17 on polar axis for polar SID.
- S05, S12, S16, S20, S22, S26 in the equatorial plane for the 6 equatorial SIDs.

The proposed experimental configurations should take these constraints into account. No flexibility in SID implantation at other positions than those listed in the previous lines is available.

The available LMJ diagnostics at the beginning of 2027 will be: GXI-1, GXI-2, SHXI, SSXI, UPXI, ULXI, ERHXI-1&2, HRXS, DMX, Mini-DMX-1, Mini-DMX-2, SPECTIX, EOS Pack, FABS1, NBI, Neutron Pack, SEPAGE, SESAME 1&2 , CRACC & CRACCOPOLE, DEDIX & DIADEM.

IX.2.1 – SID positions and insertable diagnostics compatibility

Due to diagnostics specificities, the use of insertable diagnostics in the different SIDs is subject to restrictions. The following table (IX.2) summarizes the compatibilities. The design of experimental configuration must take into account these compatibilities.

	X-ray Imagers						Spectrometers			Others					Remarks
	GXI-1	GXI-2	SHXI	SSXI	ERHXI-1	ERHXI-2	miniDMX/ miniDMX2	HRXS	SPECTIX	EOS pack	SEPAGE	CRACC	CRACCOPOLE	DEDIX/ DIADEM	
S5	Yes	Yes	Yes	No	Yes	Yes	No	Yes	Yes	No	No	Yes	Yes	No	
S12	Yes	Yes	Yes	Yes	Yes	Yes	No	Yes	Yes	No	No	Yes	Yes	No	
S16	Yes	Yes	Yes	No	Yes	Yes	Yes	Yes	Yes	No	No	Yes	Yes	Yes	
S17 polar	Yes	Yes	Yes	No	No	Yes	No	Yes	No	No	No	No	Yes	No	
S20	Yes	Yes	Yes	No	Yes	Yes	No	Yes	Yes	Yes	No	No	No	No	Dedicated to EOS pack
S22 (2027)	Yes	Yes	Yes	No	Yes	Yes	No	Yes	Yes	No	No	Yes	Yes	No	
S26	Yes	Yes	Yes	No	Yes	Yes	Yes	Yes	Yes	No	Yes	Yes	Yes	No	

Table IX.2: Compatibility of diagnostics with SIDs.

IX.2.2 – Compatibility with PETAL

During PETAL shots a high electromagnetic field may be generated which could perturb diagnostic operation. In order to reduce the risk of damage on diagnostic electronic part, two preclusions are taken.

First, a specific stalk between target holder and PETAL target has been developed [101, 102] to reduce the electric current in the target holder. All PETAL shots should use this specific stalk.

Second, some diagnostics have been purposely designed to sustain the high electromagnetic field generated by PETAL. These diagnostics comprise specific PETAL diagnostics working with passive detector, and some other LMJ diagnostic which include electromagnetic shielding.

Some diagnostics have been already used during PETAL shots and are qualified to operate with PETAL, some are not (yet) qualified.

Use of a diagnostic during PETAL shot may be restricted if the diagnostic has not been qualified for the energy level requested for PETAL. Experiment design using PETAL should only request PETAL-qualified diagnostics as primary diagnostics.

	<i>X-ray Imagers</i>					<i>X-ray Spectrometers</i>				<i>Optical diagnostics</i>			<i>Particles diagnostics</i>				
	GXI-1 & GXI-2	SHXI	SSXI	UPXI & LPXI	ERHXI-1 & ERHXI-2	DMX	MiniDMX & MiniDMX2	HRXS	SPECTIX	EOS Pack	FABS	NBI	Neutron pack	SESAME1&2	SEPAGE	CRACC & CRACCOPOLE	DEDIX & DIADEM
PETAL compatible and qualified up to 600 J	✓	✓		✓		✓			✓	✓				✓	✓	✓	
PETAL compatible but not yet qualified					✓		✓	✓					✓				✓
Not designed for PETAL			✓								✓	✓					

Table IX.3: Compatibility of diagnostics with PETAL

IX.3- Experimental platforms

In order to limit time-consuming reconfigurations of the facility, five experimental platforms have been defined. They correspond to a facility configuration with fixed SIDs and diagnostics positions. It is highly recommended to use these classical configurations already qualified by previous experiments.

The annual schedule of the facility includes two or three different platforms. The experiments will be programmed in line with the platforms selected for the year.

These platforms are made of:

- 7 fixed SID positions,
 - fixed core diagnostics (indicated by a star in table IX.3) which cannot be moved for consistency with other experiments that could be planned in the same period ; the design of the experiment should accommodate the presence of these diagnostics.
 - core diagnostics which are recommended for each platform; core diagnostics change should be avoided to ensure consistency with other experiments planned with the platform.
 - and optional diagnostics which can be used to adapt the configuration by choosing them according to table IX.2
- Up to two diagnostic changes are possible within a configuration.

Reconfiguration of polar SID is not an available option.

The 5 experimental platforms are described below :

Platform name	SID location	Core diagnostics	Optional diagnostics
SXR (Soft X-ray)	S05		
	S12	SSXI*	
	S16		
	S17 (polar)		
	S20	EOS Pack*	
	S22		
	S26	Mini-DMX*	
IMP (Implosion)	S05	GXI-2	
	S12	ERHXI	SHXI
	S16	GXI-1	HRXS, SPECTIX
	S17 (polar)	ERHXI2*	
	S20	EOS Pack*	
	S22	SHXI	ERHXI
	S26		
HXR (Hard X-ray radiography, UHI)	S05	CRAC*	
	S12	ERHXI	
	S16		CRACC, HRXS, SPECTIX
	S17 (polar)		
	S20	EOS Pack*	
	S22		
	S26		CRACC, SEPAGE
OPA (EOS, Opacity)	S05		
	S12		
	S16	HRXS*	
	S17 (polar)	ERHXI-2*	
	S20	EOS Pack*	
	S22		
	S26	Mini-DMX*	
TMS (thermomechanical studies)	S05		
	S12		
	S16	DEDIX*	DIADEM*
	S17 (polar)		
	S20		
	S22		HRXS
	S26	Mini-DMX	

Table IX.3: Configuration of the 5 experimental platforms. A star (*) indicates fixed core diagnostics.

Note : These definitions may be updated to accomodate new features planned to be included in the experimental system during the period 2027-2029 (cryogenic target holder, PETAL upgrade). Users are strongly encouraged to require assistance of CEA point of contacts to define the most appropriate experimental configuration, based on available platforms and facility schedule, to fit their needs.

X- Targets

X.1- Assembly and Metrology Process

According to the experimental process (see III.6.), the final target technological design is frozen during the Design Review (twelve months before the shots), and the metrology process definition begins. During this review, the list of all targets' materials and their respective masses is established. These data are used to check target compatibility with LMJ-PETAL facility safety rules. The MOE ensures that target design is approved according to these rules. Some other topics have also to be validated, such as target debris generation assessment, specific storage requirements, if necessary (external global target volume should be less than $40 \times 40 \times 40 \text{ mm}^3$), etc.

A gas system is available for gas-filled targets; it includes two pressure ranges : a low pressure range for gas-filled hohlraum for instance, and a high pressure range for gas-filled capsule and gas jet.

Gas target specification :

Low pressure range ($0,1 \text{ bar} < \text{Pressure} < 1,5 \text{ bars}$, $P_{\text{max}} 1,2 \text{ bars}$ for C_5H_{12})

Possible gases : H_2 , D_2 , He, CO_2 , CH_4 (methane), C_3H_8 (propane), C_5H_{12} (neopentane), N_2 , Ne, Ar, Kr, Xe.

Other gases (excluding cyanide gases) or mixture of these different gases in variable proportion is possible (must be studied during the feasibility phase of the experiment)

Tolerated leak rate for a reference target with a volume of 1 cm^3 filled at 1 bar (absolute): $10^{-4} \text{ mb.l.s}^{-1}$

High pressure range ($2 \text{ bars} < \text{Pressure} < 69 \text{ bars}$)

Possible gases : H_2 , D_2 , He, CO_2 , N_2 , O_2 , Ne, Ar, Kr, Xe.

Other gases (excluding cyanide gases) or Mixture of these different gases in variable proportion is possible (must be studied during the feasibility phase of the experiment)

The leak rate tolerated for a target will be established when defining the mounting based on experience

Gas jet

List of gases: identical to the High pressure regime

Pressure range: identical to the High pressure regime

$10 \mu\text{s} \leq \text{Gas jet opening duration} \leq 100 \text{ ms}$

Nozzle-focusing point distance $\geq 1 \text{ mm}$

CEA/CESTA Target Laboratory is in charge of target assembly and final target metrology. The final target structure study starts one year before the shots. This study requires:

- “step” format CAD target file (no later 1 than year before shots [PI]);
- laser and diagnostics experimental configuration (Supply of Visrad file: no later than 1 year before shots [MOE]).

At the design review, all components of the target assembly (including shields) must be thoroughly defined. For target elements, that are provided, detailed drawing including all dimensions and fabrication tolerances are expected.

CAD final target structure will be validated by PI and MOE between 4 and 8 months before the shots, depending on the target complexity. CEA/CESTA Target Laboratory has to receive the target 4 months before the first shot. At that time, each target must be identified and described in a dimensional characterization document.

CEA/CESTA Target Laboratory supplies target positioner interface (alignment fiducial) used by the target alignment process, and manufactures each subset assembling to obtain the final target structure. Then, it carries out metrology on the target structure (angular and dimensional controls), essential to generate target positioning data used by the LMJ target alignment system.

Targets redundancy should be sufficient to allow fulfilling the shot plan (1 to 6 shots).

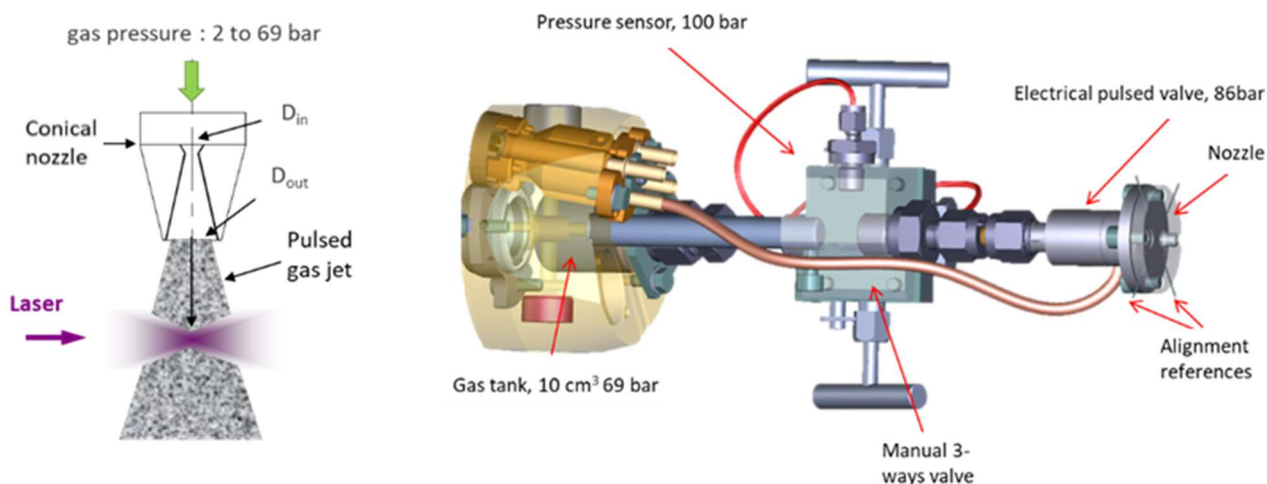


Figure X.1.1: Principle and current design of a gas jet experiment

X.2- LMJ-PETAL Target Alignment Process

The LMJ-PETAL target alignment process is based on the visualization of four spheres set around the target. Metrology, performed as described above, associates the spheres location with “strategic” target areas. So, with the LMJ target viewing station of four spheres and with the target metrology file, LMJ target alignment system can put the target at the expected location.

The LMJ target alignment process is summarized below. The first step is the preliminary insertion of target by LMJ target positioner, as seen on the three pictures given by the target viewing station (Figure X.2.1.).

The second step consists in a manual approach between target and final location represented by reticles (red circles and cylinder). When a partial superposition between spheres and red circles is reached, this step is over.

Last step is the final automatic positioning, which provides the best alignment accuracy.

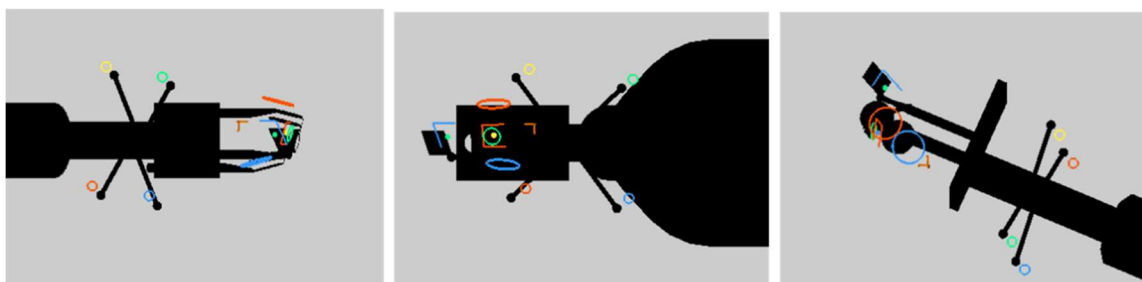


Figure X.2.1: LMJ target alignment process - first step.

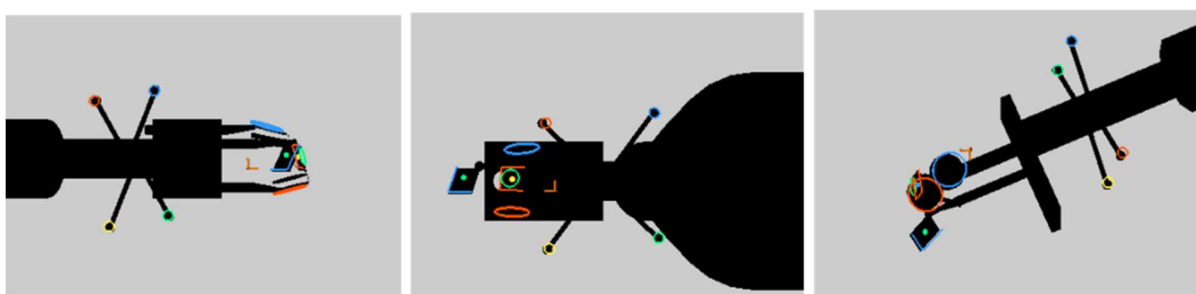


Figure X.2.2.: LMJ alignment process - last step.

XI- References

- [1] P. Monot et al, Phys. Rev. Lett. **74** (15), p.2953 (1995)
- [2] M. Schnürer et al, J. Appl. Phys. **80** (10), 5604, (1996)
- [3] G. Malka et al, Phys. Rev. Lett. **79** (11), 2053, (1997)
- [4] T. Feurer et al, Phys Rev E **56** (4), 4608, (1997)
- [5] J. Fuchs et al, Phys Rev Lett **80**, 1658, (1998)
- [6] J. Fuchs et al, Phys. Rev. Lett. **80** (11), 2326, (1998)
- [7] E. Lefebvre et al, Phys. Plasmas **5**, 2701 (1998)
- [8] P. Gibbon et al, Phys. Plasmas **6**, 947 (1999)
- [9] R.L. Berger et al, Phys. Plasmas **6**, 1043 (1999)
- [10] A. Chiron et al, Euro. Phys. Journal D **6**, 383 (1999)
- [11] C. Cherfils et al, Phys. Rev. Lett. **83**, 5507 (1999)
- [12] Th. Schlegel et al, Phys. Rev. E **60**, 2209 (1999)
- [13] L. Gremillet et al, Phys. Rev. Lett. **83**, 5015 (1999)
- [14] A. MacKinnon et al, Phys. Plasmas **6**, 2185 (1999)
- [15] J. Fuchs, Phys. of Plasmas **6** (6), 2563, (1999)
- [16] Ph. Mounaix et al, Phys. Rev. Lett. **85**, 4526 (2000)
- [17] G. Glendinning et al, Phys. Plasmas **7**, 2033 (2000)
- [18] V.N. Goncharov et al, Phys. Plasmas **7** (12), 5118 (2000)
- [19] G. Glendinning et al, Astrophys. J. Suppl. Series **127**, 325 (2000)
- [20] O. Willi et al, Nucl. Fusion **40**, 537 (2000)
- [21] C. Courtois et al, JOSA B **17** (5), 864, (2000)
- [22] B. Cros et al, IEEE Transactions on Plasma Science **28** (4), 1071, (2000)
- [23] M. Borghesi et al, Laser and particle beams **18**, 389 (2000)
- [24] J. Kuba et al, Phys. Rev. A **62**, 043808, (2000)
- [25] A. Benuzzi-Mounaix et al, Astrophysics and Space Science **277** (1), 143 (2001)
- [26] E. Dattolo et al, Phys. Plasmas **8**, 260 (2001)
- [27] D. Batani et al, Phys. Rev. Lett. **88** (23), 235502 (2002)
- [28] J.L. Bourgade et al, Rev. Sci. Instrum. **79**, 10F301 (2008)
- [29] A. Morace et al, Phys. Plasmas **16**, 12,122701 (2009)
- [30] Y. Inubushi et al, Phys. Rev. E **81** (3), 036410 (2010)
- [31] S. Jacquemot et al, Nucl. Fusion **51**, 094025 (2011)
- [32] G. Schurtz et al, Phys. Rev. Lett. **98** (9), 095002 (2007)
- [33] L. Videau et al, Plasma Physics and Controlled Fusion **50**, 12, 124017 (2008)
- [34] S. Depierreux et al, Phys. Rev. Lett. **102**, vol. 19, 195005 (2009)
- [35] C. Labaune et al, J. Phys. Conf. Series **244**, 2, 022021 (2010)
- [36] A. Casner et al, J. Phys. Conf. Series **244**, 3, 032042 (2010)
- [37] A. Benuzzi-Mounaix et al, Physica Scripta **T161**, 014060 (2014)
- [38] S.D. Baton et al, Physics of Plasmas **24**, 092708 (2017)
- [39] C. Lion, Journal of Physics: Conference Series **244**, 012003 (2010)
- [40] J.L. Miquel et al, Review of Laser Engineering **42**, 131-6 (2014)
- [41] N. Blanchot et al, EPJ Web of Conferences **59**, 07001 (2013)
- [42] J.L. Miquel et al, Nucl. Fusion **59**, 032005 (2019)
- [43] A. Casner et al, High Energy Density Physics **17**, 2-11 (2015)
- [44] F. Philippe et al, Phys. Rev. Lett. **104** (3), 035004 (2010)
- [45] S. Laffite and P. Loiseau, Phys. Plasmas **17** (10), 102704 (2010)
- [46] J.E. Ducret et al, Nuclear Instrum. Methods in Physics Research A **720**,141 (2013)
- [47] D. Batani et al, Physica Scripta **T161**, 014016 (2014)
- [48] A.F.A. Bott et al, Physical Review Letters **127** (17), 175002 (2021).
- [49] S. Baton et al, High Energy Density Physics **36**, 100796 (2020)
- [50] A. Le Cain, G. Riazuelo and J.M. Sajer, Phys. Plasmas **19** (10), 102704 (2012).
- [51] G. Duchateau, Opt. Express **17** (13), 10434-10456 (2009)
- [52] O. Morice, Optical Engineering **42** (6), p.1530-1541 (2003)
- [53] X. Julien et al, Proc. SPIE **7916**, 79610-1 (2011)
- [54] V. Brandon et al, Nuclear Fusion **54** (8), 083016 (2014)
- [55] N. Blanchot et al, Plasma Phys. Control. Fusion **50**, 124045 (2008)

- [56] E. Hugonnot et al, Appl. Opt. **45** (2), 377-382 (2006)
- [57] E. Hugonnot et al, Appl. Opt. **46** (33), 8181-8187 (2007)
- [58] C. Rouyer, Opt. Express **15**, 2019-2032 (2007)
- [59] N Blanchot, Opt. Express **18**, 10088-10097 (2010)
- [60] N Blanchot, Appl. Opt. **45** (23), 6013-6021 (2006)
- [61] J. Néauport et al, Opt. Express **15**, 12508-12522 (2007)
- [62] M. Sozet et al, Opt. Express **25**, 25767-25781 (2017)
- [63] M. Chorel et al, Opt. Express **26**, 11764-11774 (2018)
- [64] A. Ollé et al, Rev. Sci. Instrum. **90**, 073001 (2019)
- [65] N Blanchot, Opt. Express **25**, 16957 (2017)
- [66] C. Reverdin et al, Rev. Sci. Instrum. **79** (10), 10E932 (2008)
- [67] S. Hubert et al, Rev. Sci. Instrum. **81** (5), 053501 (2010)
- [68] J. Baggio et al, Fusion Engineering and Design, vol. **86**, 2762 (2011).
- [69] J. L. Dubois et al, Phys. Rev. E **89** (3), 013102 (2014).
- [70] D. Eder et al, Nuclear Fusion **53** (11), 113037 (2013)
- [71] J.L. Bourgade et al., Rev. Sci. Instrum. **79**, 10E904 (2008)
- [72] R. Rosch et al, Rev. Sci. Instrum. **78** (3), 033704 (2007)
- [73] J.P. LeBreton et al, Rev. Sci. Instrum. **77** (10), 10F530 (2006)
- [74] T. Beck et al, IEEE Trans Plasma Sci, **38**(10), 2867-72, (2010)
- [75] R. Rosch et al, Rev. Sci. Instrum. **87**, 033706 (2016)
- [76] G. Turk et al, Rev. Sci. Instrum. vol. **81**(10), 10E509, (2010).
- [77] H. Maury et al, Nucl Instrum Methods Phys Res Sect A, vol. **621**(1-3), 242-6, (2010)
- [78] P. Troussel et al, Proc. of SPIE **8139** (2011)
- [79] P. Troussel et al, Rev. Sci. Instrum. **83** (10), 10E533, (2012)
- [80] C. Troseille et al, Rev. Sci. Instrum. **85**, 11D620 (2014)
- [81] D. Denetiere et al, EPJ Web of Conferences **59**, 13005 (2013)
- [82] P. Troussel, Nuclear Instr. & Meth. A767, **14** (2014)
- [83] K.B. Fournier et al, Phys Plasmas **16**, 052703 (2009)
- [84] L. Jacquet et al, Phys Plasmas **19**, 083301 (2012)
- [85] F. Perez et al, Phys Plasmas **19**, 083101 (2012)
- [86] P. Troussel et al, Rev. Sci. Instrum. **85**, 013503 (2014)
- [87] C. Reverdin et al, J. Inst. **13**, C01005 (2018)
- [88] D. Batani et al, Acta Polytechnica **53**, 103-109 (2013)
- [89] Y. Cauchois, Journal de Physique **3**, 320 (1932)
- [90] J.F. Seely et al, Rev. Sci. Instrum. **81**(10), 10E301 (2010)
- [91] A.L. Meadowcroft et al, Rev. Sci. Instrum. **79**, 113102 (2008)
- [92] G. Boutoux et al, Rev. Sci. Instrum. **87**, 043108 (2016)
- [93] I. Thfoin et al, Rev. Sci. Instrum. **85**, 11D615 (2014)
- [94] G. Debras et al, EPJ Web of Conferences **59**, 02006 (2013)
- [95] V. Trauchessec et al. Rev. Sci. Instrum. **93**, 103519, (2022)
- [96] O. Landoas et al, Rev. Sci. Instrum. **82** (7), 073501, (2011)
- [97] I. Lantuéjoul et al, Proc of SPIE **10763**, 107630X-1 (2018)
- [98] M. Primout et al, Phys. Plasmas **29**, 073302 (2022)
- [99] G. Boutoux et al, Rev. Sci. Instrum. **94**, 033905 (2023)
- [100] S. Depierreux et al, Rev. Sci. Instrum. **91**, 083508 (2020);
- [101] M. Bardon et al, Phys Rev. Research **2**, 033502 (2020)
- [102] F. Lubrano et al, INPI patent 14 59941 (2014)

XII- Acknowledgements

LMJ is a CEA project funded by the French Ministry of Defense



PETAL is a project of the Aquitaine Region funded by the Aquitaine Region, the French Ministry of Research and Europe.



PETAL+ is an Equipex project of the University of Bordeaux funded through the PIA by the ANR (French National Research Agency).



XIII- Glossary

ALP: Association Lasers and Plasmas	LPI: Laser Plasma Interaction
ANR: French Agency for National Research	LPXI: Lower Pole X-ray Imager
APS DPP: Meeting of the Division of Plasma Physics of the American Physical Society	Mini-DMX: Mini Broad-band X-ray spectrometer
BTDP: Transfer Box for Plasma Diagnostic	MOE: CEA Experiment Manager
CAD: Computer Assisted Design	NBI: Near Backscattered Imager
CEA-DAM: Military Applications Division of CEA	NLTE: Non Local Thermodynamic Equilibrium
CELIA: Centre Lasers Intenses et Applications	OPA: Optical Parametric Amplification
CPA: Chirped Pulse Amplification	PAM: Pre-Amplifier Module
CPP: Continuous Phase Plates	PETAL: Petawatt Aquitaine Laser
CRACC: Cassette for Radiography at Chamber Center	PETAL+: PETAL diagnostics Project funded by ANR (Equipex Projects)
DEDIX: Sample holder	PFM: Pulse Forming Module
DMX: Broad-band X-ray spectrometer	PI: Principal Investigator
ECLIM: European Conference on Laser Interaction with Matter	PIA: Programme d'Investissement d'Avenir (French National program for promising investment)
EOS: Equation of State	RCE: CEA Experiment Coordinator
EOS Pack: Diagnostics set for EOS experiments	RCF: Radio Chromic Film
EPS: Conference on Plasma Physics of the European Physical Society	RH: Reference Holder
ERC: European Research Council	RMS: Root mean square
ERHXI: Enhanced Resolution Hard X-ray Imager	SBO: Shock Break Out
FABS: Full Aperture Backscattering Station	SEPAGE: Electrons and protons spectrometer
GOI: Gated Optical Imager	SESAME: Electrons spectrometer
GXI-1&2: Gated X-ray Imager	SHXI: Streaked Hard X-ray Imager
HEDLA: Conference on High Energy Density Laboratory Astrophysics	SID: System for Insertion of Diagnostics
HEDP: High Energy Density Physics	SOLEIL: French Synchrotron facility located at L'orme des Merisiers, 91190 Saint Aubin
HRXS: High Resolution X-ray Spectrometer	SOP: Streaked Optical Pyrometer
HTPD: Conference on High Temperature Plasma Diagnostics	SOPAC: System for Optical Positioning and Alignment inside Chamber
ICF: Inertial Confinement Fusion	SPECTIX: Hard X-ray spectrometer
ICHED: International Conference in High Energy Densities	SSD: Smoothing by Spectral Dispersion
IFSA: Conference on Inertial Fusion Sciences and Applications	SSXI: Streaked Soft X-ray Imager
IP: Imaging Plate	TBD: To be determined
ISAC: International Scientific Advisory Committee	TCC: Target Chamber Center
LEH: Laser Enhance Holes	TP: Thomson Parabola
LIL: Laser Integration Line	TPS: Target Positioning System
LMJ: Laser Megajoule	UPXI: Upper Pole X-ray Imager
	VISAR: Velocity Interferometer System for Any Reflector

XIV- Appendix

GPS coordinates:

- CEA-CESTA : 44° 39' 30'' N / 0° 48' 29.8'' W
- LMJ : 44° 38' 08.8 '' N / 0° 47' 12'' W

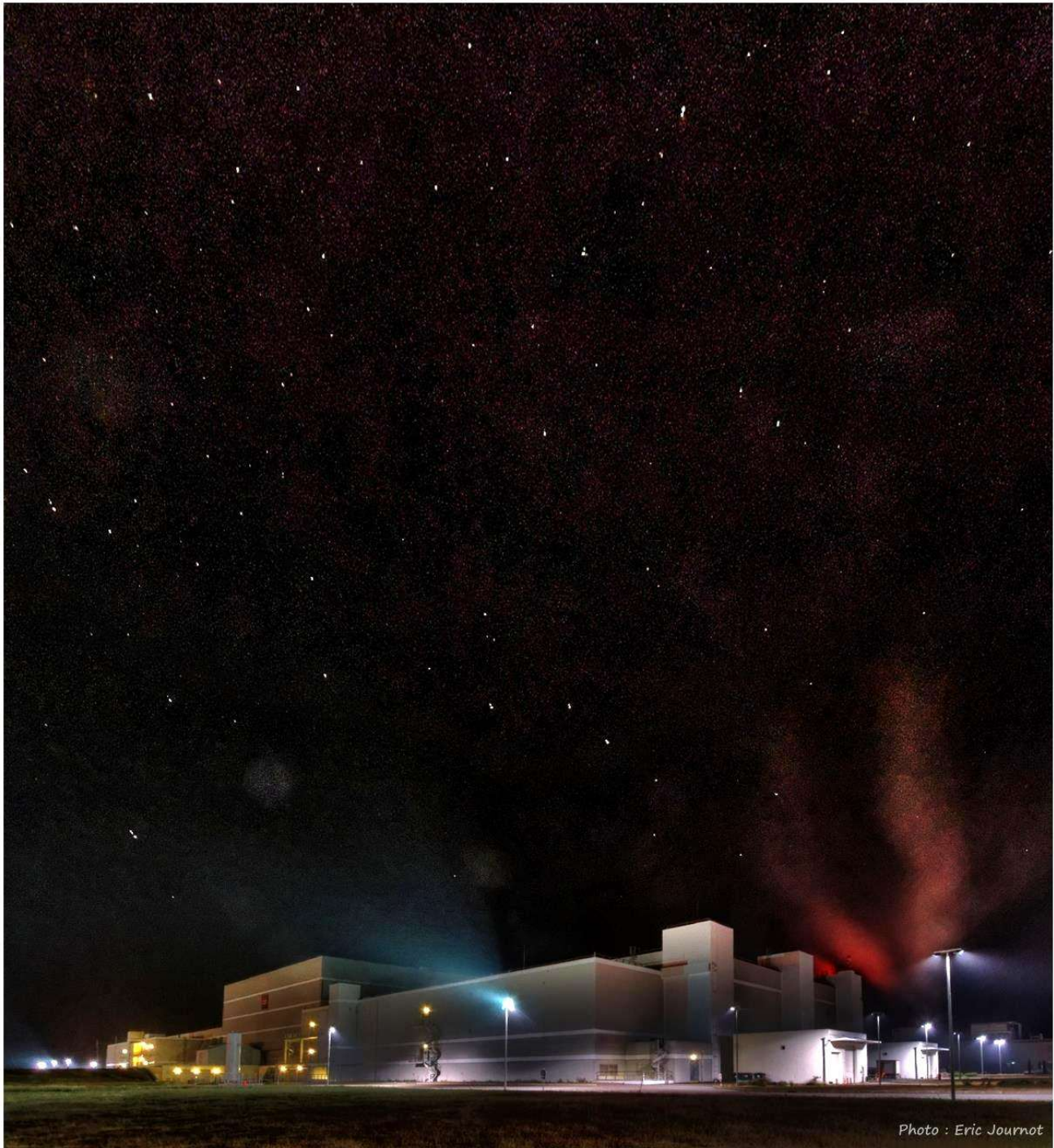
List of hotels close to CEA-CESTA, in Bordeaux and Arcachon.

Close to CEA-CESTA	Bordeaux
<p>Hôtel-Restaurant LE RÉSINIER 68, av. des Pyrénées – RN10 33114 LE BARP Tel. : +33 5 56 88 60 07 contact@leresinier.com</p>	<p>Le M & Spa by Hotels et Préférence 4* 83 avenue John Fitzgerald Kennedy 33700 Mérignac Tel : 05 57 53 21 22 Fax : 05 57 53 21 23 Reservation@hotelmbordeaux.com</p>
<p>Domaine du Pont de l'Eyre 3* 2 route de Minoy 33770 Salles Tel : +33 5 56 88 35 00 Fax : +33 5 56 88 35 99 dom.pont.de.leyre@wanadoo.fr</p>	<p>Hôtel Best Western « Bayonne Etche-Ona » 4* 4 rue Martignac 33000 BORDEAUX Tel : +33 5 56 48 00 88 bayetche@bordeaux-hotel.com</p>
<p>B&B MIOS 3* 6 rue de Galeben Parc d'activités MIOS Entreprises 33380 MIOS Tél : +33 8 92 70 20 70</p>	<p>Ténéo Apparthotel Bordeaux Saint-Jean 2* 4 cours Barbey 33800 BORDEAUX Tel : +33 5 56 33 22 00</p>
<p>ACE Hôtel BORDEAUX – CESTAS 3* Aire de Bordeaux Cestas, Autoroute A63 33610 CESTAS Tel : +33 5 57 97 87 00</p>	
Arcachon	
<p>Hôtel LE DAUPHIN 3* 7 avenue Gounod 33120 ARCACHON Tel : +33 5 56 83 02 89 hotel@dauphin-arcachon.com</p>	<p>Hôtel Le B d'Arcachon 4* 4 rue du Professeur JOLYET 33120 ARCACHON Tel : +33 5 56 83 99 91 Fax : +33 5 56 83 87 92 reservation@hotel-b-arcachon.com</p>
<p>T Boutique Hotel 3* 82 boulevard de la Plage 33120 ARCACHON Tel. : +33 5 56 83 67 70 hello@tboutiquehotel.fr</p>	<p>Zénitude Hotel Résidences Bassin Arcachon 3* 960 avenue de l'Europe 33260 LA TESTE DE BUCH Tel : +33 5 57 15 22 22 arcachon@zenitude-groupe.com</p>
<p>Hôtel LES VAGUES 3* 9 boulevard de l'Océan 33120 ARCACHON Tel. : +33 5 40 51 01 00 contact@lesvagues.fr</p>	

XV- Revision Log

Rev No	Date	Main modifications	Brief description
1.0	12 Sept 2014	-	Initial release (Jean-Luc Miquel, Alexis Casner, Emmanuelle Volant)
1.1	28 April 2015	p6: III.4- Confidentiality rules p7-8: III.5- Selection process p8: III.6- Experimental process p16: V.4- Spot sizes - Table V.2. p19: V.7- Laser performance p26: VIII- LMJ Diagnostics - Table VIII.1 p30-31: VIII.3- Mini-DMX	Rearrangement of section III (precisions on Selection process, addition of Experimental process). Modification of spot sizes. Addition of Laser performance. Addition of Mini-DMX. (JLM, EV)
1.2	6 April 2016	P3 : table II.1 : History P6: III.5 – Selection process P7: III.6 – Experimental process p10: III.11 – Calls for proposals p14: V.1 – Laser architecture – Figure V.6 and Table V.1. p16: V.4- Spot sizes - Table V.2. p19: V.7- Laser performance p22: VI.2 – PETAL performance p24: VII- Target area and associated equipment – Table VII.1 – Figure VII.5 p27 to 45 : VIII- LMJ Diagnostics p46: IX.1 - Laser beams characteristics IX.2 – Target bay equipment p47:X.1 - Assembly & metrology process X.2 – LMJ-PETAL Alignment process p49:XI – References, p52:XIII - Glossary	Update. Precisions on Selection process and Experimental process, addition of Calls for proposals. Modification of the operative quads in 2019. Modification of spot sizes. Update of laser performance. Addition of PETAL performance. Update of the 2019 locations of equipment and new Figure VII.5. Rearrangement of section VIII Update of Table IX.1. Modification of SID locations and available diagnostics. Precisions on assembly /metrology. Addition of alignment process. Update. (JLM, EV)
1.2b	2 May 2016	p3: PETAL+ project p6 : III.5 Selection process	Roles of academic community and University of Bordeaux. LOI = preliminary proposal.
1.3	24 March 2017	p10 : III.11 Calls for Proposal History p15 : Table V.1 Figure V.7 p16 : V.4 Spot sizes and table V.2 p17 : Figure V.9 and V.6 Pulse shapes p20 : V.7 LMJ performances & figure V.13 p23 : VI.2 Petal performances p28 to 46 : VIII- LMJ Diagnostics p51 : XI- References	Update Quads order Addition of disposable debris shield Modification of spot sizes, Pulse duration limited at 20 ns. Update of laser performances. Update of PETAL performances. Update of diagnostics performances Update.(JLM, EV)
1.4	Summer 2018	P44 : IX configuration 2022	Addition of new bundles
2.0	October 2020	All pages	Redesigning and update (JLM, Jean-Paul Jadaud, Bérénice Loupias)
2.1	September 2024	All pages	Update of : Selection process LMJ Laser system and characteristics LMJ Diagnostics availables Expérimental platforms Targets (JLM, JPJ, Jérôme Silva, Laurent Le Deroff)

All Photos: @CEA



Commissariat à l'énergie atomique et aux énergies alternatives
Direction des applications militaires
Centre DAM Île-de-France – Bruyères-le-Châtel - 91297 Arpajon Cedex
Etablissement public de recherche à caractère scientifique, technique et industriel | RCS Paris B 775 685 019